N73-18446
NASA CR-112241

FINAL REPORT

on

DEVELOPMENT OF HIGH TEMPERATURE STRAIN GAGES

Prepared for

NATIONAL AERONAUTICS AND SPACE ADMINISTRATION

January 5, 1973

by

M. M. Lemcoe

Contract NAS 1-11277

Langley Research Center
Hampton, Virginia

BATTELLE
Columbus Laboratories
505 King Avenue
Columbus, Ohio 43201

ABSTRACT

High temperature electric resistance wire strain gages were developed and evaluated for use at temperatures exceeding 922°K (1200°F). A special high temperature strain gage alloy (Fe-25Cr-7.5Al), designated BCL-3, was used to fabricate the gages. Pertinent gage characteristics were determined at temperatures up to 1255°K (1800°F). The results of the evaluation were reported in graphical and tabular form. It was concluded that the gages will perform satisfactorily at temperatures to at least 1089°K (1500°F) for at least one hour.

TABLE OF CONTENTS

	Page
SUMMARY	1
INTRODUCTION	2
OBJECTIVES	2
EXPERIMENTAL EVALUATION AND RESULTS	3
1. Gage Fabrication and Specimen Preparation	3
1.1 General	3
1.2 Materials	3
1.2.1 Gage	3
1.2.2 Specimen	4
1.2.3 Lead-Wire Systems	4
1.3 Gage Fabrication	4
1.3.1 Gage Winding Fixture	4
1.3.2 Gage Geometry and Fabrication Procedures	4
1.4 Specimen Preparation	5
1.4.1 Specimen Geometry and Gage Locations	5
1.4.2 Gage Attachment Procedures	5
1.4.3 Lead Tabs and Lead Wires	5
1.5 Specimen Storage	6
2. Description of Gage Evaluation Facilitites	6
2.1 High Temperature Gage Evaluation Fixture	6
2.2 Temperature Control System	7
2.3 Cooling System	8
2.4 Instrumentation for Strain, Temperature, Resistance, and Deflection Measurement	8
3. Gage Evaluation	9
3.1 Approach	9
3.2 Evaluation Procedure	9
3.3 Test Matrix	10
4. Results	10
4.1 General	10
4.2 Gage Factor and Linearity Characteristics	11
4.3 Apparent Strain	12
4.4 Drift Characteristics	12
4.5 Resistance to Ground	12
4.6 Performance History	13
5. Discussion of Results	13
5.1 General	13
5.2 Gage Factor	13
5.2.1 Specimen H-21	14
5.2.2 Specimen H-23	15
5.2.3 Specimen H-26	15
5.2.4 Specimen H-27	15
5.2.5 Specimen H-27A	15
5.3 Apparent Strain	16
5.3.1 General	16
5.3.2 Specimens H-21, H-22, H-23, H-25, H-26, H-27, H-27A	17

TABLE OF CONTENTS (Contd)

	Page
5.4 Drift Characteristics	21
5.5 Resistance to Ground	22
5.6 Performance History	23
6. Conclusions	24
ACKNOWLEDGEMENT	26
TABLES	27
FIGURES	43
APPENDIX A - GAGE FABRICATION PROCEDURE	A-1
APPENDIX B - GAGE ATTACHMENT PROCEDURE	B-1
APPENDIX C - RESISTANCE TO GROUND MEASUREMENTS	C-1

LIST OF TABLES

		Page
TABLE 1.	HAYNES 25 SPECIMEN MATERIAL PROPERTIES	29
TABLE 2.	LEAD-WIRE SYSTEMS	30
TABLE 3.	TEST MATRIX	31
TABLE 4.	APPARENT STRAIN TO 922°K (1200°F), SPECIMEN H-21	32
TABLE 5.	APPARENT STRAIN TO 978°K (1300°F), SPECIMEN H-23	33
TABLE 6.	APPARENT STRAIN TO 1033°K (1400°F), SPECIMEN H-27	34
TABLE 7.	APPARENT STRAIN TO 1089°K (1500°F) SPECIMEN H-26	35
TABLE 8.	APPARENT STRAIN TO 1144°K (1600°F), SPECIMEN H-27	36
TABLE 9.	PERFORMANCE HISTORY	37
TABLE 10.	GAGE FACTOR SUMMARY	38
TABLE 11.	GAGE FACTOR STATISTICS	39
TABLE 12.	DRIFT RATES AT VARIOUS TEMPERATURES	40
TABLE 13.	RESISTANCE TO GROUND VS SUBSTRATE THICKNESS VS TEMPERATURE	42

LIST OF FIGURES

		Page
FIGURE 1.	MICROSTRUCTURES OF 0.081 INCH-DIAMETER WIRE OF BCL-3 ALLOY	45
FIGURE 2.	GAGE GEOMETRY	46
FIGURE 3.	SPECIMEN GEOMETRY AND GAGE LOCATIONS	47
FIGURE 4.	TYPICAL GAGE INSTALLATION	48
FIGURE 5.	GAGE EVALUATION FIXTURE	49
FIGURE 6.	TEMPERATURE CONTROL SYSTEM	50
FIGURE 7.	SPECIMEN H-21, GAGE FACTOR, RT, CYCLES 1,2,3	51
FIGURE 8.	SPECIMEN H-21, GAGE FACTOR 644°K (700°F)	52
FIGURE 9.	SPECIMEN H-21, GAGE FACTOR, 978°K (1300°F)	53
FIGURE 10.	SPECIMEN H-21, GAGE FACTOR, 1033°K (1400°F)	54
FIGURE 11.	SPECIMEN H-23, GAGE FACTOR, RT	55
FIGURE 12.	SPECIMEN H-23, GAGE FACTOR, 644°K (700°F)	56
FIGURE 13.	SPECIMEN H-23, GAGE FACTOR, 1033°K (1400°F)	57
FIGURE 14.	SPECIMEN H-26, GAGE FACTOR, RT	58
FIGURE 15.	SPECIMEN H-26, GAGE FACTOR, 700°K (800°F)	59
FIGURE 16.	SPECIMEN H-26, GAGE FACTOR, 1089°K (1500°F)	60
FIGURE 17.	SPECIMEN H-26, GAGE FACTOR, 1144°K (1600°F)	61
FIGURE 18.	SPECIMEN H-27, GAGE FACTOR, RT	62
FIGURE 19.	SPECIMEN H-27, GAGE FACTOR, 700°K (800°F)	63
FIGURE 20.	SPECIMEN H-27, GAGE FACTOR, 1033°K (1400°F)	64
FIGURE 21.	SPECIMEN H-27, GAGE FACTOR, 1144°K (1600°F)	65
FIGURE 22.	SPECIMEN H-27, GAGE FACTOR, RT, CYCLES 1,2,3	66
FIGURE 23.	SPECIMEN H-27, GAGE FACTOR, 644°K (700°F), CYCLES 1,2,3	67
FIGURE 24.	SPECIMEN H-27, GAGE FACTOR, 1033°K (1400°F), CYCLES 1,2,3	68

LIST OF FIGURES
Continued

		Page
FIGURE 25.	SPECIMEN H-27, GAGE FACTOR, 1144°K (1600°F), CYCLES 1,2,3	69
FIGURE 26.	SPECIMEN H-27A, GAGE FACTOR, RT	70
FIGURE 27.	SPECIMEN H-27A, GAGE FACTOR, 700°K (800°F)	71
FIGURE 28.	SPECIMEN H-27A, GAGE FACTOR, 1144°K (1600°F)	72
FIGURE 29.	SPECIMEN H-21, APPARENT STRAIN TO 922°K (1200°F)	73
FIGURE 30.	SPECIMEN H-21, APPARENT STRAIN TO 978°K (1300°F)	74
FIGURE 31.	SPECIMEN H-21, APPARENT STRAIN TO 1033°K (1400°F)	75
FIGURE 32.	SPECIMEN H-22, APPARENT STRAIN TO 1033°K (1400°F)	76
FIGURE 33.	SPECIMEN H-23, APPARENT STRAIN TO 978°K (1300°F), CHROMEL A LEADS	77
FIGURE 34.	SPECIMEN H-23, APPARENT STRAIN TO 1033°K (1400°F), CHROMEL A LEADS	78
FIGURE 35.	SPECIMEN H-23, APPARENT STRAIN TO 1085°K (1500°F), CHROMEL A AND HOSKINS 875 LEADS	79
FIGURE 36.	SPECIMEN H-23, APPARENT STRAIN TO 1198°K (1700°F), CHROMEL A LEADS	80
FIGURE 37.	SPECIMEN H-26, APPARENT STRAIN TO 1144°K (1600°F), CHROMEL A LEADS	81
FIGURE 38.	SPECIMEN H-26, APPARENT STRAIN TO 1144°K (1600°F), HOSKINS 875 LEADS	82
FIGURE 39.	SPECIMEN H-27, APPARENT STRAIN TO 1144°K (1600°F)	83
FIGURE 40.	SPECIMEN H-27A, APPARENT STRAIN TO 1144°K (1600°F)	84
FIGURE 41.	SPECIMENS H-25, H-26, APPARENT STRAIN TO 1085°K (1500°F)	85
FIGURE 42.	SPECIMENS H-23, H-24, H-26, APPARENT STRAINS, CHROMEL A LEADS	86
FIGURE 43.	SPECIMENS H-26, H-27, H-27A, APPARENT STRAINS, HOSKINS 875 LEADS	87
FIGURE 44.	SPECIMENS H-22, H-23, H-24, INITIAL DRIFTS AT VARYING TEMPERATURES, CHROMEL A LEADS	88

LIST OF FIGURES
Continued

		Page
FIGURE 45.	SPECIMENS H-22, H-23, H-25, H-26, INITIAL DRIFTS AT VARYING TEMPERATURES, CHROMEL A LEADS	89
FIGURE 46.	SPECIMENS H-25, H-26, INITIAL DRIFTS AT 1200°K (1700°F) . .	90
FIGURE 47.	SPECIMEN H-26, INITIAL DRIFT AT 1269°K (1825°F)	91
FIGURE 48.	SPECIMENS H-25, H-26, H-27, INITIAL DRIFTS AT VARYING TEMPERATURES, HOSKINS 875 LEADS	92
FIGURE 49.	SPECIMENS H-27, H-27A, INITIAL DRIFTS AT 1158°K (1625°F) .	93
FIGURE 50.	SPECIMEN H-21, DRIFT AT 922°K (1200°F)	94
FIGURE 51.	SPECIMEN H-21, DRIFT AT 1033°K (1400°F)	95
FIGURE 52.	SPECIMEN H-23, DRIFT AT 978°K (1300°F) AND 1033°K (1400°F)	96
FIGURE 53.	SPECIMEN H-26, DRIFT AT 1089°K (1525°F) AND 1144°K (1600°F), CHROMEL A LEADS	97
FIGURE 54.	SPECIMEN H-26, DRIFT AT 1144°K (1600°F), CHROMEL A AND HOSKINS 875 LEADS	98
FIGURE 55.	SPECIMEN H-27, DRIFT AT 1033°K (1400°F) AND 1144°K (1600°F)	99
FIGURE 56.	SPECIMENS H-21, H-26, H-27, DRIFTS AT VARIOUS TEMPERATURES	100
FIGURE 57.	SPECIMENS H-23, H-26, DRIFTS AT 978°K (1300°F) AND 1089°K (1500°F), CHROMEL A LEADS	101
FIGURE 58.	SPECIMEN H-26, H-27, H-27A, DRIFTS AT 1089°K (1500°F), 1033°K (1400°F), HOSKINS LEADS	102
FIGURE 59.	GAGE FACTOR VS TEMPERATURE	103

DEVELOPMENT OF HIGH TEMPERATURE STRAIN GAGES

by

M. M. Lemcoe
Battelle Columbus Laboratories

SUMMARY

It was the overall objective of this program to develop and evaluate high temperature electric resistance strain gages for possible use for 1 hour up to 1033°K (1400°F) or 1/2 hour up to 1477°K (2200°F), utilizing a special high temperature strain gage alloy (Fe-25Cr-7.5Al) designated BCL-3, which was developed at the Battelle Columbus Laboratories for the U. S. Atomic Energy Commission.

Since the principal temperature range of interest to NASA is above 922°K (1200°F), the main effort in this program was directed to obtaining performance data above that temperature, utilizing evaluation procedures to determine pertinent gage characteristics such as gage factor vs. temperature, apparent strain vs. temperature, no-load drift, zero-shift, gage to gage and cycle to cycle uniformity, and resistance to ground vs. temperature characteristics.

The evaluation was performed by evaluating or partially evaluating a total of 34 wire wound gages, which were bonded to tapered cantilever calibration bars with high purity alumina applied by means of the flame-spray process. The specimens were machined from cobalt-base plate material. The gages are of the free-filament type and have a nominal gage length of approximately 2 cm (0.8 in.) and a nominal room temperature resistance of 70 ohms. They were fabricated from 2 mil diameter, BCL-3 alloy wire.

This report contains the pertinent results obtained during the evaluation, as well as a detailed description of the gage winding fixture and fabrication procedures used. The results are presented in both graphical and tabular form.

On the basis of the results obtained from the evaluation, it is concluded that the prototype gages should perform satisfactorily at temperatures up to 1089°K (1500°F) for periods of at least one hour. Above that temperature the overall performance of the gage appears limited, because of uncertainties associated with prediction of the apparent strain characteristics. Means of eliminating this uncertainty and extending the maximum operating temperature of the gage beyond 1089°K (1500°F) are discussed in the report.

INTRODUCTION

To obtain reliable data on magnitudes of the stresses (or strains) imposed on space shuttle vehicles or hypersonic aircraft during flight, and to provide a check on the validity of existing analytical methods for predicting these stresses, electric resistance strain gages with higher operating temperatures (1400 to 2200°F max.) will be required.

Further, monitoring of the strains during each flight should lead to a better understanding of the cyclic or cumulative effects of the reentry environment upon reuseable space vehicle structures such as heat shields vehicle experience cumulative creep deformation.

Unfortunately, there are no commercially available electric resistance strain gages that are reliable enough for consideration in the 1400°F to 2200°F maximum operating temperatures, above mentioned. In fact, there are no commercially available electric resistance strain gages that are reliable for static applications much above 950°F. For this reason, the Atomic Energy Commission through its Liquid Metal Engineering Center sponsored a program at Battelle for the development of strain gages capable of operating at 1200°F for periods of time up to 1000 hours. In attempting to achieve this objective, it was necessary to develop special high temperature strain gage alloys of high purity and uniformity (freedom from defects). One of these alloys, BCL-3 (Fe-25Cr-7.5Al), showed the most promise of meeting the 1200°F/1000 hr requirement.

Based on the data obtained in the AEC program, at maximum temperatures up to 1200°F, there was reason to believe that it should be possible to develop strain gages from BCL-3 alloy with a maximum operating temperature greater than 1200°F, but for much shorter periods of time (1/2 to 1 hour instead of 1000 hours).

This report contains information relating to the development and evaluation of wire gages fabricated from the above-mentioned BCL-3 alloy. Included in the report is a detailed description of gage fabrication and evaluation procedures, and gage performance data (gage factor, apparent strain, drift, etc.) up to 1800°F.

OBJECTIVES

It was an overall objective of this program to develop and evaluate high temperature electric resistance strain gages for possible use up to 1 hour up to 1400°F or 1/2 hour up to 2200°F, utilizing special strain gage alloys, including BCL-3 alloy (Fe-25Cr-7.5Al), which were developed at Battelle for the Atomic Energy Commission.

Since the principal temperature range of primary interest to NASA is above 1200°F, effort was directed to obtaining performance data at temperatures

above 1200°F utilizing evaluation procedures to determine pertinent gage characteristics, such as apparent strain, gage factor vs. temperature, no-load drift, mechanical hysteresis (zero-shift), gage resistance to ground, linearity, maximum useable strain, and gage to gage uniformity.

EXPERIMENTAL EVALUATION AND RESULTS

1. Gage Fabrication and Specimen Preparation

1.1 General

During the course of this program, 8 specimens were prepared for various kinds of evaluations. These specimens were given designations H-21 through H-27 and H-27A. The gages on Specimens H-21 and H-22 were fabricated from 1 mil diameter wire, and have a nominal gage length of 0.8 inch and nominal gage resistance of 240 ohms. The gages on all other specimens were fabricated from 2 mil diameter wire, and also have a gage length of 0.8 inch, and a nominal resistance of 70 ohms.

1.2 Materials

1.2.1 Gage

All gages evaluated in this program were made of a special high temperature electric resistance strain gage wire. The alloy, designated BCL-3, having a composition Fe-25Cr-7.5Al, was one of several alloys developed at Battelle for high temperature strain gages. It was selected because of its relatively good oxidation resistance, excellent ductility, and relatively low apparent strain. One other alloy, BCL-5, having a composition Fe-12Cr-10Al, was also considered during the preliminary screening because of its good ductility, but was eliminated during the preliminary screening because of its relatively high oxidation rate and steepness of the apparent strain curve at the high temperature end of the curve.

Figure 1 shows the microstructures of BCL-3 alloy in the as-drawn and process annealed conditions. The cleanliness and fine grain structure of the annealing can be clearly seen.

The BCL-3 alloy was processed and drawn into wire of various sizes, including 1 and 2 mil diameter wire.

To enhance the resistance to oxidation, in use, the wire was pre-oxidized in air at 1600°F for approximately 10 minutes. The result of this treatment in the formation of a Al_2O_3 coating on the surface of the wire vehicle inhibits further oxidation.

The lead tab ribbons were made from 1/32 x 0.002 inch Nichrome V ribbon. The perforated gage carrier was made from teflon impregnated glass fiber tape. The gage backing was made from 1/32 inch thick teflon sheet. See Appendix A for additional information.

1.2.2 Specimen

The specimens were machined from Haynes 25 plate, which was aged at 1850°F for one hour. The mechanical and chemical properties are summarized in Table 1. It should be noted that the room temperature mechanical properties and chemical composition were obtained from the mill report, and that the elevated temperature properties were taken from the manufacturer's literature for sheet material, in the absence of any other elevated temperature information.

1.2.3 Lead-Wire Systems

Table 2 describes the materials used for the various types of lead wire systems.

1.3 Gage Fabrication

1.3.1 Gage Winding Fixture

The gages evaluated in this program were produced with a fixture which was designed and fabricated at Battelle for an earlier high temperature strain gage program. Special features incorporated in the design of the fixture include the capability for welding the lead tab ribbons to the gage filament, without having to remove the gage from the fixture for welding or other reasons (insuring precise control of gage resistance and constant wire tension), recessing pins, variable gage length, and precise pre-stressing of the gage filament, after winding, to maintain filament straightness.

Photographs and a detailed description of the fixture are contained in Appendix A.

1.3.2 Gage Geometry and Fabrication Procedures

The gage geometry for the 240 ohm and 70 ohm gages is shown in Figure 2. Procedures for fabricating the gages, with the fixture mentioned in 1.3.1, are also described in detail in Appendix A.

1.4 Specimen Preparation

1.4.1 Specimen Geometry and Gage Locations

The specimens were prepared from Haynes 25 plate, having the properties mentioned in 1.2.2. The geometry of the specimens and typical gage locations are shown in Figure 3. It should be noted that the holes at the shank end of the specimen are for four Inconel clamping bolts and the Inconel pin for precise positioning, which is installed prior to insertion of the bolts and removed after tightening of the bolts.

1.4.2 Gage Attachment Procedures

Gages were bonded to the Haynes 25 calibration bar by means of the flame-spray process, using high purity aluminum oxide rod. For a detailed description of the procedures, refer to Appendix B. Figure 4 is a photograph (enlarged 3X) of a typical BCL-3 strain gage installation on a specimen in position in the evaluation fixture. Also shown in the photograph are details relating to attachment of the lead wires to the lead tab ribbons, lead wire dress, thermocouple location, and dress of the thermocouple leads.

Initially, the Al_2O_3 substrate thickness was 3 mils. This thickness proved to be satisfactory up to 1500°F at which temperature erratic behavior of the gages was observed. Inspection revealed partial separation of the substrate from the calibration bar due to oxidation at the interface resulting from permeation of air through the relatively porous Al_2O_3. To minimize interface oxidation, the substrate thickness was progressively increased to 5 mils and a somewhat thicker final coating, extending to the edges of the substrate, was used on Specimen H-25 and in all subsequent specimens.

1.4.3 Lead Tabs and Lead Wires

On Specimens H-21, the lead wire was spot-welded directly to the gage lead tab ribbons. For gages with 13 ga. Chromel A lead wire, it was necessary to provide a transition section between the 0.002 x 1/32 in. lead tab ribbon and the much larger lead wire. This was accomplished with the use of an intermediate Nichrome V 0.005 in. x 1/8 in. ribbon. For gages with 20 ga. lead wire, use of the intermediate Nichrome V ribbon was found unnecessary. Flexibility loops were provided for all leads to minimize stressing of the joints or lead tabs caused by mechanical or thermal deformations. The 13 gage rather than 20 gage Chromel A wire was used because of its lower temperature coefficient of resistivity and ready availability.

Flexible high temperature quartz fiber sleeving or alumina beads were used at all locations such as bends, etc., where use of rigid aluminum oxide tubing was not possible. The high temperature quartz fiber sleeving was also used to insulate the wires for a short distance outside of the furnace, where

the temperatures were still too high for the PVC room temperature lead wire which was spliced to the high temperature lead wire approximately one foot from the furnace end.

Where an intermediate ribbon was used, the joint between the lead tab ribbon and the intermediate ribbon was made by resistance spot-welding.

For more detailed information relating to joining or other fabrication aspects of the lead tabs and lead wires, refer to Appendix B.

1.5 Specimen Storage

To minimize the deleterious effects of humidity and oxidation, all specimens not in test were stored in an inert atmosphere (argon) can containing desiccant.

2. Description of Gage Evaluation Facilities

2.1 High Temperature Gage Evaluation Fixture

With the exception of Specimen H-21, all specimens were evaluated in a special fixture designed and fabricated at Battelle. Figure 5 is a photograph of the fixture, without the tubular 3-zone resistance furnace in place. The furnace, of conventional design, is 24 inches long with a 3-1/2 inch bore, and is capable of continuous operation up to at least 2200°F. In use the furnace surrounds the specimen, truss structure, and box beam.

The fixture basically consists of an exterior carbon steel support frame mounted on legs with leveling screws, the cantilever box beam assembly, deflection gage support structure, deflection gages, and loading mandrels.

The exterior box frame was designed to resist the mandrel loads and moment induced at the root end of the box beam, with a minimum amount of deflection in the frame.

The box beam which was fabricated as a weldment from Inconel 600 was heavily reinforced with an interior web plate to provide additional stiffness. The outer dimensions of the box were the maximum permissible in terms of the furnace bore. The box beam was clamped to the support structure by means of 6 Inconel bolts, four of which go through the specimen shank. To minimize the flow of heat from the box beam into the cooler support structure, rigid Al_2O_3 thermal insulation spacer blocks were used between the support structure and the side faces of the box beam. A thermal insulating block was also provided on the underside of the box beam to thermally isolate it from the support structure.

The deflection gages were protected from the heat by thermally isolating the deflection gage yoke from the deflection gage support truss.

Further protection of the gages and external lead wire was provided by plugging the furnace ends with insulation.

The deflection gage truss, fabricated from Inconel X-750 was welded to the end of the box beam. Consequently, the deflections measured by the dial gages represent the relative deflection on the beam at the point of contact with the dial gage with respect to the shank of the specimen. The deflection measurement is therefore independent of the deflection of the box beam itself, which is relatively small.

With loading mandrels on each side of the specimen, it is possible to subject a gage to reverse strain cycles, i.e., $0, +\varepsilon, 0, -\varepsilon, 0$, or the opposite sequence, $0, -\varepsilon, 0, +\varepsilon, 0$, without removing and repositioning the specimen.

The fixture was calibrated by accurately measuring the dial deflection vs. specimen strain relations over the full deflection ranges with a specimen instrumented with 4 room temperature foil gages of known gage factor. It should be noted, at the higher temperatures, it was necessary to position the specimen closer to the center of the furnace, to insure uniformity of temperature along the length of the specimen. This required the use of a longer extension than the one shown in Figure 5. Consequently, it was necessary to perform two fixture calibrations, i.e., one with the short extension on the fixture and one with the long extension on the fixture.

The calibrations were found to be quite linear over the full ranges, and linear best-fit lines through the data points resulted in the following equations for use at all temperatures, since calibration is independent of the specimen stiffness or mandrel load.

With short extension: (Specimens H-21 through H-24) $\varepsilon_T = 2.209\ \Delta$

With long extension: (Specimens H-25 through H-27A) $\varepsilon_T = 1.045\ \Delta$

where,

Δ = dial gage deflection, mils

ε_T = strain on surface of specimen at gage location, $\mu\varepsilon$.

In the actual calibration of the gages, it was than merely necessary to deflect the cantilever specimen by means of the loading mandrel until the required strain was induced at the gage location.

2.2 Temperature Control System

The temperature control system consisted of a solid-state temperature programmer and temperature controller, and a solid-state SCR power controller. Figure 6 is a block diagram of the system.

Specimen temperature was monitored by means of Type K or Type S thermocouples, depending upon the temperatures involved. For tests up to 1400°F, Type K thermocouples were used. For tests above that temperature, Type S (Pt/Pt - 10% Rh) thermocouples were used. The thermocouples were attached to the specimen midway between each gage, with one thermocouple so located on each face of the specimen.

The temperature programmer expedited evaluation of the gage apparent strain characteristics. The predetermined temperature-time history for each test series was drawn on the electrically conducting program chart with a stylus. The temperature control system then imposed this temperature-time history on the specimen with a minimum amount of temperature deviation or over-shoot during heating. It also should be pointed out that the temperature controller incorporated circuitry to provide proportional band, rate time, and reset action, which also minimized temperature over-shoot during heating.

2.3 Cooling System

To expedite evaluation, a simple forced convection air cooling system was later incorporated into the fixture design. It was found that, because of the large thermal inertia of the fixture and furnace, a considerable amount of time was consumed during furnace cool-down. By symmetrically directing a gentle flow of air through the furnace, after the specimen had cooled to a certain point, it was possible to substantially reduce the time to cool to room temperature. Readings, of course, were not taken during this period (nor at any other time) until isothermal conditions existed.

An additional filter was installed in the supply air line to prevent possible contamination of the specimen or furnace with any traces of moisture, oil, or other contaminants that were not filtered out by the main line filter.

2.4 Instrumentation for Strain, Temperature, Resistance, and Deflection Measurement

A conventional strain indicator and 10 channel switch and balance unit were used to measure gage output, in a 1/4 bridge hook-up, with a 3-lead wire system to minimize lead wire errors. A precision decade box was used in the dummy leg of the bridge, and in series with the active gage when required.

Temperatures were determined with a millivolt potentiometer, whose reference junction temperature was measured by means of a precision laboratory thermometer. Resistance and resistance to ground measurements were made with a vacuum tube voltmeter.

Specimen deflection was measured by means of 0 to 2 in mechanical dial gages, having a least count of 0.0254 mm (0.001 inch).

All instruments were calibrated with standards traceable to the National Bureau of Standards.

3. Gage Evaluation

3.1 Approach

Since no previous information was available on the performance of BCL-3 gages above 1200°F, an exploratory gage evaluation procedure was established which, although not comprehensive in every respect, would provide indications of the performance of these gages to the maximum temperature possible, above 1200°F.

It was originally proposed to begin the study at 1200°F and to evaluate the gages every 200°F, above that temperature, to 2200°F, or the maximum temperature possible. However, because of difficulties encountered during early tests, it was found often necessary to go up in 100°F rather than 200°F increments to provide a clearer understanding of the effects of increasing temperature on gage and lead wire behavior.

3.2 Evaluation Procedure

Unless otherwise indicated, the evaluation procedure consisted of performing the following steps at each maximum step temperature level (hereinafter referred to as maximum run temperature), until erratic gage behavior of failure occurred:

(1) Measure and record gage assembly resistance and resistance to ground at room temperature (R.T.) from ends of lead wire, and replace or repair obviously bad gages or joints.

(2) Prestabilize the gages by soaking for 40 hours, unless otherwise indicated, at a temperature 25°F higher than the maximum test temperature (M.T.T.).

(3) Thermally precycle to M.T.T. three times. Record gage output, at R.T. and M.T.T. only, and resistance to ground.

(4) Hold at M.T.T. for 3/4 hour, and then precycle, mechanically, three times to 1000 microstrain ($\mu\epsilon$) and record gage output at zero and maximum deflection, and resistance to ground.

(5) Hold at M.T.T. for 3/4 hour, and then determine gage factor, zero shift, and linearity characteristics, by going up at least four deflection steps to 1000 $\mu\epsilon$. Record gage output at each step going up, and at each return step to R.T. Repeat procedure two more times. Repeat entire procedure at temperature equal to 1/2 M.T.T. and at R.T.

(6) Determine apparent strain vs. temperature characteristics from R.T. to M.T.T. and at each return step to R.T., at least every 250°F. Hold gage at each temperature level for 3/4 hour to

insure achievement of isothermal conditions. Record gage output at each temperature. Repeat procedure two more times. Record zero-shifts at end of each cycle.

(7) Bring specimen to M.T.T. and record gage output, periodically, for a period of about 12 hours, to permit determination of drift characteristics as a function of time at temperature.

3.3 Test Matrix

Table 3 summarizes the number of steps in the above-mentioned evaluation procedure to which each of the specimens was subjected to for each run. It should be noted that steps 4 and 5 for the 1300°F and 1400°F runs for Specimen H-22 were omitted, since the primary purpose of performing measurements on this specimen was to determine the apparent strain and drift characteristics of 1 mil dia. BCL-3 gages used in conjunction with Chromel A lead wire. Having established the feasibility of using the Chromel A lead wire on the basis of the results for the 1300°F and 1400°F runs, an attempt was made to do a complete evaluation at 1500°F. However, failure occurred during step 3, and the test was therefore terminated. (See Section 4 for details relating to failures.)

Steps 4 and 5 were also omitted on Specimen H-25, since the primary purpose of the measurements on this specimen was to obtain data on the apparent strain and drift characteristics of 2 mil dia. BCL-3 gages used in conjunction with the Hoskins Alloy 875 lead wire.

4. Results

4.1 General

The results from the data obtained from evaluation of the gages on Specimens H-21 through H-27 and H-27A have been analyzed in terms of the following gage characteristics:

(a) gage factor and linearity

(b) apparent strain

(c) drift (during and after prestabilization)

(d) zero shift

(e) resistance to ground

(f) performance history.

Unless stated otherwise the above characteristics were obtained for a gage factor setting of 2.05.

4.2 Gage Factor and Linearity Characteristics

Figures 7 through 28 are plots showing gage factor and linearity characteristics at selected test temperatures for Specimens H-21, H-23, H-26, H-27, and H-27A. Included on these plots are the zero shifts after return to "zero", as well as the data points for each strain level. The zero shift data points are represented by solid (filled-in) symbols. Unless otherwise indicated, the plots were constructed by passing a best-fit straight line through the data points. The deviation of individual data points from the straight line serves as an indication of the linearity of the strain response.

The gage factor, GF, was obtained from the slopes of the lines in the above-mentioned figures by means of the following equation:

$$GF = \frac{\epsilon_M}{\epsilon_T} \text{ (GFS)}$$

where

GFS = gage factor setting

ϵ_M = measured strain at given deflection, $\mu\epsilon$

ϵ_T = true strain on surface of specimen at given deflection, $\mu\epsilon$.

The relations between ϵ_T and Δ, established by calibration of the fixture with gages of known gage factor are given on Page 38. Using these relations gage factor may then be expressed directly in terms of Δ as follows:

$$GF = \left(\frac{\epsilon_M}{\Delta}\right) \times \frac{GFS}{2.209} \quad , \quad \text{with short extension, (Specimens H-21 through H-24)}$$

$$GF = \left(\frac{\epsilon_M}{\Delta}\right) \times \frac{GFS}{1.045} \quad , \quad \text{with long extension, (Specimens H-25 through H-27A)}$$

It should be noted that ϵ_M/Δ represents the line slopes in the gage factor plots and that GFS = 2.05 unless otherwise stated.

The above relations were used in computing the gage factors for all gages summarized in Table 10 on Page 38 except for the 600°F and 1200°F gage factors for H-21, whose values were obtained in another fixture. A sufficient number of data points were not taken in that fixture to warrant plotting curves.

4.3 Apparent Strain

Figures 29 through 43 are plots of apparent strain vs. temperature over the range in temperatures investigated in this program. For ease of comparison, curves have been grouped together, whenever similarity permitted doing so. The data were first divided into "first run" and non-first run data. "First run" data are defined here as data from a specimen that had not previously been evaluated at a lower elevated temperature. For example, the 1300°F apparent strain data for Specimen H-23 are "first run" data, since 1300°F was the first elevated run for this specimen. However, the 1400°F data for this specimen are not "first run" data since the specimen had previously been evaluated at the next lower maximum test temperature (M.T.T.) of 1300°F. Without this separation of the data, it would be difficult to assess the uniformity of apparent strain characteristics from cycle to cycle, since prior thermal history at temperature can alter the apparent strain characteristics.

The data were next divided into additional groups to take into account possible differences in gage characteristics due to the three different lead wire systems (copper, Chromel A, and Hoskins Alloy 875) that were used during the program. The apparent strain curves shown on each figure were grouped together, unless otherwise indicated, in accordance with this separation of the data into the three mutually exclusive groups. This permits a more meaningful comparison of gage to gage variations, or differences in apparent strain from run to run at different M.T.T.'s. In those instances where it was not feasible to group an apparent strain cycle or a set of apparent strain cycles with other gages, the cycle or set was plotted on a separate figure. Zero-shift data points after return to zero are represented by solid (filled-in) symbols.

Tables 4 through 8 tabulate apparent strain data for gages on Specimens H-21, H-23, H-26, and H-27 for M.T.T.'s of 922°K (1200°F), 978°K (1300°F), 1033°K (1400°F), 1089°K (1500°F), and 1144°K (1600°F). These data permit ready assessment of the uniformity of apparent strain from gage to gage.

4.4 Drift Characteristics

Figures 44 through 49 are plots of initial drift vs. time (Step 2) at the various M.T.T.'s. Information on the drift occurring during prestabilization (defined herein as initial drift) is presented, since information of this kind may be valuable in assessing the feasibility of getting "first-time" data in those instances where prestabilization of the gages is not possible, or feasible. Figures 50 through 58 are plots of drift vs. time (Step 7).

The data have been separated into groups similar to those for the apparent strain data, to permit a more meaningful and easier comparison. The instantaneous or average drift rate may readily be obtained from these curves.

4.5 Resistance to Ground

Appendix C summarizes in tabular form the resistance to ground measurements taken at various times during the evaluation.

4.6 Performance History

Table 9 summarizes the performance history of the gages and overall specimen/lead wire assembly performance. The word "failure" with respect to gage performance is defined as a gage condition in which the gage opens, or exhibits erratic behavior, not attributed to substrate separation or lead wire failure. Failure with respect to the specimen/lead wire assembly is defined as gross failure such as deterioration of lead wire insulation, partial or complete substrate separation, or joint failure at lead wire to lead tab ribbon caused by thermal movement of the lead wire.

5. Discussion of Results

5.1 General

The developmental work and evaluations relating to the gages on Specimens H-21 through H-25 were exploratory in nature. It was the primary purpose of those evaluations to determine whether 1 mil or 2 mil dia. BCL-3 wire should be used for the prototype gages, what type of lead wire system should be used above 1200°F, what type of transition section between the lead wire tab and the heavier lead wire should be used to accommodate the large thermal expansions that occurred during evaluation at the higher temperatures, and how thick a substrate would be required to prevent excessive oxidation of the metal at the interface between the substrate and the specimen.

Having determined the answers to the above questions, it was then possible, as evident from the performance results presented in Table 9, to arrive at a prototype gage system which would not exhibit premature failure below 1089°K (1500°F). Gages 2 and 4 on Specimen H-26, and all gages on Specimens H-27 and H-27A have Hoskins Alloy 875 lead wires, 5 mil thick substrates, and 2 mil diameter BCL-3 wire filaments, and they represent the final prototype gage system developed in this program. Being prototype gages they were consequently subjected to a more comprehensive evaluation than the gages on Specimens H-21 through H-25 which were only partially evaluated as a part of the exploratory study. Therefore, in some of the following subsections, only limited, or no discussion is included on the exploratory gages.

5.2 Gage Factor

Table 10 contains the gage factors obtained for the gages on Specimens H-21, H-23, H-26, H-27, and H-27A at temperatures up to 1144°K (1600°F). Table 11 contains gage factor statistics relating to scatter of the gage factor data points shown in Figure 59, which is a plot of the gage factors in Table 10 vs. temperature. The following subsections briefly discuss the gage factor plots from which the gage factor values were obtained, as well as linearity and zero-shift characteristics.

During several of the gage factor runs at temperature, a variation from the set point temperature of at least 5.5°K (10°F) occurred. When the effect of this temperature change was deemed significant, the data points, including the zero-shift points, were corrected on the basis of the incremental change in strain as obtained from the apparent strain curve at the set point temperature.

In reviewing the zero-shift data (return to "zero" points) on the figures in this subsection, it should be borne in mind that these points represent not only the shifts due to hysteresis in the gage, itself, but also the shift due to any difference between the initial gage temperature and the gage temperature upon completion of the cycle. In addition, these zero-shift points include the effects of any permanent set developed during loading of the specimen at the higher deflection levels. In those instances where temperature fluctuations or permanent set occurred, the data were corrected, provided sufficient information was available to make the correction. If sufficient information was not available to make the correction, the zero-shift point was omitted from the figure.

5.2.1 Specimen H-21

Figure 7 is a plot of true strain vs. measured strain at room temperature for 3 consecutive cycles. The data points represent the average of the 6 operating gages on this specimen. It is noted that the plots in tension and compression are quite linear, that in tension, the second and third cycles are virtually identical, whereas in compression the first and second cycles are identical, that there was no zero shift, and that the gage factor in tension is somewhat larger than in compression.

Figure 8 shows the gage to gage variation at 644°K (700°F) for the same gages. It is noted that the plots are quite linear in tension and compression, that there is some variation from gage to gage, that there is a zero shift of about + 90 $\mu\epsilon$, and that the gage factor in tension again is somewhat larger than that in compression.

Figure 9 shows similar behavior at 978°K (1300°F), except that the zero-shift is negative and considerably less.

In Figure 10, which shows results at 1033°K (1400°F), no attempt was made to pair a straight line through the tensile data points, because of their upward deviation from a straight line relationship. The cause of this nonlinearity has not been firmly established. However, it is believed that it may be due to microcracking which causes an increase in gage resistance due to opening of the cracks when in tension. A gradual increase in furnace temperature could also cause the nonlinearity in tension; however, this was ruled out as a possibility since it would have also caused a nonlinearity in the compression gages, which was not the case. The effects of microcracks and subsequent oxidation would, of course, be more pronounced in gages fabricated from one mil dia. wire than two mil dia. wire.

5.2.2 Specimen H-23

Figures 11 through 14 show the gage factor characteristics at R.T., 644°K (700°F) and 1033°K (1400°F). Some initial nonlinearity is observed in the room temperature run in both tension and compression, and in compression for the 644°K run. However, the gage to gage variation is virtually zero. The zero shifts are in general small, and do not exceed 100 με. Again, the gage factors are somewhat larger in tension than compression.

5.2.3 Specimen H-26

Figures 14 through 17 show gage factor characteristics at R.T., 700°K (800°F), 1089°K (1500°F), and 1144°K (1600°F). Excellent linearity is noted. Gage to gage variation in tension is generally smaller than that in compression. Zero-shifts at R.T. are about ± 50 με. For the 1144°K run the average zero shift was -50 με. The maximum zero shift for all runs is -100 με.

Referring to Figures 15 and 16, it is noted that the gage factors in compression are somewhat higher than those in tension for both runs. This is due to small temperature drops (< 10°K) during the measurements period. It is also noted that there is no gage factor plot for Gage No. 1 in Figure 15. The data were not plotted because of unusually high readings.

5.2.4 Specimen H-27

Figures 18 through 21 show gage factor characteristics at R.T., 700°K (800°F), 1033°K (1400°F), and 1144°K (1600°F). It is noted that, with the exception of the 700°K run, the linearity is excellent and the gage to gage variation is small. Small temperature fluctuations were responsible for the scatter in data points at the upper end of the 700°K run. Zero shifts are also small, the maximum one being less than + 70 με. Gage factors in tension and compression are approximately equal.

Figures 22 through 25 show the cycle to cycle variations in terms of true strain vs. measured strain. Each data point represents the average of the gages. It is noted that the linearity is excellent, and that the variation from cycle to cycle is, in general, small. The zero-shifts are also small, except for the 1144°K run, where zero-shifts are about + 55 με, and -68 με. Gage factors in tension are, in general, slightly higher in tension. Also shown on the plots for the 1033°K and 1144°K runs (Figures 24 and 25) are the ± 10% "error" bands, which represent ± 10% deviations from the solid mean value line. It is noted that all points but one fall within these bands.

5.2.5 Specimen H-27A

Figures 26, 27, and 28 show the gage factor characteristics at R.T., 700°K (800°F), and 1144°K (1600°F). It is noted that the linearity is, in

general, excellent, and the gage to gage variation is small, with the exception of the compression gages for the 700°K run. The greater than average scatter here was due to small temperature fluctuations in the furnace. Shown on the plot for the 1144°K run are the ± 10% "error" bands. It is noted that all data points fall well within this band. The reason for the zero-shifts of -160 and -172 for Gages 3 and 4 and no zero-shifts for Gages 1 and 2 during the R.T. run is not clear, particularly since the zero-shifts for the 1144°K (1600°F) run were quite small ($< 50\ \mu\varepsilon$).

5.3 Apparent Strain

5.3.1 General

Figures 29 through 43 are plots of apparent strain vs. temperature for the gages on Specimens H-21, H-22, H-23, H-25, H-26, H-27, and H-27A, for temperatures up to 1198°K (1700°F). Unless otherwise indicated, the data points represent the average apparent strain of all gages on the specimen (generally, 4 gages), for three consecutive cycles from essentially ambient to the maximum test temperature (M.T.T.). On the return cycle, only the "zero"-return point (shaded) is shown on the plot. The second cycle begins at the end of the first cycle and the third cycle begins at the end of the second cycle.

One of the most interesting gage behavioral patterns exhibited in these figures is the tendency of the gages to converge to the same terminal point, cycle after cycle, even though the cycles themselves were by no means identical. It seems that the gage material in effect has a "memory" which causes it to repeatedly exhibit the same apparent strain at its maximum temperature, regardless of cycle to cycle differences in apparent strain at the lower temperatures of the cycle. The significance of this characteristic with respect to acquisition of strain data is discussed in Section 6.

With respect to the return-zero points for each cycle, it should be noted that, while there was an effort to return to the same temperature at the end of each cycle, it was not always possible to do so because of variations in room temperature and the expediency considerations. Consequently, it should be borne in mind that differences in location between the initial point at the start of the test and subsequent return points do not necessarily indicate gage instability. To assess the zero-shift due to gage instability, the apparent strain curve should be extended away from the return-point to the temperature line corresponding to the initial temperature. The gage zero-shift may then be assessed by comparing the location of the "extended" terminal point with that of the initial point. This should be done particularly where there is a difference between initial temperature and return temperature and the curve in that region is steep. For example, in Figure 31, there is a difference of about 20°K (37°F) between the two temperatures. The true zero-shift is not -1000 $\mu\varepsilon$, as might be inferred from casual inspection (if the curve had not been extended), but only -250 $\mu\varepsilon$. In general, the curves in these figures were not extended beyond the data points.

In the following, the apparent strain behavior of each specimen is discussed in terms of the apparent strain plots contained in the above-mentioned figures and the apparent strain data in Tables 4 through 8.

5.3.2 Specimens H-21, H-22, H-23, H-25, H-26, H-27, H-27A

Figures 29, 30, and 31 are apparent strain plots for Specimen H-21 at M.T.T.'s of 922°K (1200°F), 978°K (1300°F), and 1033°K (1400°F), respectively. Referring to Figure 29 it is noted that the cycle to cycle variations and zero-shifts are negligible, and that the apparent strain up to M.T.T. is everywhere negative, the maximum value being -8500 με at 755°K (900°F). Most commercial gages are rated for use at 1200°F and have maximum apparent strains in the neighborhood of 40,000 to 60,000 με.

Referring to Figure 30, one notes a distinct change in the shape of the curve for the 978°K (1300°F) run. Up to about 811°K (1000°F) the curve has the same general shape as the curve for the previous run, but with a slightly reduced maximum strain of about -7500 με instead of -8500 με. However, at 811°K, a reversal begins, then a subsequent peaking occurs, which is followed by a downward turn. It is further noted that the zero-shifts between cycles are -650 με and -400 με.

For the 1033°K (1400°F) run, the downward turn becomes much steeper and, as noted in Figure 31, the maximum strain of -8700 με occurs at M.T.T., rather than at some intermediate temperature. It is also observed that there is virtually no difference between the second and third cycle, except at the M.T.T. The zero-shifts of -250 με and zero are less than those for the previous run.

Figure 32 shows the apparent strain curves to 1033°K (1400°F) for the gages on Specimen H-22. The variations, including zero-shifts, are small and the tendency to converge at M.T.T. is clearly evident. It is also noted that there is no steep down turn in the curve, as exhibited by Specimen H-21 (see Figure 31) after exceeding 1033°K (1200°F). The only basic difference between the gage systems is that Specimen H-22 has the Chromel A leads whereas Specimen H-21 has stainless steel clad copper leads. It is further observed that the maximum apparent strain to 1033°K does not exceed 4400 με, which is low in comparison to that of the other gages.

Figures 33 and 34 show the apparent strain curves to 978°K (1300°F) and 1033°K (1400°F) for the gages on Specimen H-23. It is noted that the shape of the curve has changed again. The maximum apparent strain, -10,250 με now occurs at 672°K (750°F). It is further noted that the curves tend to converge as the M.T.T. is approached. (For differences in the gage construction for this specimen and H-21, refer to Table 3.) It is noted that the zero-shifts between the first and second cycles and second and third cycles are about -800 με and -900 με, respectively, which is significantly larger than observed for most of the other gages.

Figures 35 and 36 are apparent strain plots to 1089°K (1500°F) and 1200°K (1700°F) for Specimen H-25.

Specimen H-25 was prepared primarily for comparison of the apparent strain and drift characteristics of gages with Chromel A and Hoskins Alloy 875 lead wire systems. It is noted in Figure 35 that both lead wire systems have similarly shaped curves, the Chromel A, however, having an apparent strain approximately 29% greater at M.T.T. than the Hoskins lead wire. This was one of the reasons for giving further consideration to using Hoskins instead of Chromel A lead wire. See Figures 37 and 38 for additional information on lead wire characteristics.

Referring to Figure 36, it is noted that there is little scatter or zero-shift from cycle to cycle. The third cycle is not shown because erratic gage behavior occurred prior to the commencement of the third cycle.

Figures 37 and 38 are apparent strain plots to 1144°K (1600°F) for Specimen H-26 with Chromel A and Hoskins 875 lead wires. It is noted that there is virtually no cycle to cycle variation or zero-shift for either lead wire system, that both systems have curves of essentially the same shape, the Chromel A system again having the highest apparent strain. The curves are much straighter than the curves at the lower gage temperatures, and have no abrupt changes in slope. Nevertheless, because of the appreciable apparent strain at M.T.T. (+ 63,500 $\mu\varepsilon$ and + 56,000 $\mu\varepsilon$), the average slope is still appreciable (> 66 $\mu\varepsilon$/°K or 37 $\mu\varepsilon$/°F).

Figure 39 is an apparent strain plot to 1144°K (1600°F) for Specimen H-27, which has Hoskins lead wires. It is noted that up to 811°K (1000°F) there is some variation between Cycle 1 and 2 and virtually no variation between Cycles 2 and 3. Above 811°K, there is virtually no variation from cycle to cycle, all curves characteristically converging to the same terminal point. The maximum zero-shift is about -4500 $\mu\varepsilon$. The curves are similar in shape and magnitude to those for Specimen H-26, shown in Figure 38.

During the apparent strain evaluation of Specimen H-27 at 1144°K (1600°F), it was noted that there appeared to be a "pairing off" of the data points, in spite of the fact that there was excellent repeatability of gage readings from cycle to cycle. For example, at the end of the third apparent strain cycle, Gages 1 and 3 read 44,524 $\mu\varepsilon$ and 43,305 $\mu\varepsilon$, respectively, whereas Gages 2 and 4 read 69,419 $\mu\varepsilon$ and 70,901 $\mu\varepsilon$, respectively. This corresponds to a difference of 26,246 $\mu\varepsilon$ between the two pairs of gages (see Table 8).

Various checks were made in an endeavor to establish why this occurred. A shunt calibration of the system was performed, as well as a complete check of the equipment and temperature distribution in the furnace and on the specimen. Resistance checks across joints at various points in the gage-lead wire systems were also made. It was found that the room temperature resistances of Gages 1 and 3 were 59.43 ohms and 59.87 ohms, respectively, whereas Gages 2 and 4 had resistances of 52.06 ohms and 51.35 ohms, respectively. It is believed that this pairing off of the data points at 1144°K is associated with these differences

in gage resistances. However, it is not known whether the difference is due to resistance differences across the lead tab-gage filament joint, or whether it is due to a metallurgical change in the gage filament, or affected portions of the lead tabs. (It was not feasible to make resistance measurements across the 2 mil dia. filaments embedded in the Rokide.)

It should be mentioned that no such pairing off took place during any of the 1033°K (1400°F) apparent strain runs. Readings for this run, obtained by small extrapolations of the Specimen H-27 data in Table 6, were as follows:

Cycle No.	Apparent Strain, με			
	Gage 1	Gage 2	Gage 3	Gage 4
1	- 4388	- 3902	- 3880	- 3743
2	- 4312	- 3831	- 3838	- 3712
3	- 4335	- 3864	- 3878	- 3756

It is evident that no pairing off took place and that, with the exception of Gage 1, the gage to gage variations are relatively small. The cycle to cycle variations, even for Gage 1, are also small.

A check of the gage readings for the 1144°K (1600°F) apparent strain run on Specimen H-26 revealed no large differences. It will be recalled that this specimen has two gages with Hoskins lead wire. Their apparent strain readings were as follows:

Cycle No.	Apparent Strain, με	
	Gage 2	Gage 4
1	58143	54064
2	57958	53890
3	58017	53928

To provide additional information on the apparent strain behavior at 1144°K, a supplemental evaluation not originally planned was performed at 1144°K (1600°F) on a Specimen H-27A, having Hoskins lead wires. The following apparent strain data were obtained.

Cycle No.	Apparent Strain, με			
	Gage 1	Gage 2	Gage 3	Gage 4
1	43988	34553	36027	45903
2	41737	34264	35738	45333
3	41749	34421	35887	45295

The gage to gage variations appear to be random with no strong indications of pairing off. In any event, if pairs were selected, they would be Gage pairs 2 and 3, and 1 and 4, and not Gage pairs 1 and 3, and 2 and 4. These findings fairly well ruled out the possibility that the pairing off had something to do with the position of the specimen in the furnace, or a peculiarity in the read-out equipment.

Finally, it may be that the pairing off was purely a coincidence and that 1144°K (1600°F) approaches a temperature that no longer permits the present type of joints and/or gage alloy to behave in a precisely predictable manner.

Figure 40 is an apparent strain plot to 1144°K (1600°F) for Specimen H-27A which also has Hoskins lead wires. It is noted that the curves have the same general shape as those for Specimen H-27. However, the magnitudes of the apparent strain are less (+ 40,000 $\mu\epsilon$ vs. + 57,000 $\mu\epsilon$ at M.T.T.). The larger apparent strains for H-27 may be due to the fact that the gages were exposed to a longer time-temperature history than those on H-27A, as evident from Table 3.

It is noted that the variations from cycle to cycle and zero-shifts are similar to those of Specimen H-27.

Figure 41 is an apparent strain plot to 1089°K (1500°F) for Specimens H-25 and H-26. Both specimens have Chromel A lead wires and were subjected to essentially the same history, except for the elimination of Steps 4 and 5 which relate to gage factor (see Table 3). It is noted that the zero-shifts for Specimen H-26 are relatively small in comparison to those for Specimen H-25 (+ 500 $\mu\epsilon$ vs. -2500 $\mu\epsilon$). It is believed that the greater zero-shift is due to the lack of mechanical cycling of the specimen in Steps 4 and 5, and does not necessarily represent gage to gage variations.

Figure 42 is an apparent strain plot for Specimens H-23, H-25, and H-26 for M.T.T.'s of 978°K (1300°F) and 1085°K (1500°F). The plots are for those gages on these specimens having Chromel A lead wires. Figure 43 is a similar plot for Specimens H-26, H-27, and H-27A at M.T.T.'s of 1030°K (1400°F), 1085°K (1500°F), 1140°K (1600°F), for those gages having Hoskins lead wires. The solid lines on these curves represent the mean value lines. It is evident that for both lead wire systems, the curves rotate in counterclockwise direction as the M.T.T. is increased, starting out negative and then becoming positive. It is also observed that the zero-shifts for all gages are small, except for Specimen H-25, which did not have the benefits derived from mechanical cycling during Steps 4 and 5. It is also noted that the cycle to cycle data points tend to converge to the M.T.T., and that the cycle to cycle scatter is less for the gages with the Hoskins lead wire even though the M.T.T.'s are higher.

Tables 4 through 8 represent a portion of the apparent strain data used in plotting the above-mentioned figures, for the range in temperature from 922°K (1200°F) to 1144°K (1600°F). From Table 4 it is evident that at 922°K (1200°F) the gage to gage and cycle to cycle variations and zero-shifts are small. It is further noted that these variations and zero-shifts, except for Specimen H-23, remain relatively small and gradually increase in magnitude. Even at 1089°K (1500°F), the apparent strains do not exceed + 18,084 $\mu\epsilon$, which is considerably

less than that of commercially available gages rated for use up to 922°K (1200°F). However, at 1144°K (1600°F), as evident from Table 8, the apparent strain becomes appreciably larger, as well as the cycle to cycle, gage to gage variations and zero-shifts. Reasons for the large differences in apparent strain values between Gage pairs 1 and 3 and 2 and 4 are discussed on Page 19. It should be noted that, in spite of these larger gage to gage variations, the cycle to cycle variations are remarkably small after about 811°K (1000°F) due to the characteristic convergence of the cycles at the M.T.T.

In assessing the cycle to cycle zero-shifts, meaningful comparisons can be made only by comparisons at the same initial and return temperatures, since relatively small temperature differences (for reasons mentioned in the discussion of the zero-shifts in the apparent strain plots) can significantly affect the magnitude of the zero-shift. For example, for Gage 1 in Table 5, the zero-shift change from + 2044 (at the end of the first cycle) to + 1118 at the end of the second cycle is not truly indicative of the true gage zero-shift, because of the 16°K (30°F) difference in temperature. Meaningful comparisons can readily be made, however, by means of small interpolation or extrapolation of the apparent strain data.

5.4 Drift Characteristics

Figures 44 through 49 are plots of initial drift vs. time (Step 2) of the gages on Specimens H-22 through H-27A at the various M.T.T.'s up to 1269°K (1825°F). Figures 50 through 58 are drift vs. time (Step 7) plots for these same specimens, up to the same M.T.T.

In reviewing these plots, it should be noted that, in some instances, there is a considerable variation in the time intervals between data points. In general, the long time interval between data points was a result of the evaluation extending beyond normal working hours, such as into evenings and weekends. Although this introduced some uncertainty in the precise location of the curve between the widely separated data points, it is believed that sufficient data points have been obtained to characterize the overall drift behavior of these gage systems.

The solid lines in these plots represent a best-fit curve through the data points which, in general, are an average of the gages on that particular specimen. Where the number of data points was insufficient to permit plotting the curve back to the origin, the data points were left unconnected, as was done, for example, with the data points for H-24, Figure 44.

The instantaneous and average drift rates at any temperature, or over a given time interval may be readily obtained from these curves. However, to permit an easy comparison of the drift rates of the various gage systems evaluated at temperatures up to 1269°K (1825°F), the average drift rates over a 10-hour span were computed and summarized in Table 12.

Regarding initial drift rates, it is evident that there is a fair amount of scatter, as is often the case with drift data. However, a general

trend does exist. Because of the data scatter, it appears that there is no significant difference in drift rates between 991°K (1325°F) and 1103°K (1525°F), the values ranging from -27 με/hr. to -40 με/hr. At 1158°K (1625°F) the rate increased to -81 με/hr., and at 1200°K (1700°F), the average drift rate increased to nearly -100 με/hr., and finally at 1269°K (1825°F), the average drift increased to -189 με/hr.

The following average drift rates were obtained by averaging the drift rates (Step 7) for those specimens in Table 12 that were evaluated at the same temperature.

Temperature		Ave. Drift Rate, με/hr.
°K	°F	
922	1200	< -1
978	1300	-14
1033	1400	-16
1089	1500	-26
1144	1600	-97

It is evident that there is a gradual increase in drift rate with increasing temperature, the maximum value being -97 με/hr. at 1144°K (1600°F). These values, as would be expected, are substantially less than the initial drift rates (Step 2), because of the stabilizing effects of the prior thermal history.

5.5 Resistance to Ground

Tables 1 through 7 of Appendix C summarize the resistance to ground values obtained with a VTVM for each specimen. The gage substrate thickness is indicated in the table heading.

Inspection of the numerous individual values of resistance to ground shows sizeable variations, making it difficult to establish trends or establish correlations between substrate thickness and resistance to ground as a function of temperature. To facilitate correlation, these data have been regrouped in Table 13 into a different format. Minimum and maximum values of resistance to ground are presented in terms of substrate thickness, temperature, and step number. It should be noted that resistance to ground performance is affected by the time-temperature history imposed on the gage after the thermal prestabilization in Step 2. Account of this fact was taken by dividing the resistance data into two basic categories, namely, Step 2 data and Steps 3, 4, 5, 6, and 7 data. No further separation was attempted. If more detailed information on the effect of step number on resistance to ground values is required, such information can be obtained directly from Appendix C.

The effect of increasing substrate thickness is immediately evident from Table 13. For example, increasing the substrate thickness from 4 to 4-1/2 to 5 mils resulted in increasing the resistance to ground value at 1033°K (1400°F) from 5 to 9 to 12 megohms. Likewise, increasing the substrate thickness from 3 to 4 to 4-1/2 mils increased the resistance to ground values from 1 to 4.4 to 11.5 megohms at 1033°K (1400°F).

At 1144°K (1600°F), it appears that a 5 mil thick substrate is quite adequate, since the minimum resistance to ground for the Steps 3 through 7 grouping was 12 megohms, and the maximum value 45 megohms. It is also interesting to note that even at 1255°K (1800°F), the minimum resistance was 2.2 megohms and the maximum value 5.8 megohms.

Finally, it should be mentioned that inconsistently low resistance to ground values may be a result of low resistance to ground values for the lead-wire system, itself, rather than the substrate.

5.6 Performance History

Because of lead wire and substrate failures, none of the gages on exploratory Specimens H-21 through H-24 could be evaluated above 1089°K (1500°F). After minimizing failures from these two causes, it was possible to fabricate and evaluate gage systems through all 7 steps by the evaluation procedure without premature failures.

As noted in Tables 3 and 9, it was possible to perform complete evaluations on Specimens H-26, H-27, and H-27A through all 7 steps in the evaluation procedure, without failure, up to 1144°K (1600°F), and partial evaluations to 1255°K (1800°F), before bond failures occurred.

Regarding gage factor performance, it is evident, from Figure 59 and Table 11, that the gages perform in a predictable manner up to 1144°K (1600°F), with maximum deviations from the average value not exceeding 7.63% over the entire temperature range. The average gage factors of 2.62 at room temperature and 1.92 at 1144°K (1600°F) are considered quite satisfactory in terms of sensitivity.

Regarding apparent strain, the performance, in general, is found to be satisfactory up to at least 1089°K (1500°F). However, at 1144°K, as mentioned in Section 5.3.2, the apparent strain on two of the four gages on Specimen H-27 became appreciable (~ 70,000 $\mu\varepsilon$). This large a value was in contrast to average values of about 44,000 $\mu\varepsilon$ for the remaining two gages on that specimen, and an average value of about 40,000 $\mu\varepsilon$ for the gages on Specimen H-27A. The value of 70,000 $\mu\varepsilon$ is also larger than the 63,000 $\mu\varepsilon$ experienced by the gages on Specimen H-26.

Since considerable care was exercised in preparing the alloy and subsequent processing of the wire to insure high purity, uniformity, and freedom from defects, it is believed that the appreciably larger value of 70,000 $\mu\varepsilon$

and perhaps the value of 63,000 με, may be a result of resistance instabilities in the gage filament to lead tab joints. Only by detailed post-mortem analyses of these joints and/or evaluation of a larger number of gage samples, however, can statistically sound conclusions be arrived at regarding the apparent strain performance of this gage system at 1144°K (1600°F).

Regarding drift, the performance was at least equal to or exceeded that generally specified for commercial high temperature electric resistance strain gages. At 922°K (1200°F), the average drift rate was less than -1 με/hr. over a 10-hour period, with correspondingly increasing values to -97 με/hr. at 1144°K (1600°F).

The drift rate of -97 με/hr. is an average of the specimen drift rates which includes Gages 2 and 4 on Specimen H-27. The drift rates of -220 με/hr. and -220 με/hr. are for these two gages and they are more than four times as large as the drift rates for the other two gages (Gages 1 and 3) on Specimen H-27. It is interesting to note that Gages 2 and 4 were also the gage pair that gave the very high apparent strain readings of about 70,000 με at 1144°K (1600°F). Whether this significantly higher drift rate was caused by the same factors (such as joint resistivity or metallurgical changes in the alloy) that may have been responsible for the high apparent strain is a moot question.

Regarding resistance to ground performance, it is evident from Table 13 (and prior substrate failure history) that a substrate thickness of 5 mils is required to insure adequate resistance to ground. In view of the excellent resistance to ground of 2.2 to 5.8 megohms at 1225°K (1800°F), it is believed that the 5 mil substrate will permit utilizing the full potential of the BCL-3 alloy. However, even with a 5 mil substrate, high quality 3-conductor, moisture-free MgO insulated lead wire with a stainless steel or Inconel sheath and sealed ends will be required to maintain a high resistance to ground.

6. Conclusions

Based on the information obtained in this study, it appears that satisfactory performance up to about 1089°K (1500°F) for at least one hour may be expected from the prototype gage developed in this program. Because of the "pairing off" of apparent strain data points during the 1144°K (1600°F) run for Specimen H-27, there is some question of the predictability of the apparent strain data obtained at that temperature or, more precisely, at any temperature above 1089°K (1500°F). Nevertheless, since the large apparent strain difference (26,246 με) that occurred for the paired-off data points did not occur on other specimens evaluated at 1144°K (1600°F), there is a possibility that the difficulty may be associated with the gage filament to lead tab joints rather than metallurgical changes in the gage alloy. Post-mortem examination of the joints on Specimen H-27 and evaluation of a larger number of gage samples should pin-point whether the joints are responsible for the difficulty. If it should turn out to be a joint problem, then it may be possible to improve the joint design and extend the operating temperature of the gage to a temperature as high as

1477°K (2200°F) for periods of time up to 1/2 hr. On the other hand, if it should turn out that the difficulty stems from metallurgical changes in the gage alloy due to differential oxidation effects, then additional protection of the gage filament against oxidation may then make it possible to extend the operating temperature to as high as 1477°K (2200°F).

Based on the gage factor and drift data obtained during this study there appears to be no limitation of extending the gage maximum operating temperature to 1144°K (1600°F), or an even higher temperature. The present limitation on maximum operating temperatures of 1089°K (1500°F) for the prototype gage is therefore one dictated by the large magnitude and apparent lack of predictability of the apparent strain above that temperature.

Nevertheless, because of the characteristic tendency of the apparent strain cycles to characteristically converge to the maximum test temperature, it should be possible to correct the strain data obtained during test for apparent strain to a higher degree of accuracy than otherwise would be possible. For example, referring to Figures 32, 33, 36, and 37, it is observed that above 811°K (1000°F) the apparent strain cycles converge to the degree that the cycle to cycle variations due to zero-shift or other causes are essentially eliminated. This means that if one can establish the apparent strain vs. temperature curve for each gage (within prescribed limits of accuracy) by means of statistical sampling of other gages, or by individual precalibration of the gage in a furnace (gages bonded to a coupon or shim), it should then be possible to correct the test data to a relatively high degree of accuracy, in spite of the fact that the apparent strains are relatively large. An analysis of the apparent strain curves obtained during this program seems to bear out the fact that changes in the apparent strain curve occur on the return portion of the cycle, presumably when the alloy goes through the transformation temperature. Since no change occurs during the up cycle, this means that on the subsequent up cycle the apparent strain curve should retrace its previous return cycle. It appears that it is for this reason the curves characteristically converge to the maximum test temperature. Consequently if the gage were precalibrated for a complete cycle (up and return), it appears that the return portion of that cycle could be used to predict the apparent strain corrections with confidence over a relatively large span in temperature from about 811°K (1000°F) to the maximum operating temperature. Since the critical stresses often occur at the higher temperatures, it appears that the convergence characteristic can be utilized to considerably enhance the accuracy in making high temperature strain or stress measurements at temperatures in excess of 811°K (1000°F).

ACKNOWLEDGEMENT

Battelle Columbus Laboratories wish to express their appreciation to the U. S. Atomic Energy Commission, Division of Reactor Development and Technology, Washington, D. C., and the Liquid Metal Engineering Center, Canoga Park, California, for permission to use a special strain gage winding fixture and BCL-3 alloy wire developed under LMEC Contract N083-0004.

TEXT TABLES

TABLE 1. HAYNES 25 SPECIMEN MATERIAL PROPERTIES

Mechanical Properties							Chemical Composition	
Temperature		Ultimate Tensile Strength		Yield Strength (0.2% Offset)		% Elongation (in 4 Diameters)		
^{o}K	^{o}F	N/m^2	psi	N/m^2	psi		Element	%
R.T.	R.T.	9.786×10^8	141,950	4.622×10^8	67,050	61	Cr	19.17
							W	14.91
922	1200	7.100×10^8	103,000	2.412×10^8	35,000	35	Ni	10.50
							Fe	2.68
							Mn	1.48
1089	1500	3.447×10^8	50,000	2.482×10^8	36,000	16	Si	0.36
							C	0.10
							P	0.010
1255	1800	2.343×10^8	34,000	1.586×10^8	23,000	41	S	0.002
							Co	balance

TABLE 2. LEAD WIRE SYSTEMS

Specimen	Description of Lead-Wire Systems	
	High Temperature Section	Low Temperature Section
H-21	3-conductor #26 gage stainless steel clad copper wire, with glass glass fiber insulation	#25 ga, 3-conductor stranded copper wire, insulated with PVC
H-22	13 gage Chromel A wire in 4 mm x 2-hole porcelain tubes (hereinafter referred to as porcelain tubing)	
H-23	" " " " " " " "	
H-24	" " " " " " " "	
H-25	One gage with 13 gage Chromel A wire, and one gage with 20 ga Hoskins Alloy 875 wire with all wires in porcelain tubing	
H-26	2 gages with 13 gage Chromel A wire, and two gages with 20 ga Hoskins Alloy 875 wire with all wires in porcelain tubing	
H-27	20 gage Hoskins Alloy 875 in porcelain tubing	
H-27A	20 gage Hoskins Alloy 875 in porcelain tubing	

TABLE 3. TEST MATRIX

Specimen	Specimen Description	Run M.T.T. °K	Run M.T.T. °F	Step 1	Step 2	Step 3	Step 4	Step 5	Step 6	Step 7
H-21	8, 240Ω gages; 1 mil dia. BCL-3 wire; 26 ga., 3-conductor S.S. clad copper, glass fiber insulated lead wire; 3 mil thick Al_2O_3 substrate	922	1200	x	x	x	x	x	x	x
		978	1300	x	x	x	x	x	x	
		1033	1400				x	x	x	x
H-22	4, 240Ω gages; 1 mil dia. BCL-3 wire; 13 ga. Chromel A lead wire; 3 to 4 mil thick Al_2O_3 substrate	978	1300	x	x	x	omitted	omitted	x	x
		1033	1400	x	x	x	omitted	omitted	x	x
		1089	1500	x	x	x	failure	--	--	--
H-23	4, 70Ω gages; 2 mil dia. BCL-3 wire; 13 ga. Chromel A lead wire; 4.5 mil thick Al_2O_3 substrate	978	1300	x	x	x	x	x	x	x
		1033	1400	x	x	x	x	x	x	x
		1089	1500	x	failure	--	--	--	--	--
H-24	4, 70Ω gages; 2 mil dia. BCL-3 wire; 13 ga. Chromel A lead wire; 5 mil thick Al_2O_3 substrate, and thicker final Al_2O_3 coat	1089	1500	x	x	x	failure	--	--	--
H-25	2, 70Ω gages; 2 mil dia. BCL-3 wire; gage #1 with 13 ga. Chromel A lead wire, and gage #2 with Hoskins 20 ga. Alloy 875 lead wire; Al_2O_3 same as for H-24	1089	1500	x	x		omitted	omitted	x	x
		1200	1700	x	x	x	omitted	omitted	failure	--
H-26	4, 70Ω gages; 2 mil dia. BCL-3 wire; gages 1 and 3, 13 ga. Chromel A lead wire, gages 2 and 4 with 20 ga. Hoskins Alloy 875 lead wire; Al_2O_3 same as for H-24	1089	1500	x	x	x	x	x	x	x
		1144	1600	x	x	x	x	x	x	x
		1255	1800	x	x	x	failure	--	--	--
H-27	4, 70Ω gages; 2 mil dia. BCL-3 wire; 20 ga. Hoskins Alloy 875 lead wire; Al_2O_3 same as for H-24	1033	1400	x	x	x	x	x	x	x
		1144	1600	x	x	x	x	x	x	x
H-27A	4, 70Ω gages; 2 mil dia. BCL-3 wire; 20 ga. Alloy 875 lead wire; Al_2O_3 same as for H-24	1144	1600	x	x	x	x	x	x	x

TABLE 4. APPARENT STRAIN TO 922°K (1200°F), SPECIMEN H-21

Temperature		Apparent Strain, με				
°K	°F	Gage 1	Gage 2	Gage 4	Gage 5	Gage 8
			Cycle 1			
299	78	0	0	0	0	0
394	250	-3513	-3467	-3467	-3488	-3434
533	500	-6776	-6667	-6670	-6719	-6613
672	750	-8200	-8036	-8032	-8112	-7957
755	900	-8589	-8426	-8435	-8511	-8347
922	1200	-7176	-6936	-6958	-7064	-6896
			Cycle 2			
299	78	-70	-63	-12	-35	63
394	250	-3602	-3545	-3501	-3535	-3406
533	500	-6877	-6751	-6715	-6779	-6608
672	750	-8423	-8267	-8231	-8303	-8103
755	900	-8702	-8533	-8531	-8623	-8438
922	1200	-7182	-6946	-6957	-7064	-6901
			Cycle 3			
299	78	-153	-157	-163	-134	-119
394	250	-3604	-3559	-3568	-3552	-3497
533	500	-6850	-6741	-6749	-6963	-6655
672	750	-8453	-8297	-8298	-8340	-8184
755	900	-8721	-8550	-8565	-8632	-8477
922	1200	-7188	-6930	-6948	-7068	-6905

TABLE 5. APPARENT STRAIN TO 978°K (1300°F)
SPECIMEN H-23

Temperature		Apparent Strain, με			
°K	°F	Gage 1	Gage 2	Gage 3	Gage 4
		Cycle 1			
315	108	0	0	0	0
394	250	3217	3216	3218	3196
533	500	6736	6769	6738	6736
672	750	8895	8916	8949	8916
811	1000	8435	8533	8489	8553
978	1300	9323	9365	9318	9403
		Cycle 2			
316	110	2044	2071	2028	2057
394	250	5069	5110	5085	5092
533	500	8252	8308	8281	8289
672	750	10271	10312	10285	10277
811	1000	8455	8540	8477	8563
978	1300	9420	9464	9448	9547
		Cycle 3			
300	80	1118	1073	1087	1071
394	250	4498	4469	4484	4458
533	500	7957	7959	7944	7939
672	750	9779	9821	9776	9799
811	1000	8433	8510	8445	8538
894	1150	8924	8966	8916	9016
978	1300	9444	9474	9415	9529

TABLE 6. APPARENT STRAIN TO 1033°K (1400°F)
SPECIMEN H-27

Temperature		Apparent Strain, με			
°K	°F	Gage 1	Gage 2	Gage 3	Gage 4
		Cycle 1			
259	72	0	0	0	0
389	240	-2744	-2694	-2688	-2685
522	480	-5369	-5226	-5232	-5214
663	733	-6482	-6232	-6177	-6150
801	983	-3893	-3504	-3435	-3367
951	1252	-4130	-3663	-3613	-3504
1025	1385	-4308	-3822	-3800	-3673
		Cycle 2			
321	118	120	157	187	203
394	250	-2068	-1998	-2031	-2013
523	481	-4680	-4523	-4476	-4438
667	741	-5726	-5484	-5420	-5380
801	983	-3822	-3443	-3392	-3321
917	1191	-3950	-3508	-3483	-3383
1026	1391	-4262	-3781	-3788	-3662
		Cycle 3			
304	88	620	636	640	658
394	250	-2210	-2160	-2123	-2113
589	600	-5304	-5115	-5088	-5043
689	780	-6356	-6096	-6056	-6007
803	985	-3829	-3456	-3428	-3350
908	1174	-3915	-3489	-3480	-3383
1022	1380	-4235	-3764	-3778	-3656

TABLE 7. APPARENT STRAIN TO 1089°K (1500°F)
SPECIMEN H-26

Temperature		Apparent Strain, με			
°K	°F	Gage 1	Gage 2	Gage 3	Gage 4
			Cycle 1		
302	85	0000	0000	0000	0000
394	250	0078	0224	0080	- 0122
536	506	1592	1911	1598	1101
676	758	4439	4954	4462	3668
807	994	12168	12715	12202	10821
950	1251	15597	16304	15684	14001
1089	1500	17361	18139	17475	15630
			Cycle 2		
298	77	0149	0081	0134	0120
396	254	0152	0244	0215	- 0092
535	504	1666	1930	1649	1104
672	750	4482	4929	4447	3614
811	1000	12250	12776	12255	10861
950	1250	15565	16246	15624	13946
1089	1500	17328	18069	17407	15560
			Cycle 3		
304	88	0049	- 0079	0024	- 0005
394	250	0047	0065	0008	- 0208
533	500	1514	1741	1486	0952
672	750	4636	5048	4620	3780
811	1000	12248	12754	12249	10854
950	1250	15565	16185	15581	13900
1089	1500	17353	18084	17431	15586

TABLE 8. APPARENT STRAIN TO 1144°K (1600°F)
SPECIMEN H-27

Temperature		Apparent Strain, με			
°K	°F	Gage 1	Gage 2	Gage 3	Gage 4
		Cycle 1			
297	75	0	0	0	0
422	300	5365	10958	5167	11318
581	586	13274	24616	12821	25332
726	847	21147	37206	20460	38120
807	993	30653	49094	29761	50078
983	1310	40005	63426	38819	64736
1121	1558	43879	68878	42636	70292
		Cycle 2			
293	67	-1727	-2160	-1858	-2352
446	343	4783	10735	4409	10970
582	588	11796	22716	11234	23275
692	786	17797	32408	17131	33209
804	987	30116	48133	29237	49116
978	1300	39931	63203	38768	64522
1141	1595	44386	69353	43170	70811
		Cycle 3			
305	89	-728	-2542	-801	-2567
449	348	5662	10464	5348	10824
581	587	12614	22673	12107	23322
694	790	18411	32311	17770	33167
803	986	30153	47610	29312	48647
978	1300	39854	62766	38720	64125
1144	1600	44524	69419	43305	70901

TABLE 9. PERFORMANCE HISTORY

Specimen	Gage No.	Gage Performance	Specimen/Leadwire Assembly Performance
H-21	1	No failure	Complete failure of lead wire insulation after 1400°F run, all gages
	2	Failed prior to Step 6, 1400°F run	
	3	Failed during Step 3, 1200°F run	
	4	Damaged during installation	
	5	No failure	
	6	Damaged during installation	
	7	Damaged during installation	
	8	No failure	
H-22	1	Failed after Step 2, 1400°F run	Substrate separation noted after removal of specimen from furnace after 1500°F run
	2	No failure	
	3	No failure	
	4	No failure	
H-23	1	No failure	Substrate separation noted after removal of specimen from furnace after 1500°F run
	2	No failure	
	3	Lead wire failure during Step 6, 1400°F run	
	4	No failure	
H-24	1	No failure	Substrate separation noted after Step 4, of 1500°F run. Also possible joint failure due to lead wire thermal movement
	2	No failure	
	3	Failure at joint of tab to lead wire, during Step 4, 1500°F run	
	4	No failure	
H-25	1	No failure	Complete substrate separation after Step 4, 1700°F run
	2	No failure	
	3	No failure	
	4	No failure	
H-26	1	No failure	Complete substrate separation during Step 4, 1800°F run
	2	No failure	
	3	No failure	
	4	No failure	
H-27	1	No failure	No failure
	2	No failure	
	3	No failure	
	4	No failure	
H-27A	1	No failure	No failure
	2	No failure	
	3	No failure	
	4	No failure	

TABLE 10. GAGE FACTOR SUMMARY

Specimen		Temperature, ^{o}K and (^{o}F)								
		RT[c]	589 (600)	644 (700)	700 (800)	922 (1200)	978 (1300)	1033 (1400)	1089 (1500)	1144 (1600)
H-21	T[a]	2.71[e] 2.69[d]	2.40	2.47[e]	--	2.05	1.92	1.83	--	--
	C[b]	2.19[e] 2.28[d]	2.16	2.14[e]	--	2.02	1.92	1.88	--	--
H-23	T	2.63	--	2.43	--	--	--	1.97	--	--
	C	2.31	--	2.08	--	--	--	1.71	--	--
H-26	T	2.72	--	--	2.28	--	--	--	2.07	1.84
	C	2.42	--	--	2.37	--	--	--	2.13	1.95
H-27	T	2.42	--	2.19	2.25	--	--	1.90	--	2.06
	C	2.14	--	2.15	2.13	--	--	1.92	--	1.94
H-27A	T	2.55	--	--	2.27	--	--	--	--	1.87
	C	2.41	--	--	2.09	--	--	--	--	1.87

(a) Tension
(b) Compression
(c) Room Temperature
(d) From 922°K Run
(e) From 1033°K Run

TABLE 11. GAGE FACTOR STATISTICS

Temperature		Average Gage Factor		Max. Deviation in Gage Factor (% of Average Value)			
				Tension		Compression	
^{o}K	^{o}F	Tension	Compression	+	-	+	-
R.T.	R.T.	2.62	2.29	3.82	7.63	5.68	6.55
589	600	2.40	2.16	*	*	*	*
644	700	2.36	2.12	*	*	*	*
700	800	2.20	2.11	3.18	5.00	0.95	0.95
922	1200	2.05	2.02	*	*	*	*
978	1300	1.92	1.92	*	*	*	*
1033	1400	1.90	1.84	3.68	3.68	4.35	7.06
1089	1500	2.07	2.13	*	*	*	*
1144	1600	1.92	1.92	7.29	4.16	1.56	2.60

* Deviation not computed, since there was only one data point.

TABLE 12. DRIFT RATES AT VARIOUS TEMPERATURES

a) Initial Drift Rates (Step 2)

Specimen	Temperature °K	Temperature °F	Lead-Wire System: Chromel A	Lead-Wire System: Hoskins 875	Lead-Wire System: Stainless Steel Clad Copper	Drift Rate at end of 10 hrs, με/hr.	Ref. Figure
H-22	991	1325	x			-40	45
H-23	991	1325	x			-30	45
H-22	1047	1425	x			-38	44
H-23	1047	1425	x			-27	44
H-27	1047	1425		x		-28	48
H-25	1103	1525	x			-29	45
H-26	1158	1625	x			-81	45
H-26	1158	1625		x		-74	48
H-27	1158	1625		x		-24	49
H-27	1158	1625		x		-25	49
H-27	1158	1625		x		-30	49
H-25	1200	1700	x			-120	46
H-25	1200	1700		x		-100	46
H-26	1200	1700		x		-70	46
H-26	1200	1700	x			-90	46
H-26	1269	1825	x			-200	47
H-26	1269	1825		x		-180	47
H-26	1269	1825	x			-235	47
H-26	1269	1825		x		-140	47

TABLE 12. DRIFT RATES AT VARIOUS TEMPERATURES (Contd.)

b) Drift Rates (Step 7)

Specimen	Temperature °K	Temperature °F	Lead-Wire System: Chromel A	Lead-Wire System: Hoskins 875	Lead-Wire System: Stainless Steel Clad Copper	Drift Rate at end of 10 hrs, με/hr.	Ref. Figure
H-21	922	1200			x	-0.4	50
H-21	922	1200			x	-0.7	50
H-21	922	1200			x	-0.7	50
H-21	922	1200			x	-1.0	50
H-21	922	1200			x	~0	56
H-23	978	1300	x			-8	52
H-26	978	1300	x			-20	57
H-21	1033	1400			x	-20	51
H-23	1033	1400	x			-38	52
H-27	1033	1400		x		-10	55
H-27	1033	1400		x		-10	55
H-27	1033	1400		x		-10	55
H-27	1033	1400		x		-12	55
H-27	1033	1400		x		-10	59
H-26	1089	1500	x			-15	53
H-26	1089	1500	x			-20	56
H-26	1089	1500		x		-30	56
H-23	1089	1500	x			-30	57
H-26	1089	1500		x		-35	59
H-26	1144	1600	x			-25	53
H-26	1144	1600	x			-70	54
H-26	1144	1600		x		-48	54
H-27	1144	1600		x		-50	55
H-27	1144	1600		x		-50	55
H-27	1144	1600		x		-220	55
H-27	1144	1600		x		-220	55
H-27A	1144	1600		x		-90	59

TABLE 13. RESISTANCE TO GROUND VS. SUBSTRATE THICKNESS VS. TEMPERATURE

Substrate Thickness, Mils	Temperature °K	Temperature °F	Step 2 Resistance to Ground Min. Kilohms	Step 2 Resistance to Ground Min. Megohms	Step 2 Resistance to Ground Max. Kilohms	Step 2 Resistance to Ground Max. Megohms	Steps 3, 4, 5, 6, or 7 Resistance to Ground Min. Kilohms	Steps 3, 4, 5, 6, or 7 Resistance to Ground Min. Megohms	Steps 3, 4, 5, 6, or 7 Resistance to Ground Max. Kilohms	Steps 3, 4, 5, 6, or 7 Resistance to Ground Max. Megohms
3 (Specimen H-21)	922 to 936	1200 to 1225	3.5	--	--	7.0	3.8	--	--	7.5
	978 to 991	1300 to 1325	4.0	--	--	3.0	3.6	--	--	3.8
	1033 to 1047	1400 to 1425	--	--	--	--	1.6	--	--	1.0
4 (Specimen H-22)	R.T.	R.T.	--	--	--	--	--	--	--	150
	978 to 991	1300 to 1325	350	--	--	1.0	3.0	--	--	200
	1033 to 1047	1400 to 1425	3.0	--	--	5.0	13.0	--	--	4.4
	1089 to 1103	1500 to 1525	--	--	--	--	10.0	--	300	--
4-1/2 (Specimen H-23)	R.T.	R.T.	--	150	--	500	--	50	--	∞ (>1000)
	978	1300	350	--	--	10	3.0	--	--	200
	1033	1400	--	2.5	--	9	20	--	--	11.5
	1089	1500	--	--	--	--	40	--	--	1000
5 (Specimens H-24, H-25, H-26, H-27, H-27A)	R.T.	R.T.	--	∞ (>1000)	--	∞ (>1000)	--	500	--	∞
	1033	1400	--	--	--	--	--	--	--	--
	1089	1500	--	1	--	12	40	--	--	70
	1144	1600	--	10	--	30	--	12	--	45
	1200	1700	--	--	--	--	100	--	--	100
	1255	1800	--	4	--	10	--	2.2	--	5.8

TEXT FIGURES

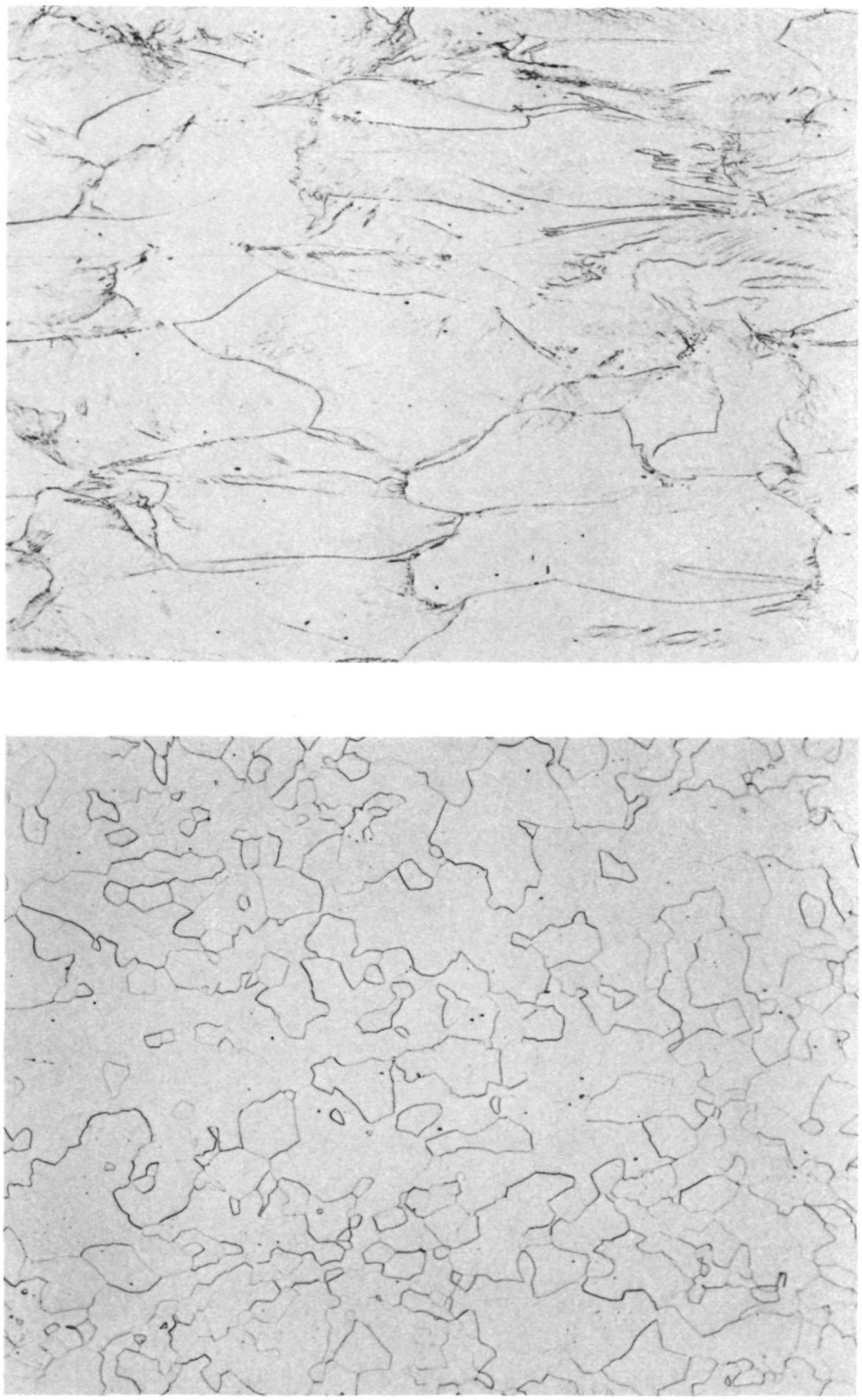

FIGURE 1. MICROSTRUCTURES OF 0.081 (2.05mm) IN-DIA WIRE OF BCL-3 ALLOY

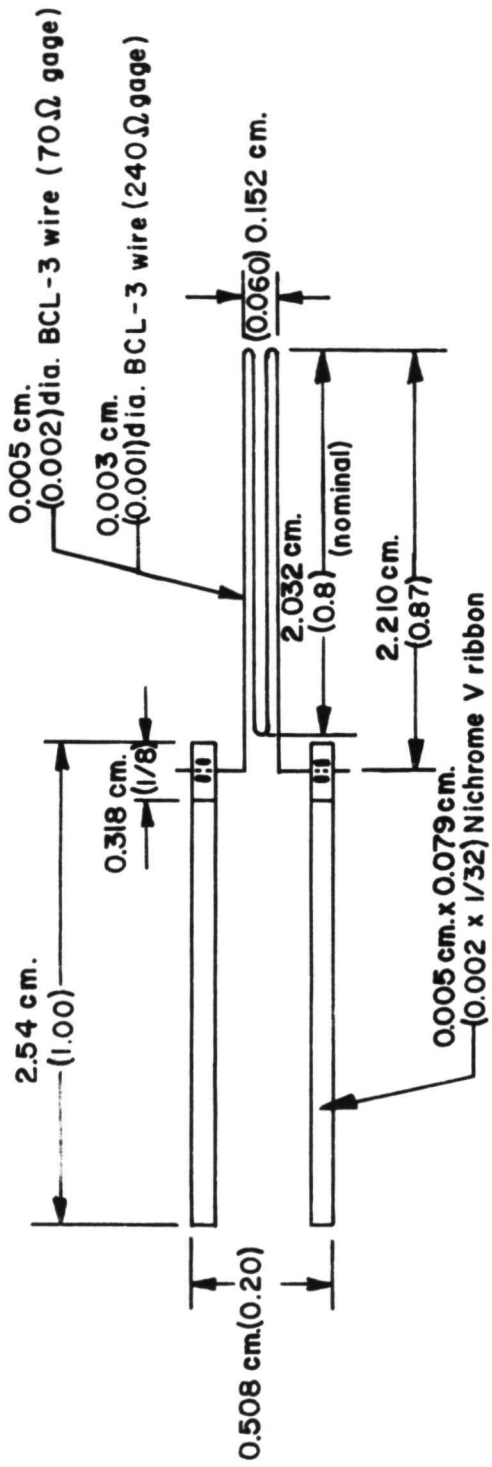

FIGURE 2. GAGE GEOMETRY

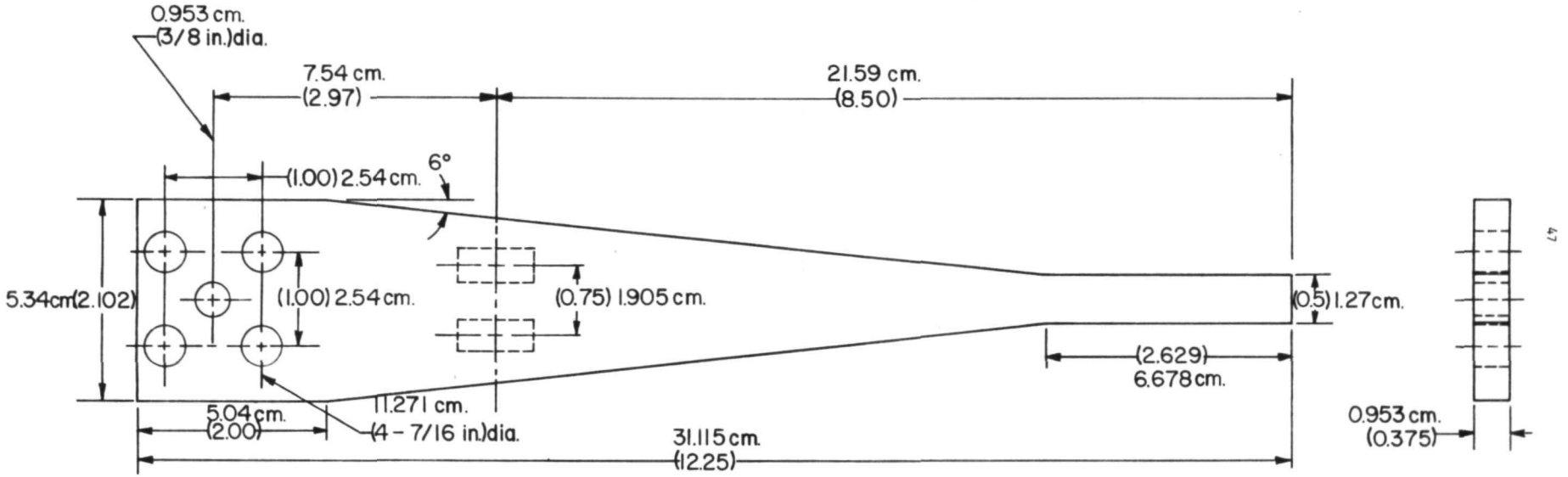

FIGURE 3. SPECIMEN GEOMETRY AND GAGE LOCATIONS

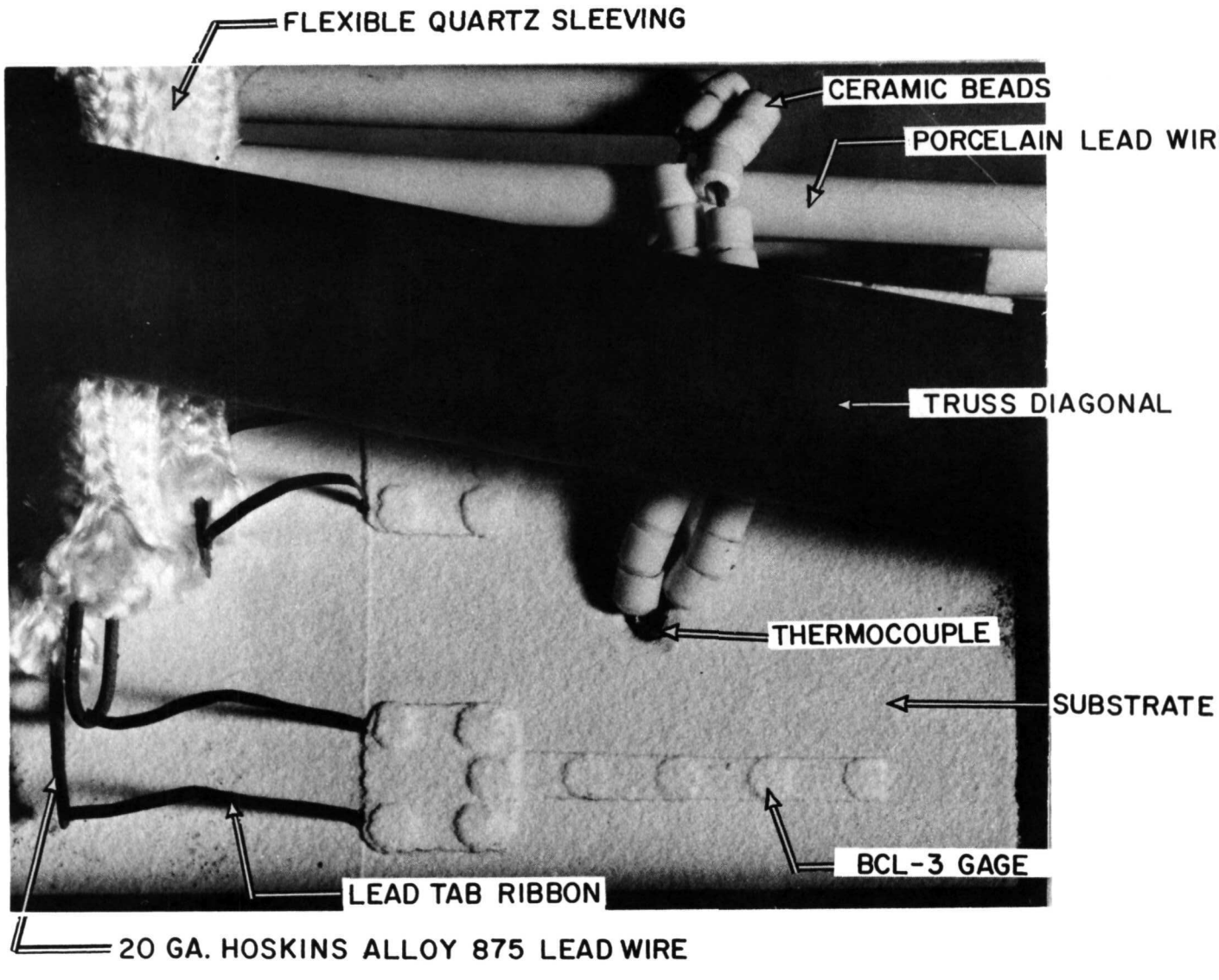

FIGURE 4. TYPICAL GAGE INSTALLATION

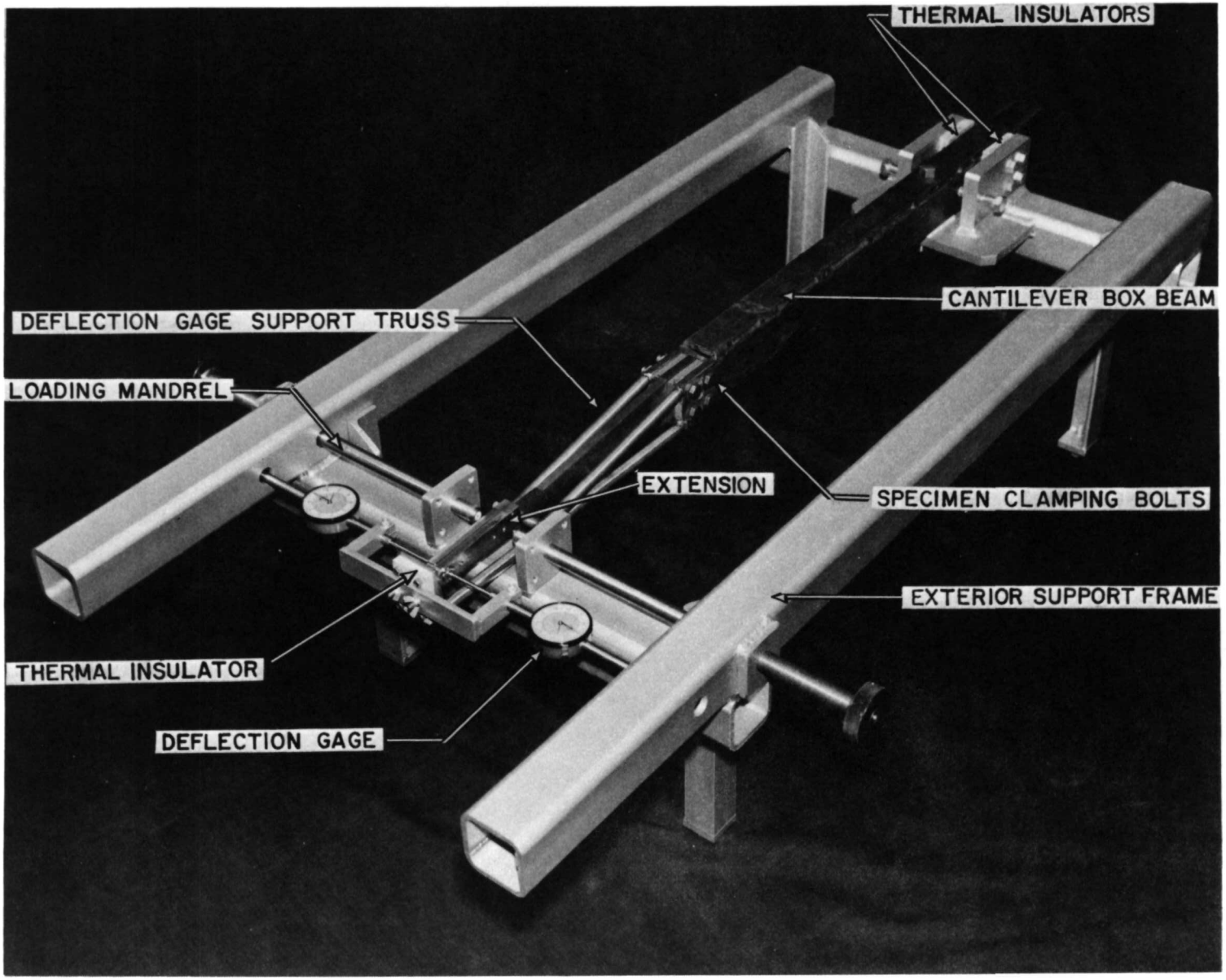

FIGURE 5. GAGE EVALUATION FIXTURE

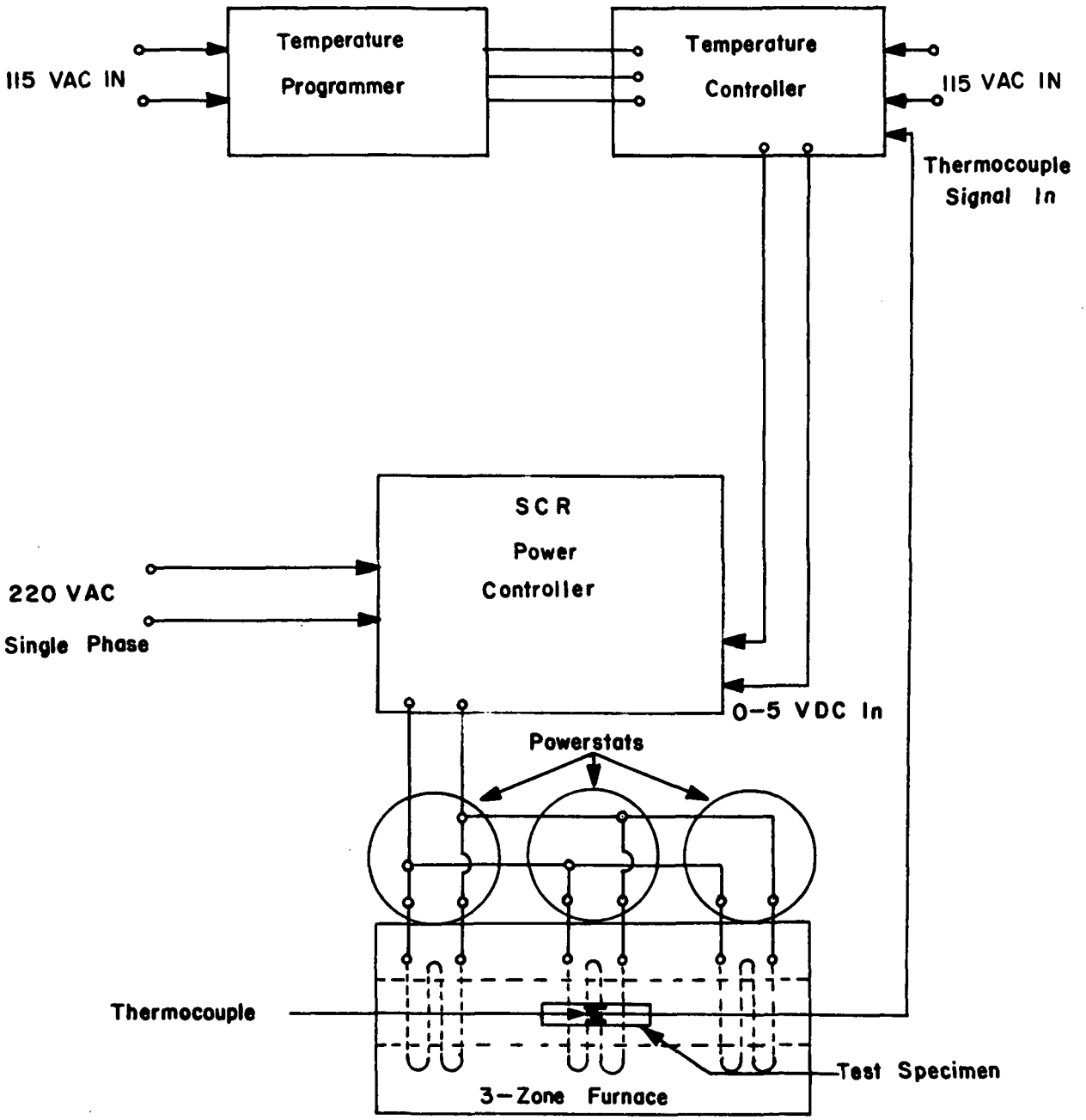

FIGURE 6. TEMPERATURE CONTROL SYSTEM

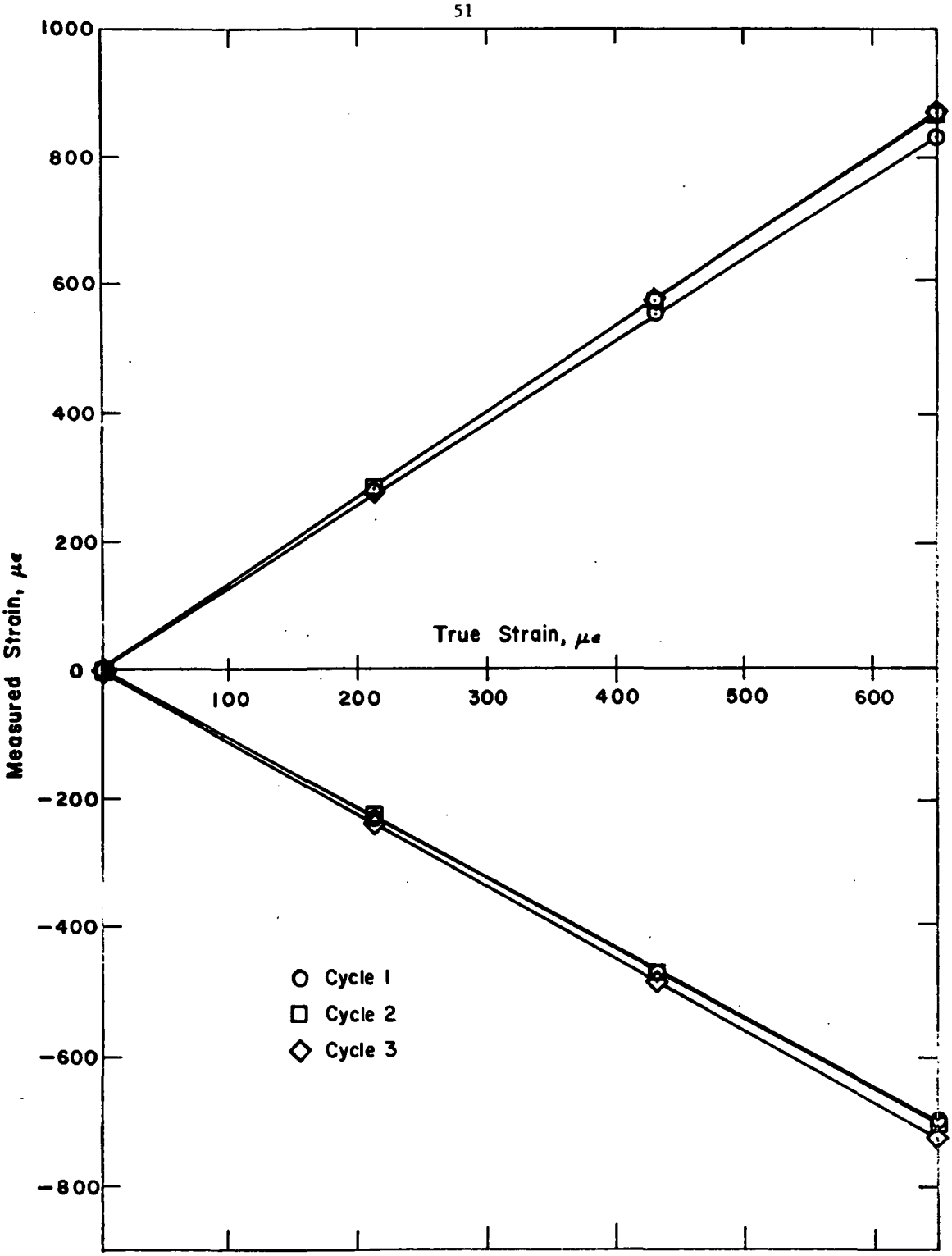

FIGURE 7. SPECIMEN H-21, GAGE FACTOR, R. T., CYCLES 1,2,3

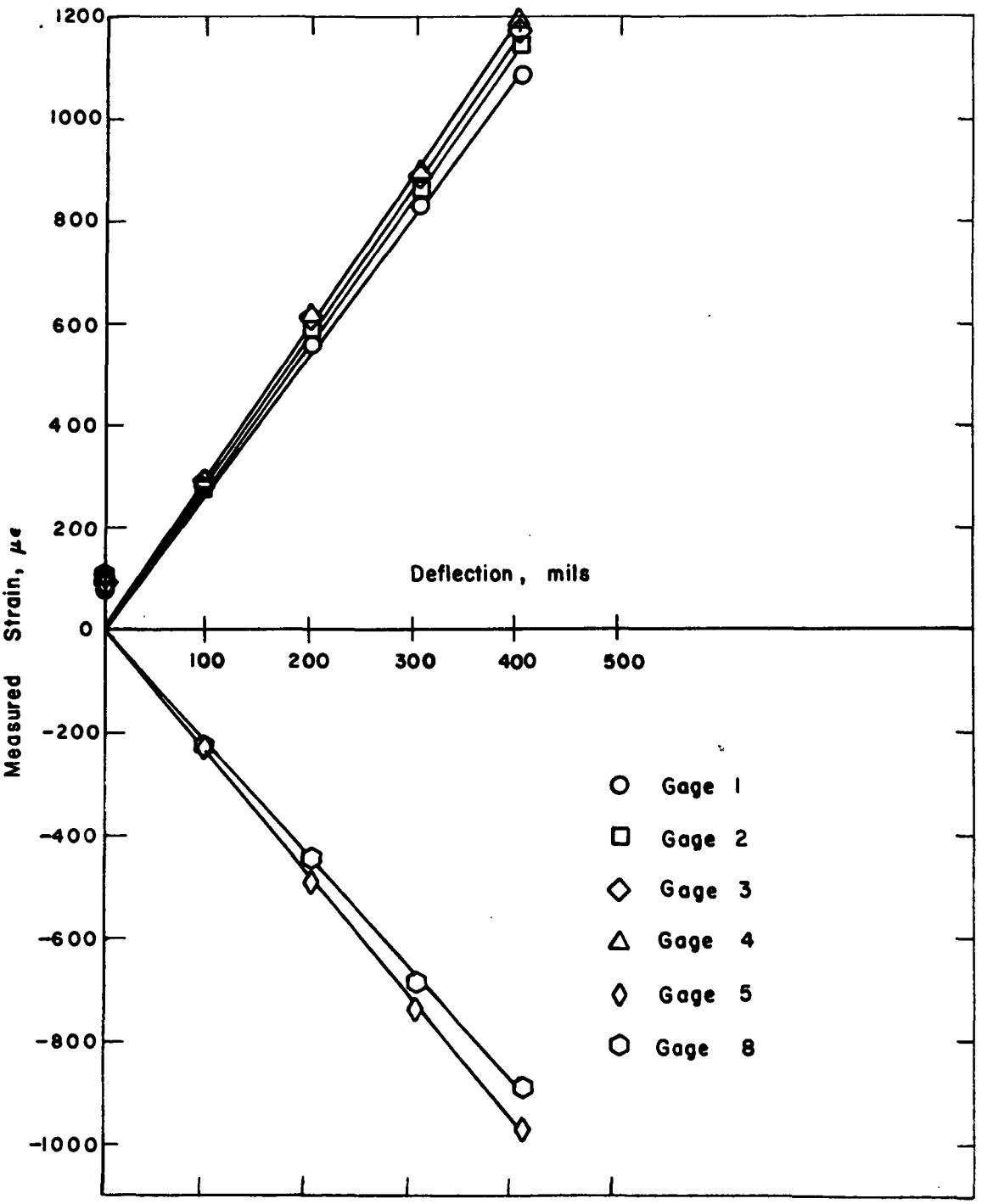

FIGURE 8. SPECIMEN H-21, GAGE FACTOR, 644°K (700°F)

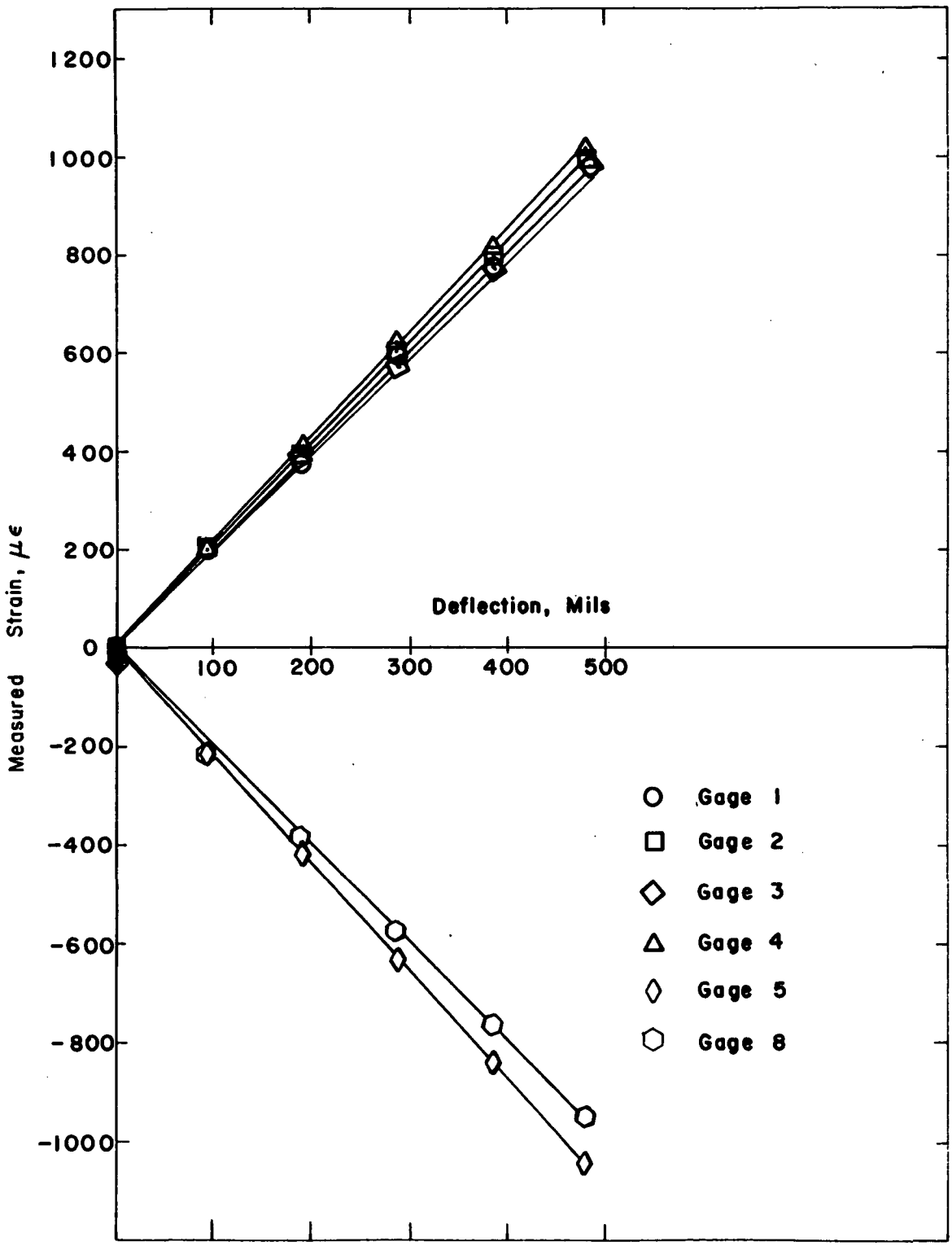

FIGURE 9. SPECIMEN H-21, GAGE FACTOR, 978°K (1300°F)

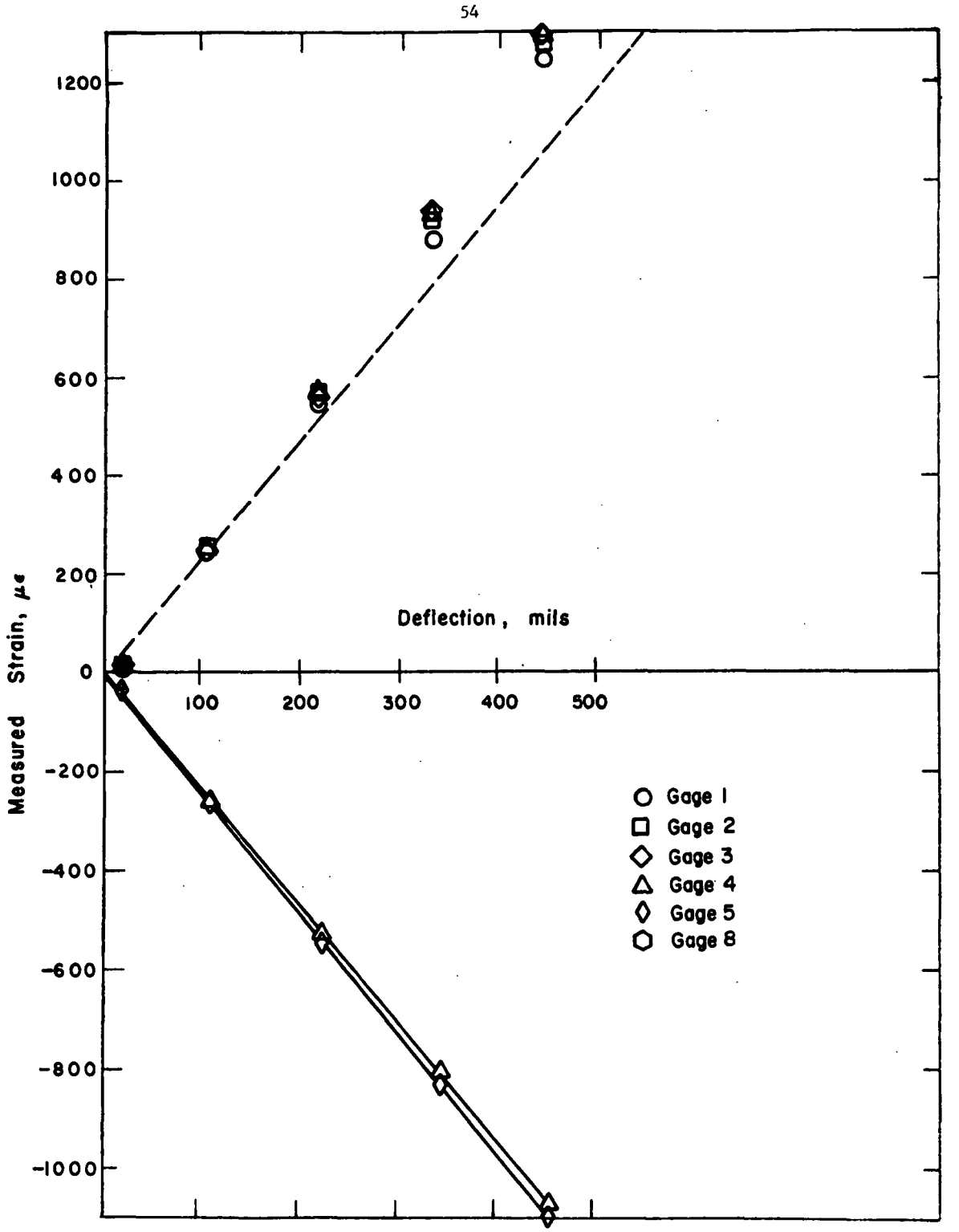

FIGURE 10. SPECIMEN H-21, GAGE FACTOR, 1033°K (1400°F)

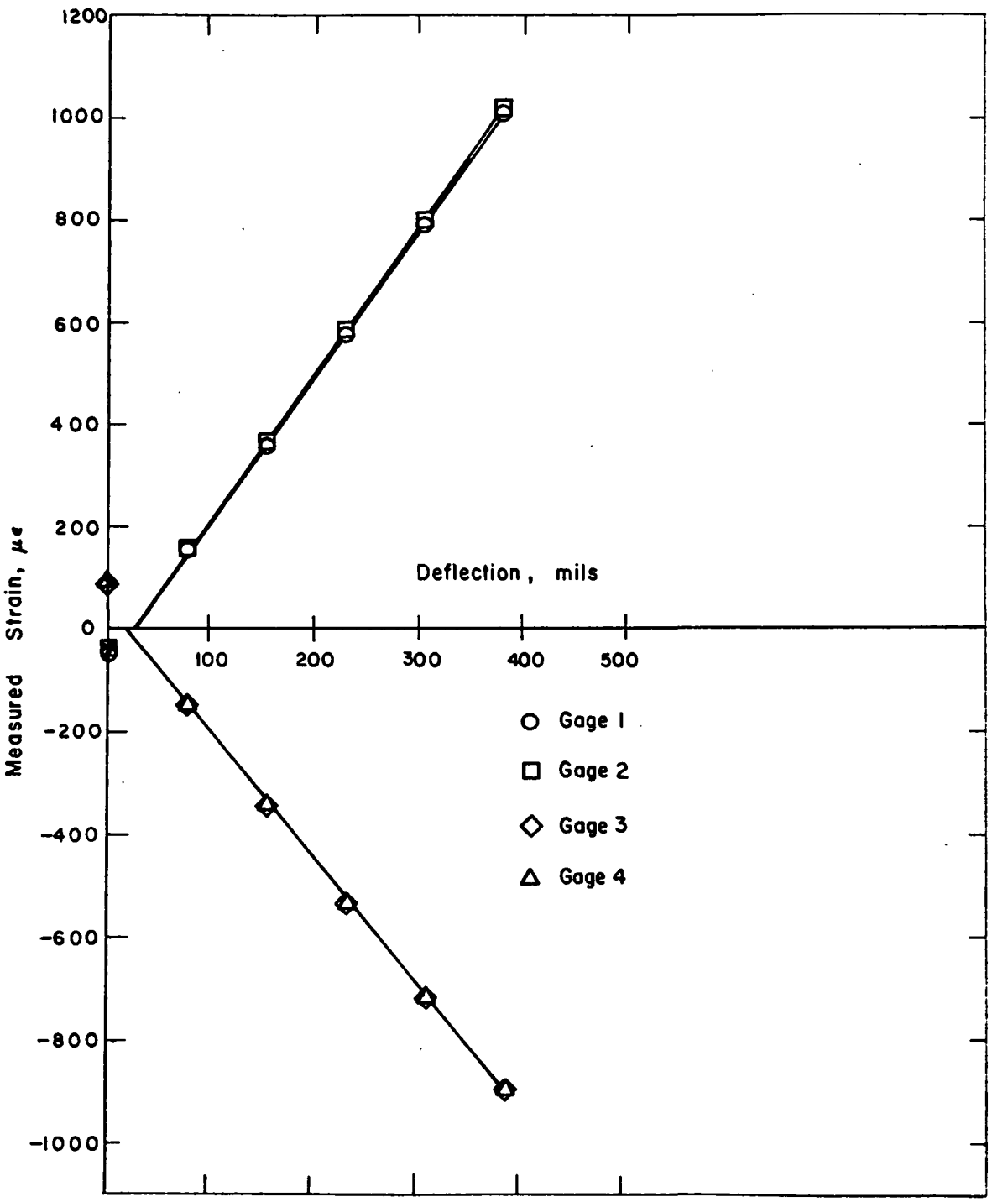

FIGURE 11. SPECIMEN H-23, GAGE FACTOR, R. T.

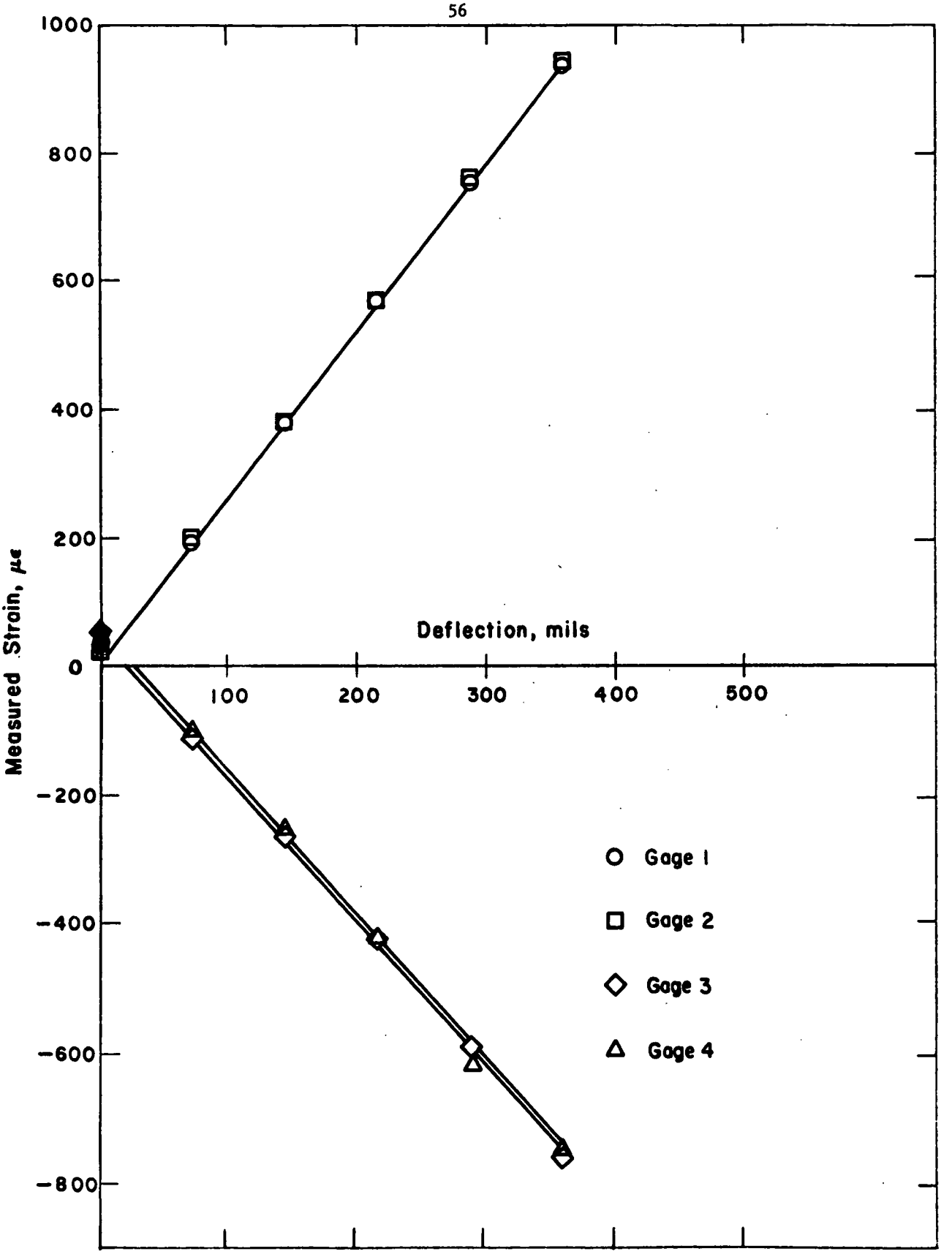

FIGURE 12. SPECIMEN H-23, GAGE FACTOR, 644°K (700°F)

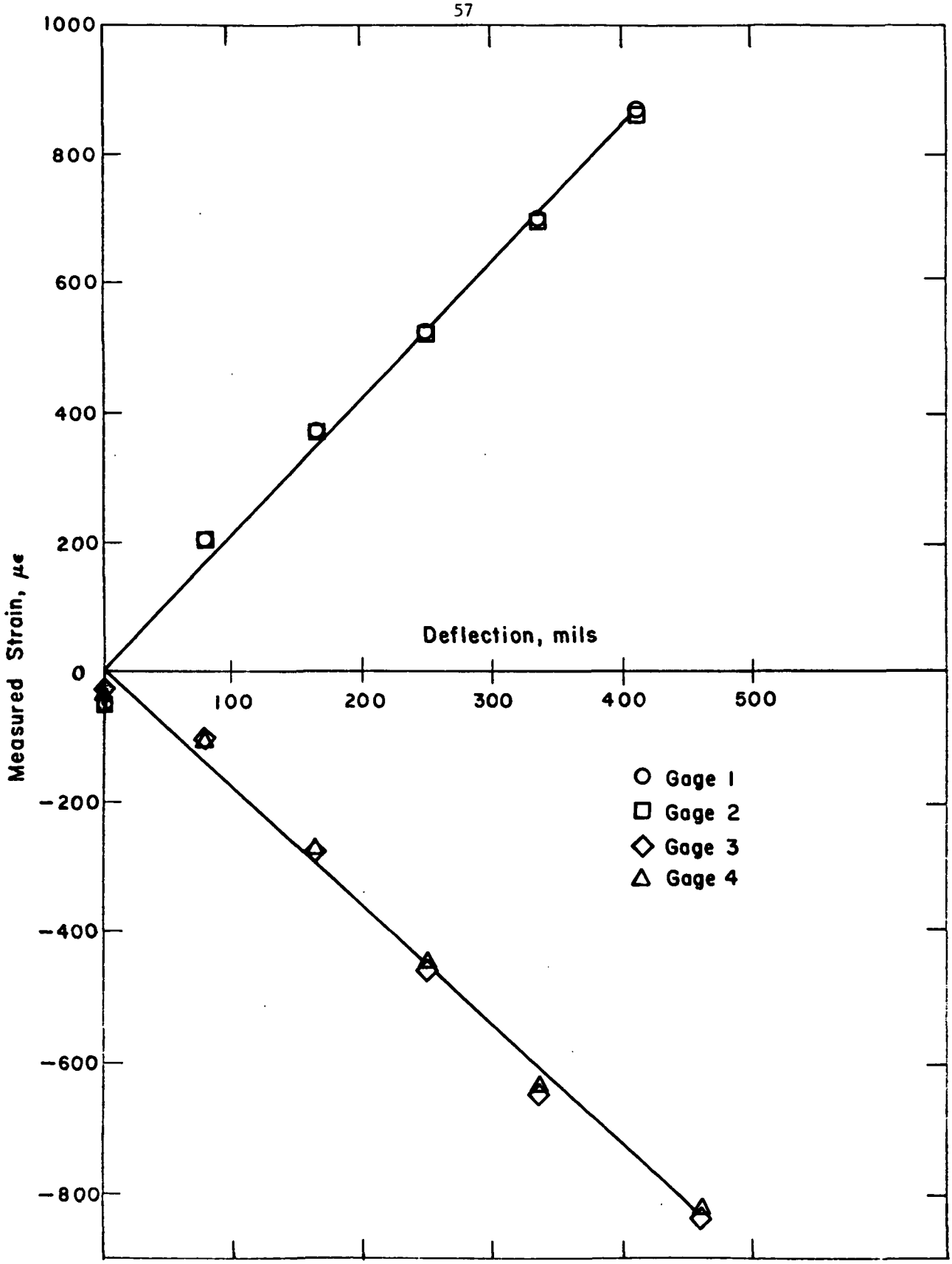

FIGURE 13. SPECIMEN H-23, GAGE FACTOR, 1033°K (1400°F)

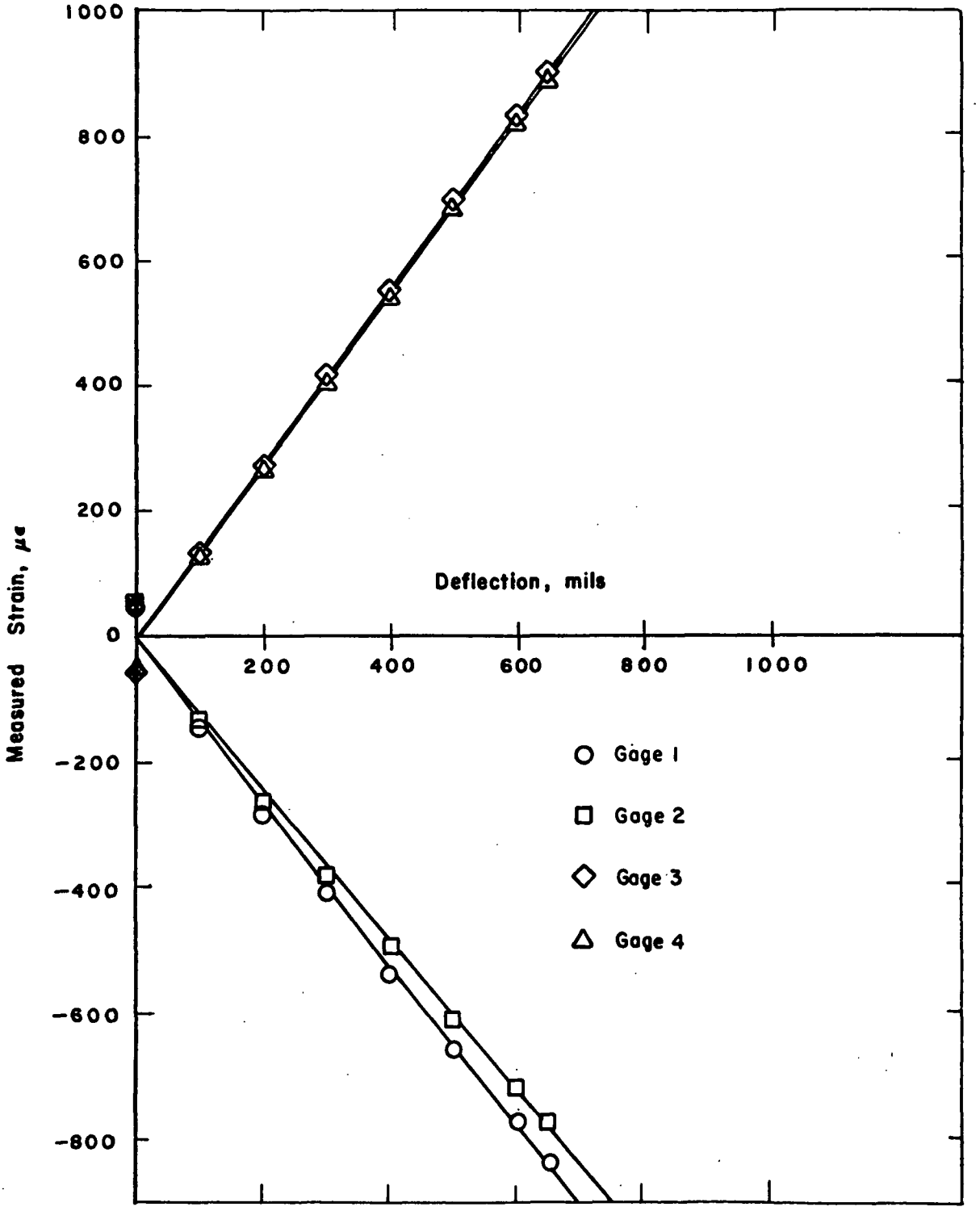

FIGURE 14. SPECIMEN H-26, GAGE FACTOR, R. T.

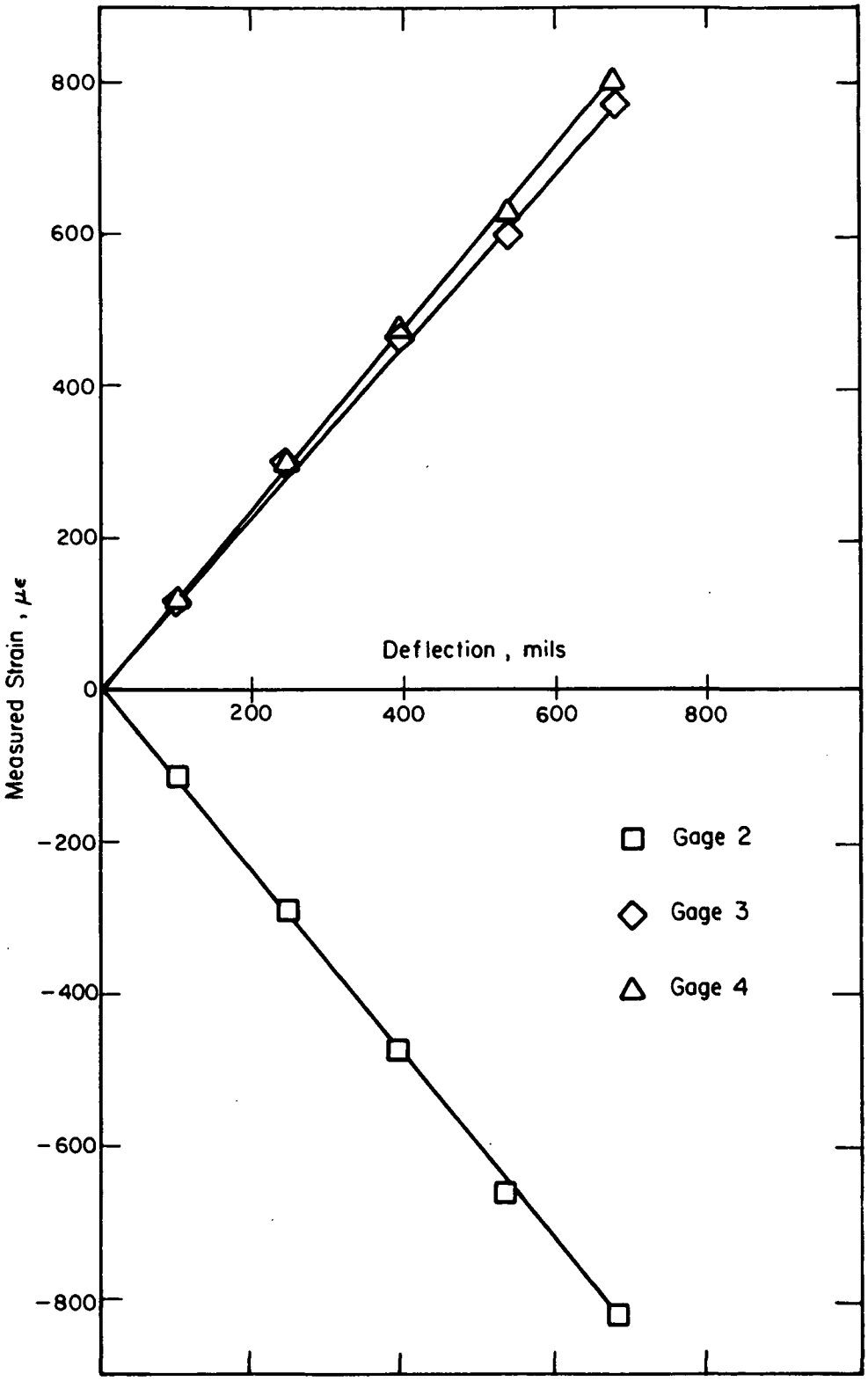

FIGURE 15. SPECIMEN H-26, GAGE FACTOR, 700°K(800°F)

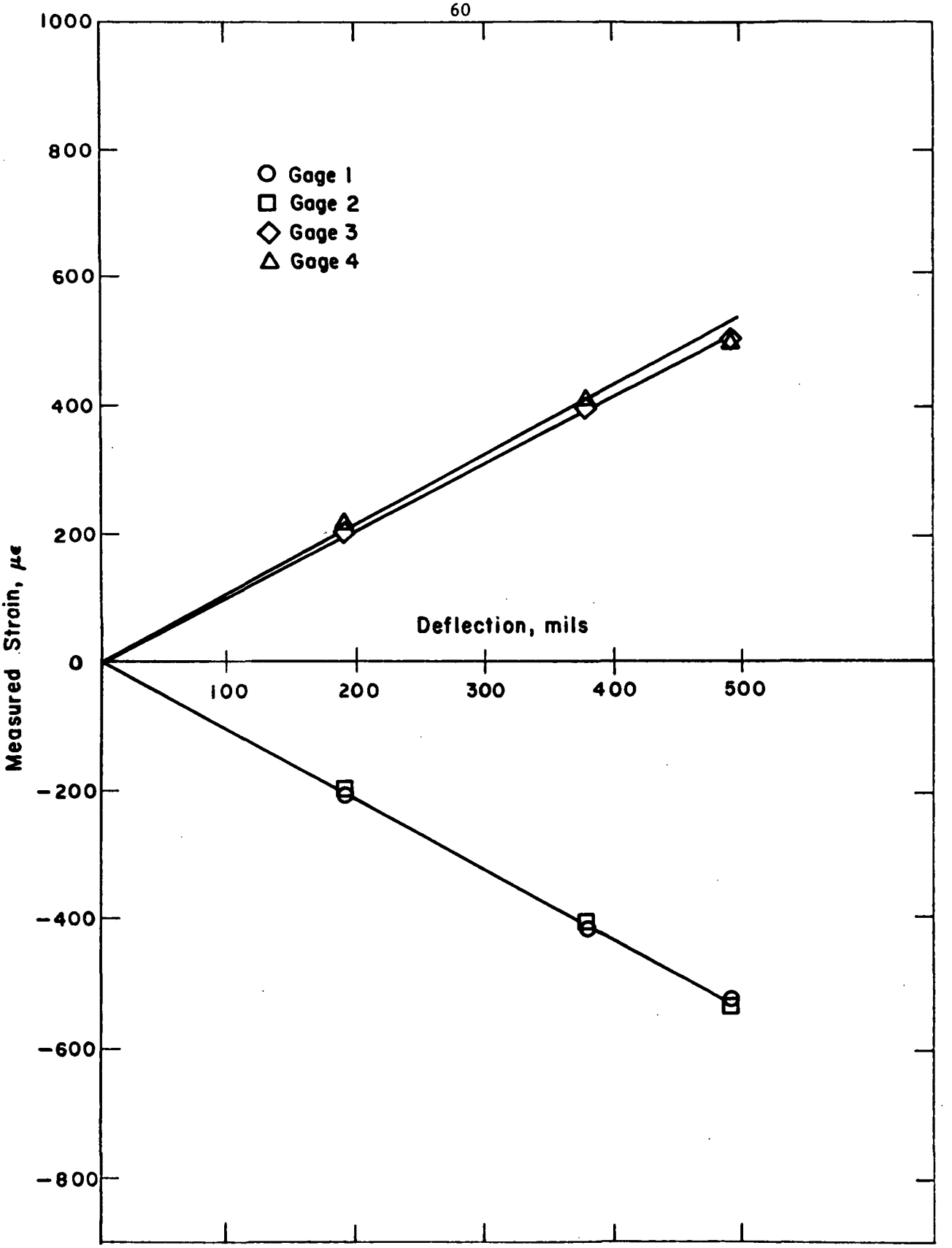

FIGURE 16. SPECIMEN H-26, GAGE FACTOR, 1089°K (1500°F)

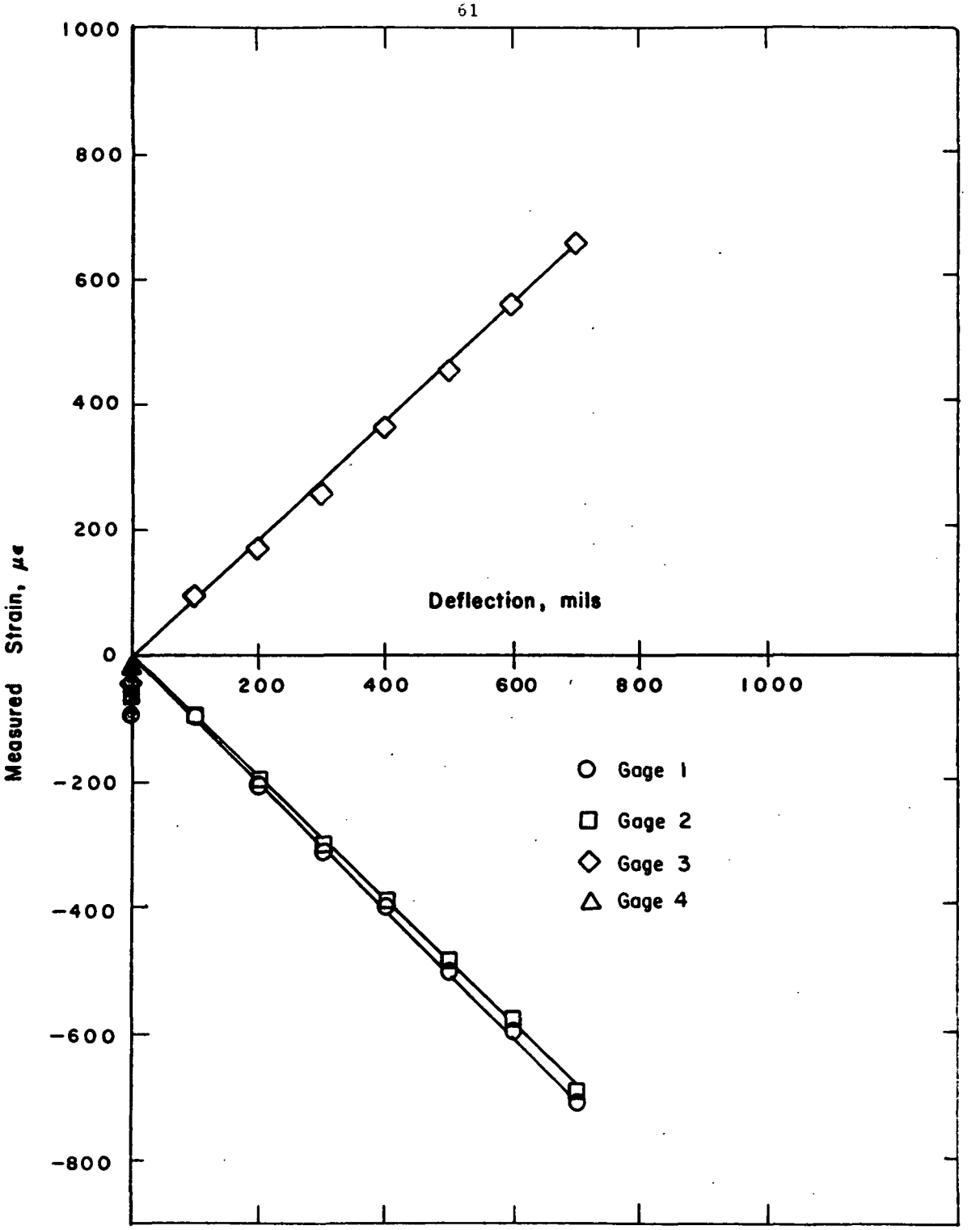

FIGURE 17. SPECIMEN H-26, GAGE FACTOR, 1144°K (1600°F)

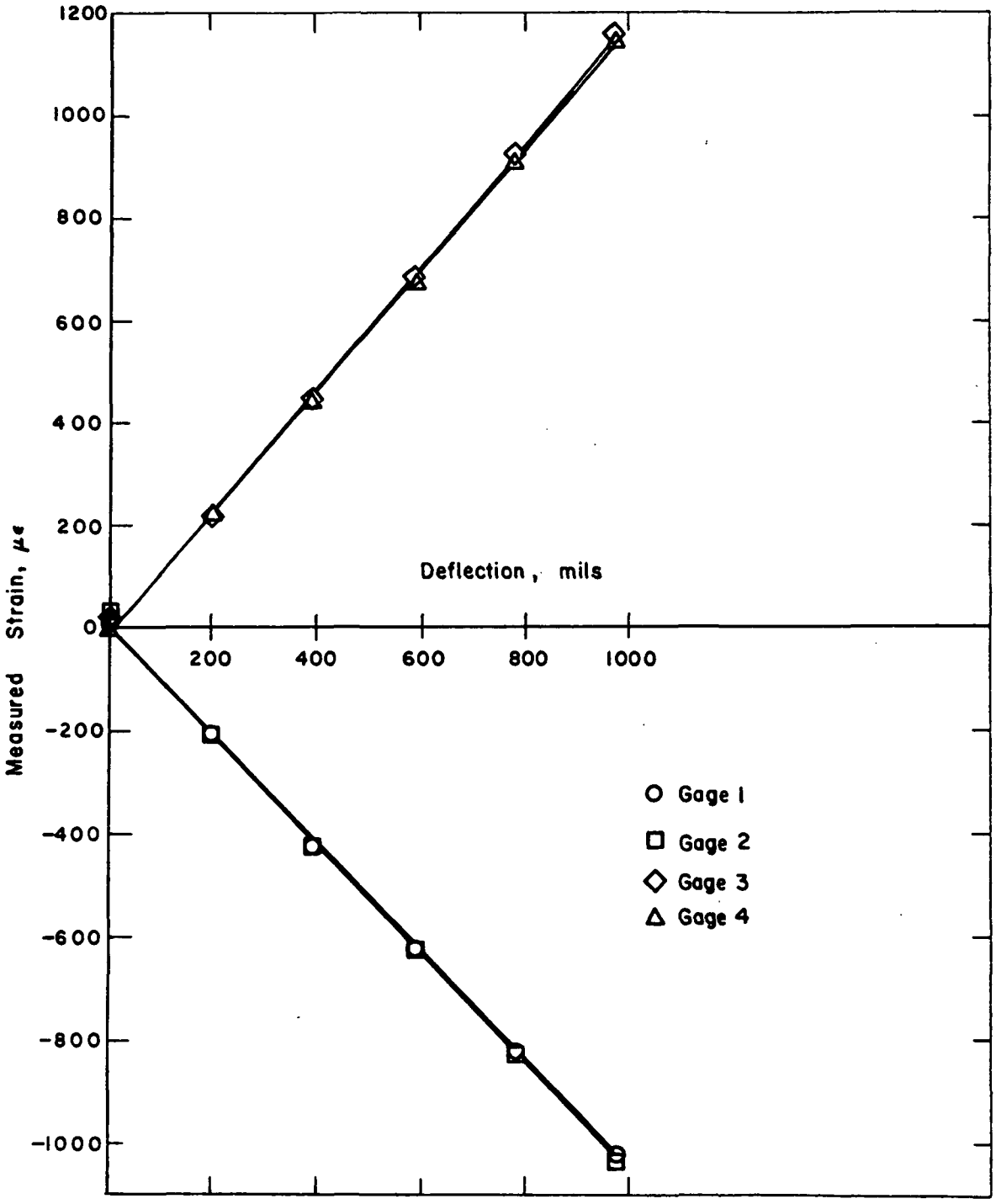

FIGURE 18. SPECIMEN H-27, GAGE FACTOR, R.T.

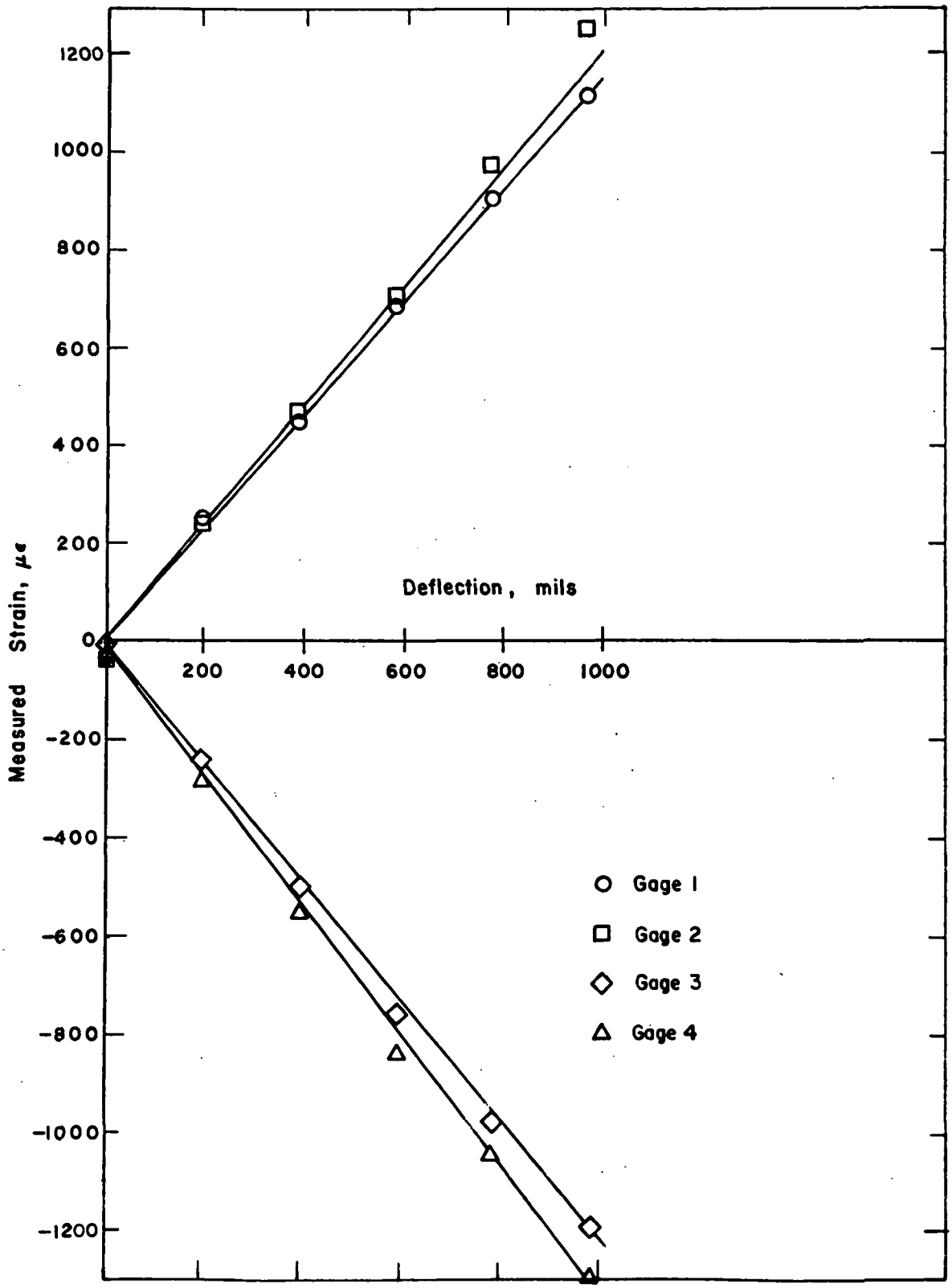

FIGURE 19. SPECIMEN H-27, GAGE FACTOR, 700°K (800°F)

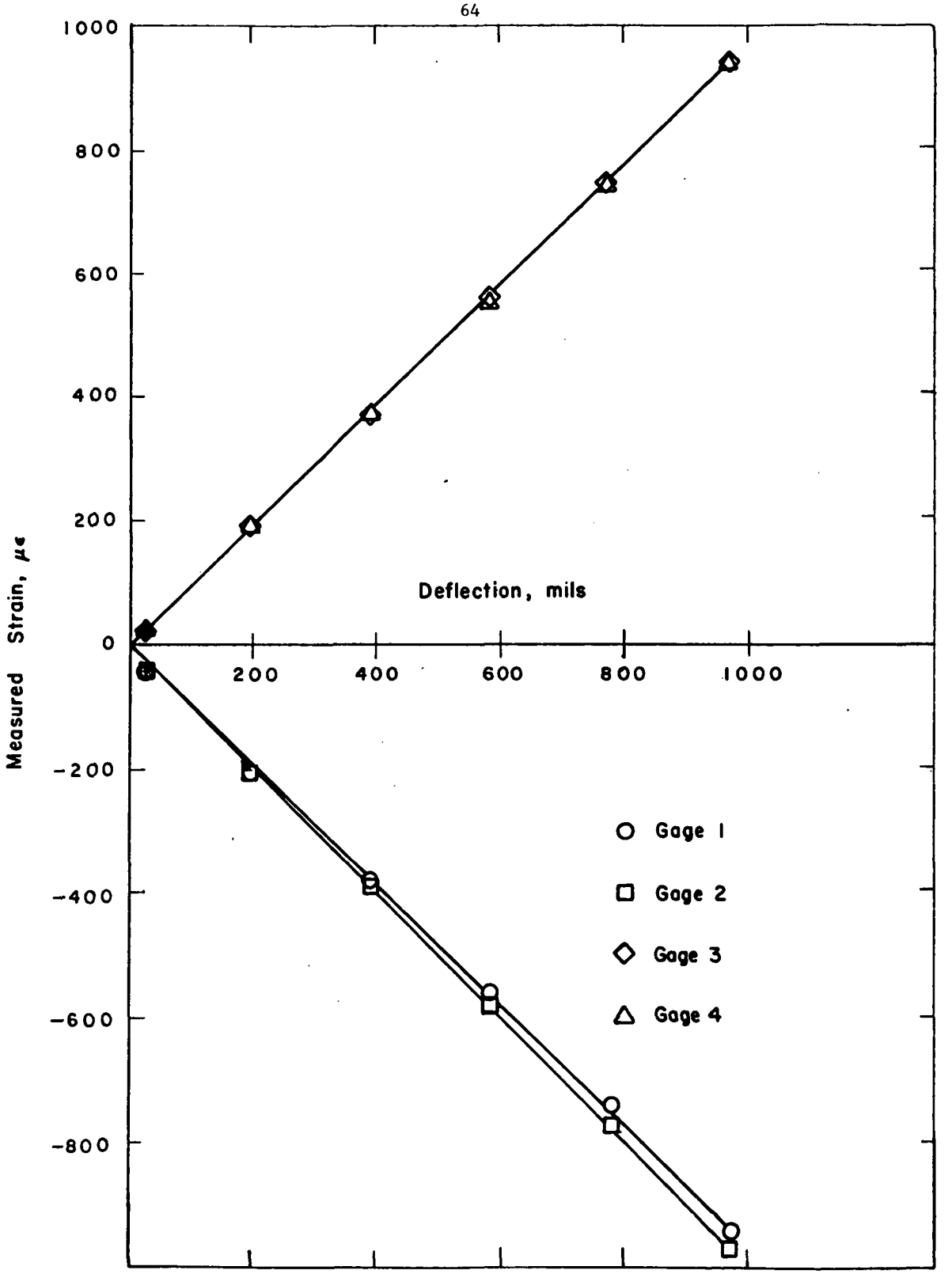

FIGURE 20. SPECIMEN H-27, GAGE FACTOR, 1033°K (1400°F)

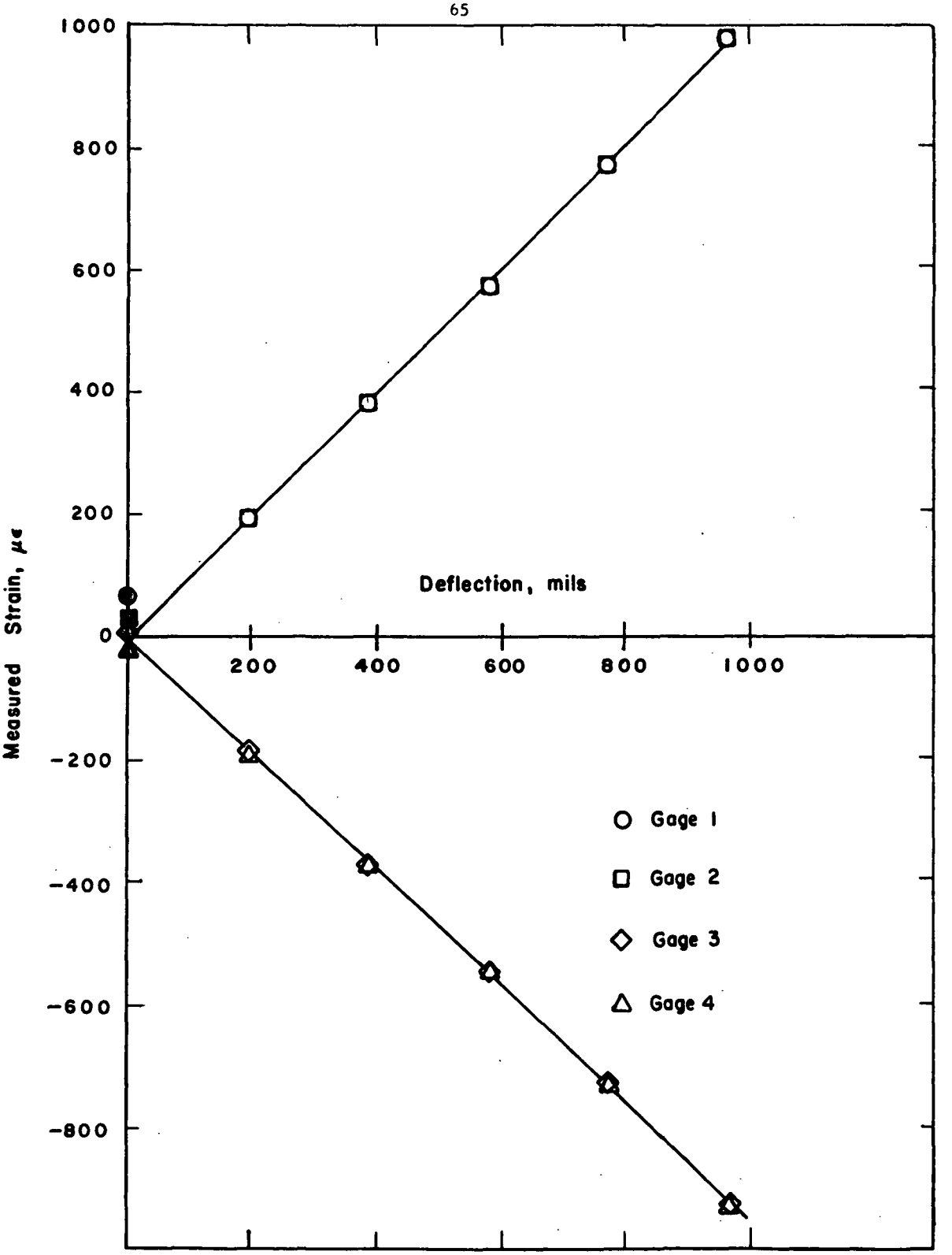

FIGURE 21. SPECIMEN H-27, GAGE FACTOR, 1144°K (1600°F)

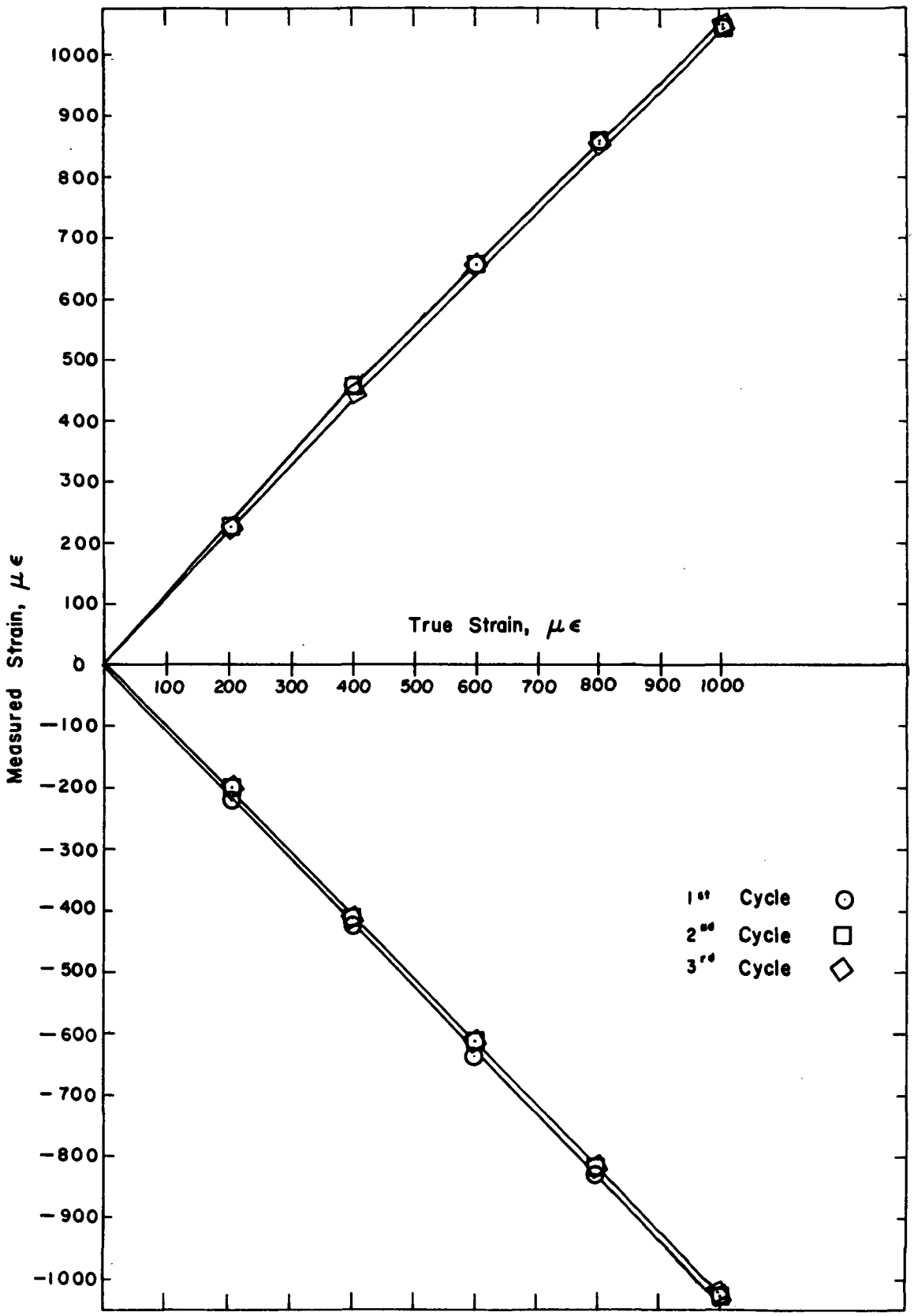

FIGURE 22. SPECIMEN H-27, GAGE FACTOR, R. T., CYCLES 1,2,3

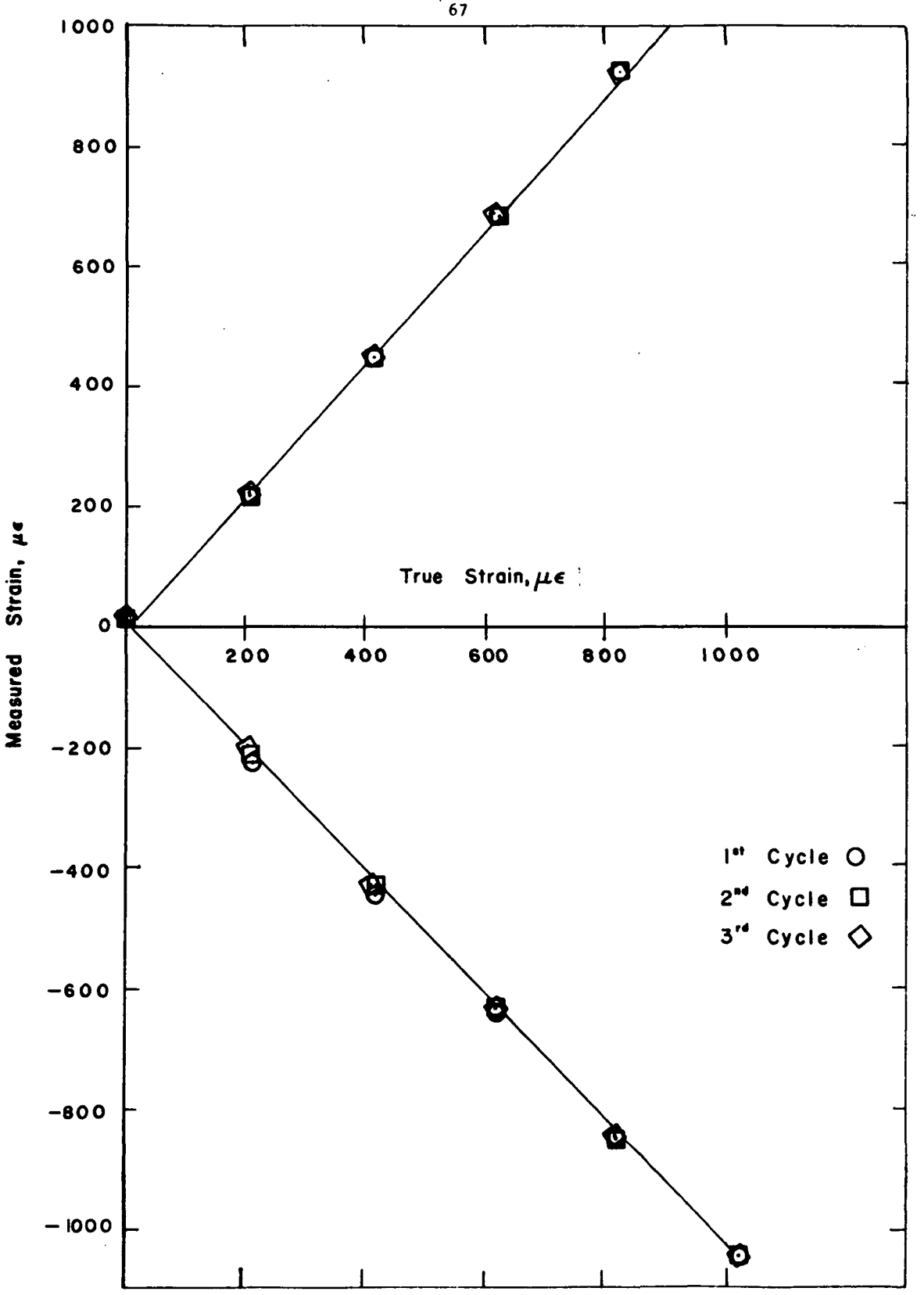

FIGURE 23. SPECIMEN H-27, GAGE FACTOR, 644°K (700°F), CYCLES 1,2,3

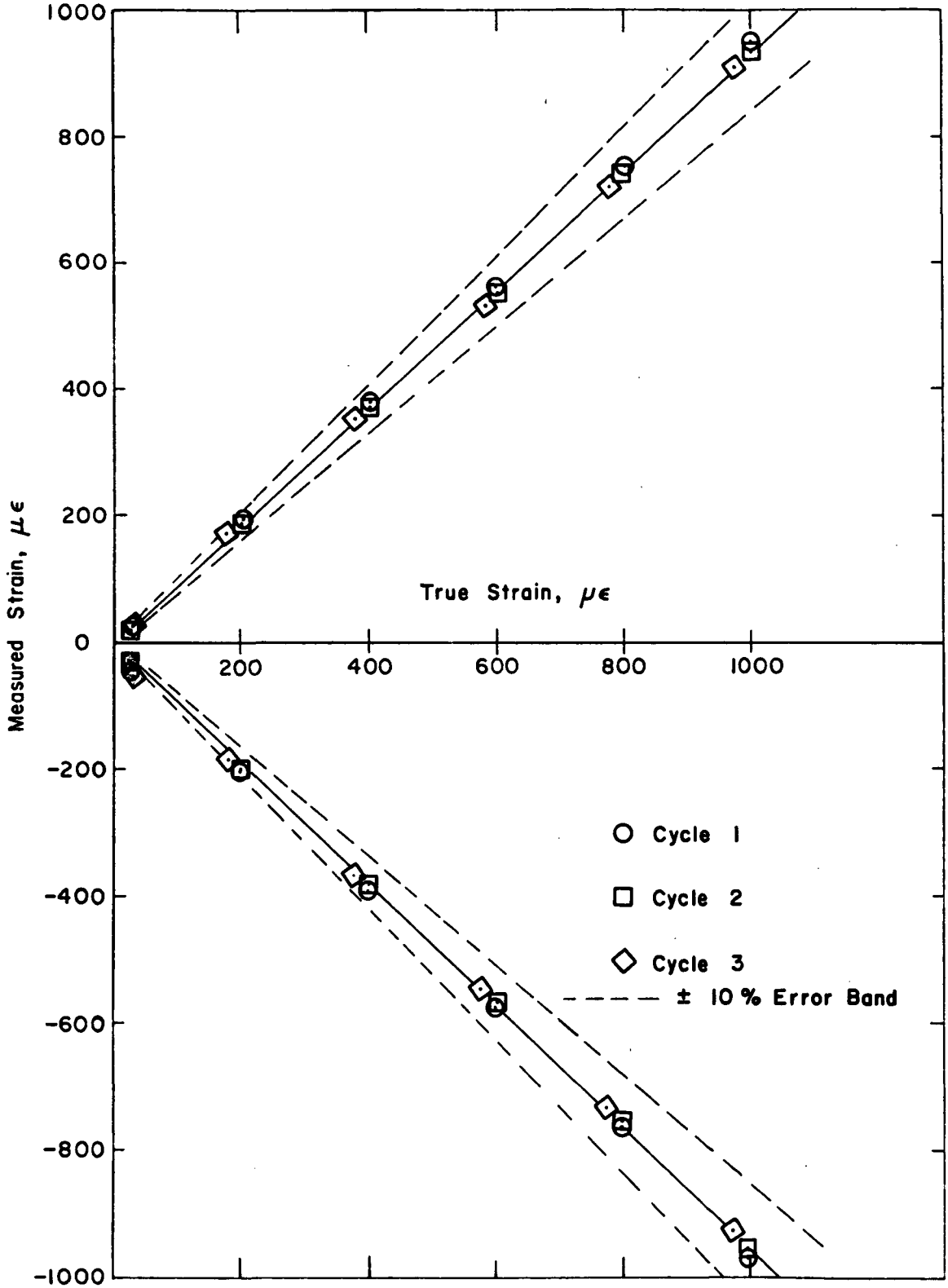

FIGURE 24. SPECIMEN H-27, GAGE FACTOR,1033°K (1400°F), CYCLES 1,2,3

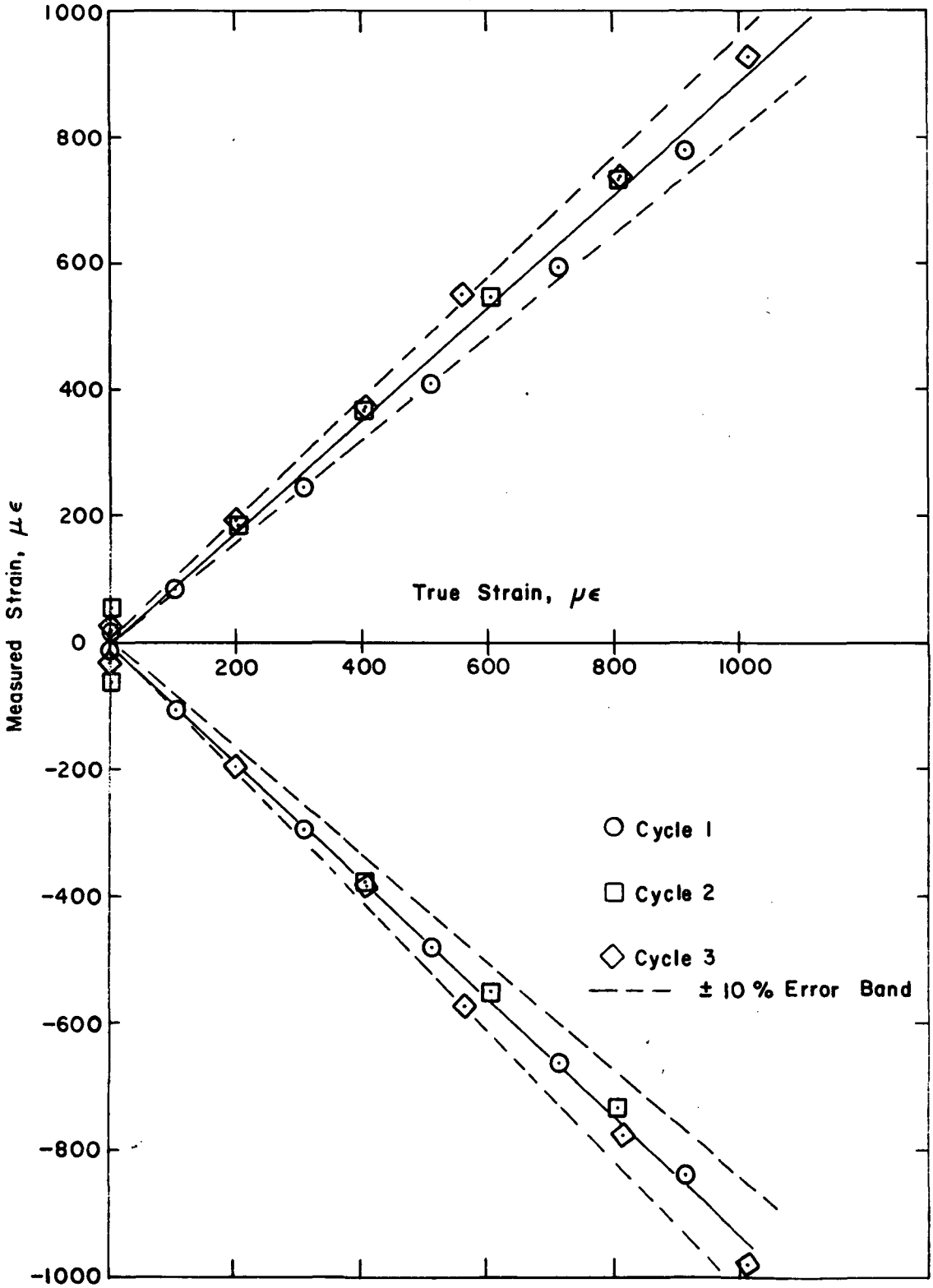

FIGURE 25. SPECIMEN H-27, GAGE FACTOR, 1144°K (1600°F), CYCLES 1,2,3

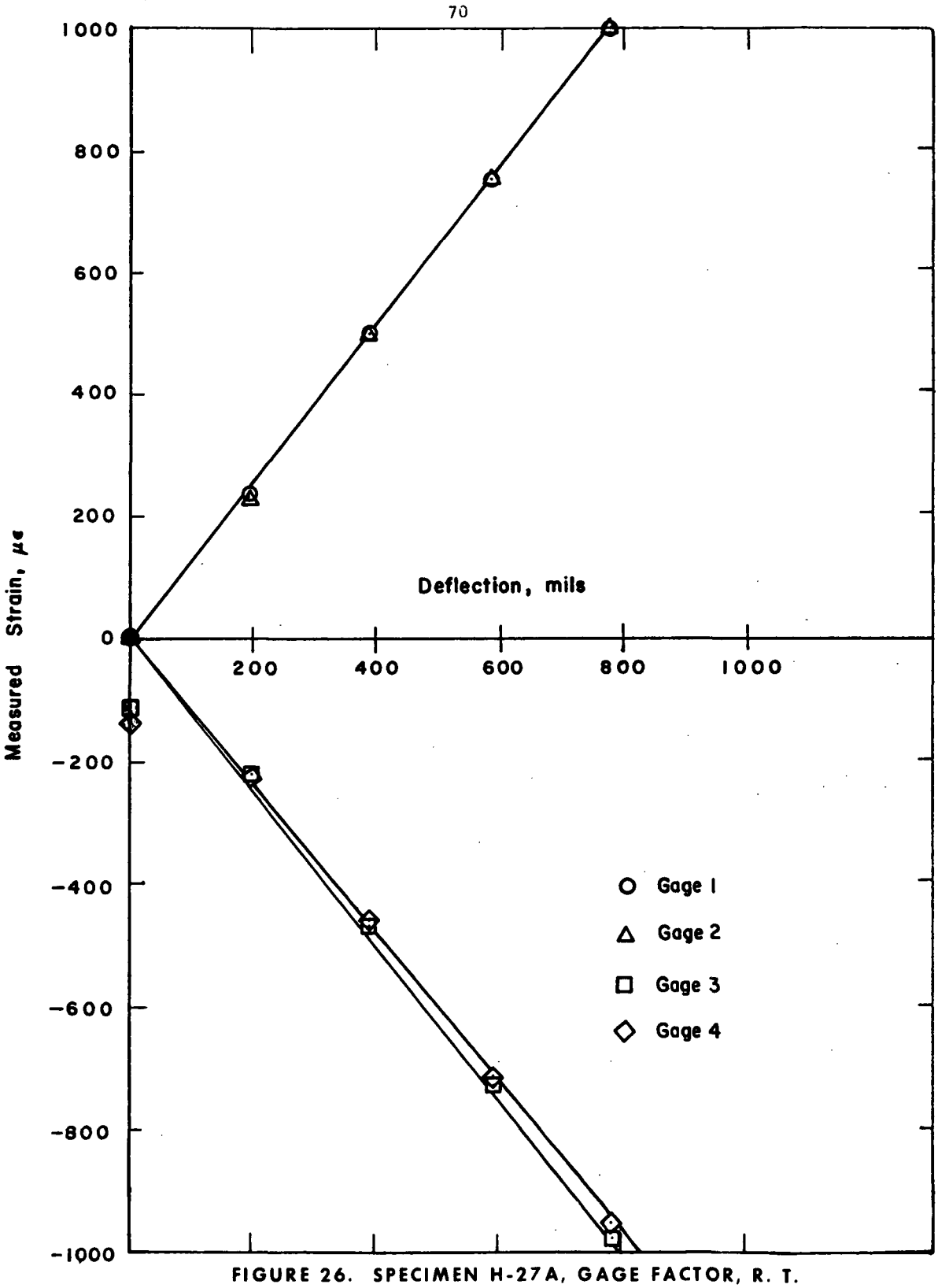

FIGURE 26. SPECIMEN H-27A, GAGE FACTOR, R. T.

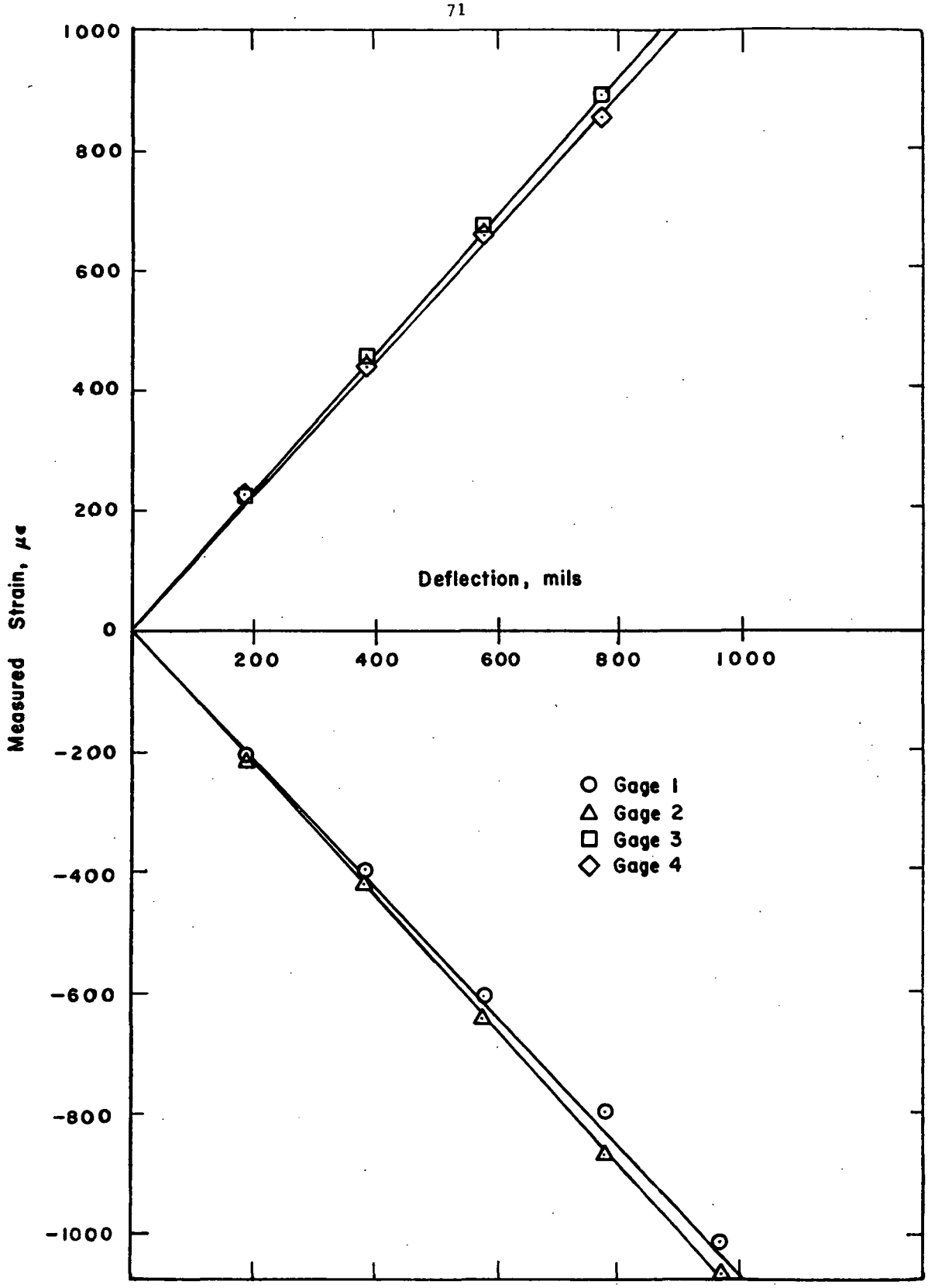

FIGURE 27. SPECIMEN H-27A, GAGE FACTOR, 700°K (800°F)

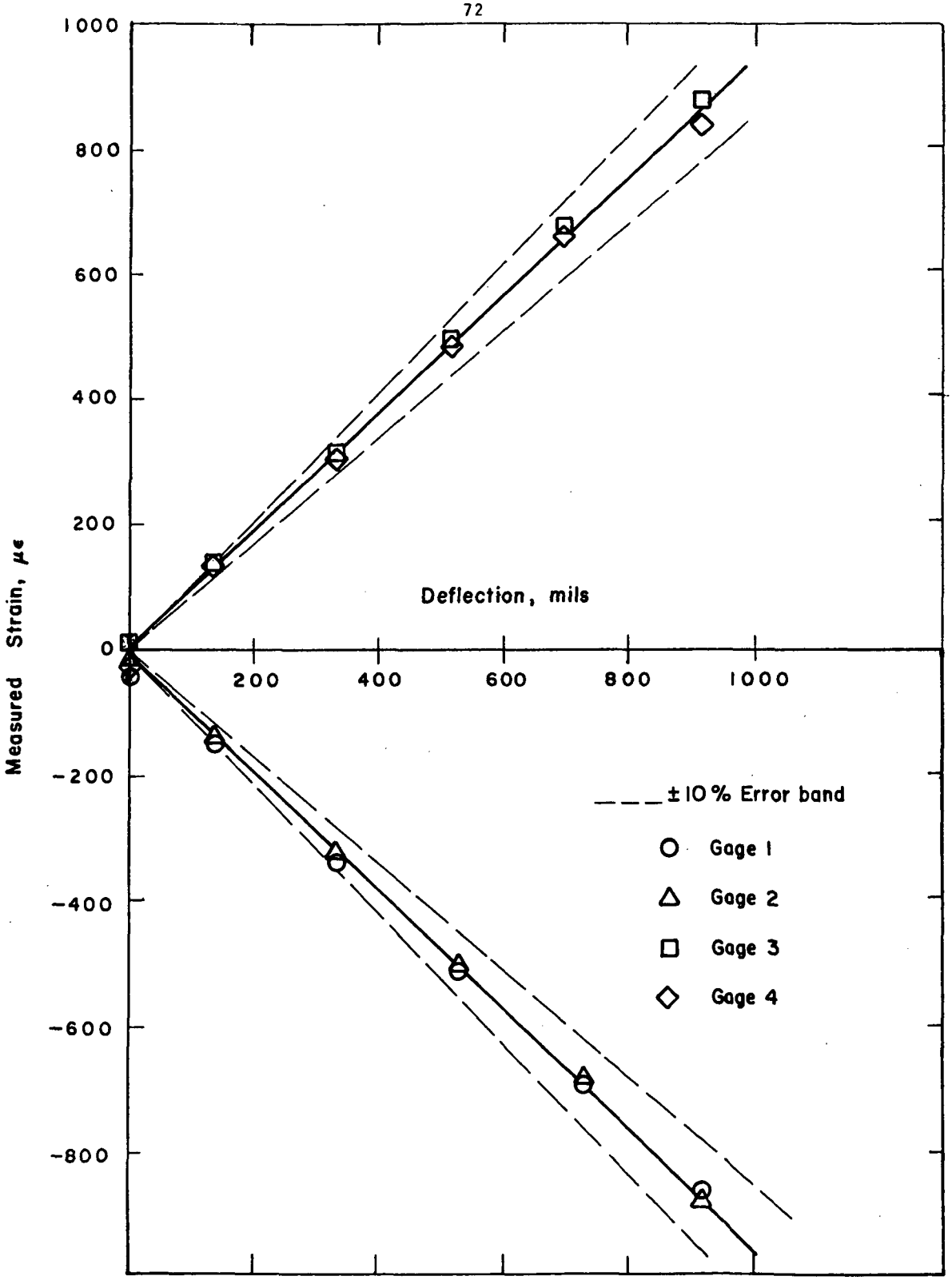

FIGURE 28. SPECIMEN H-27A, GAGE FACTOR, 1144°K (1600°F)

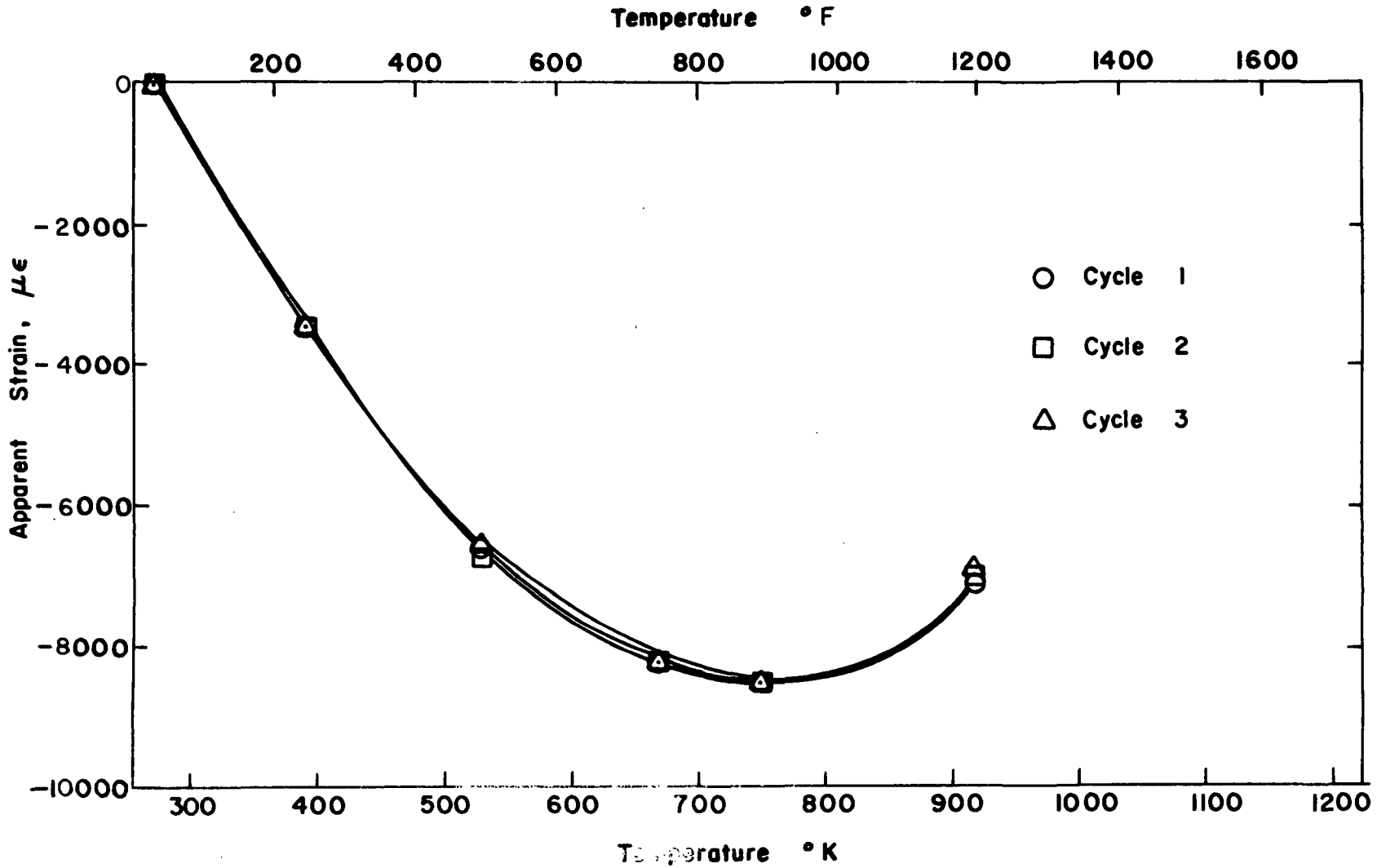

FIGURE 29. SPECIMEN H-21, APPARENT STRAIN TO 922°K (1200°F)

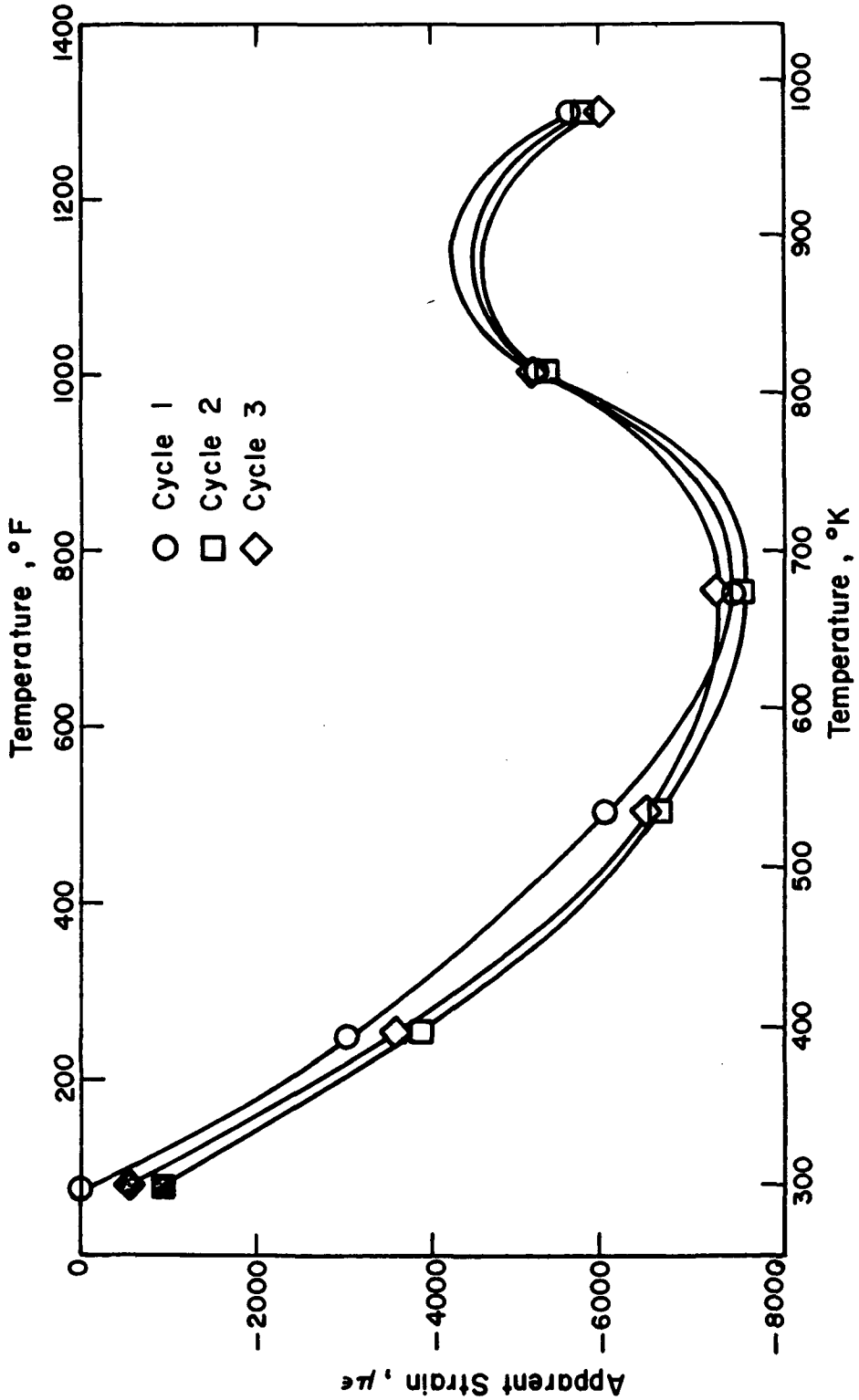

FIGURE 30. SPECIMEN H-21, APPARENT STRAIN TO 978°K (1300°F)

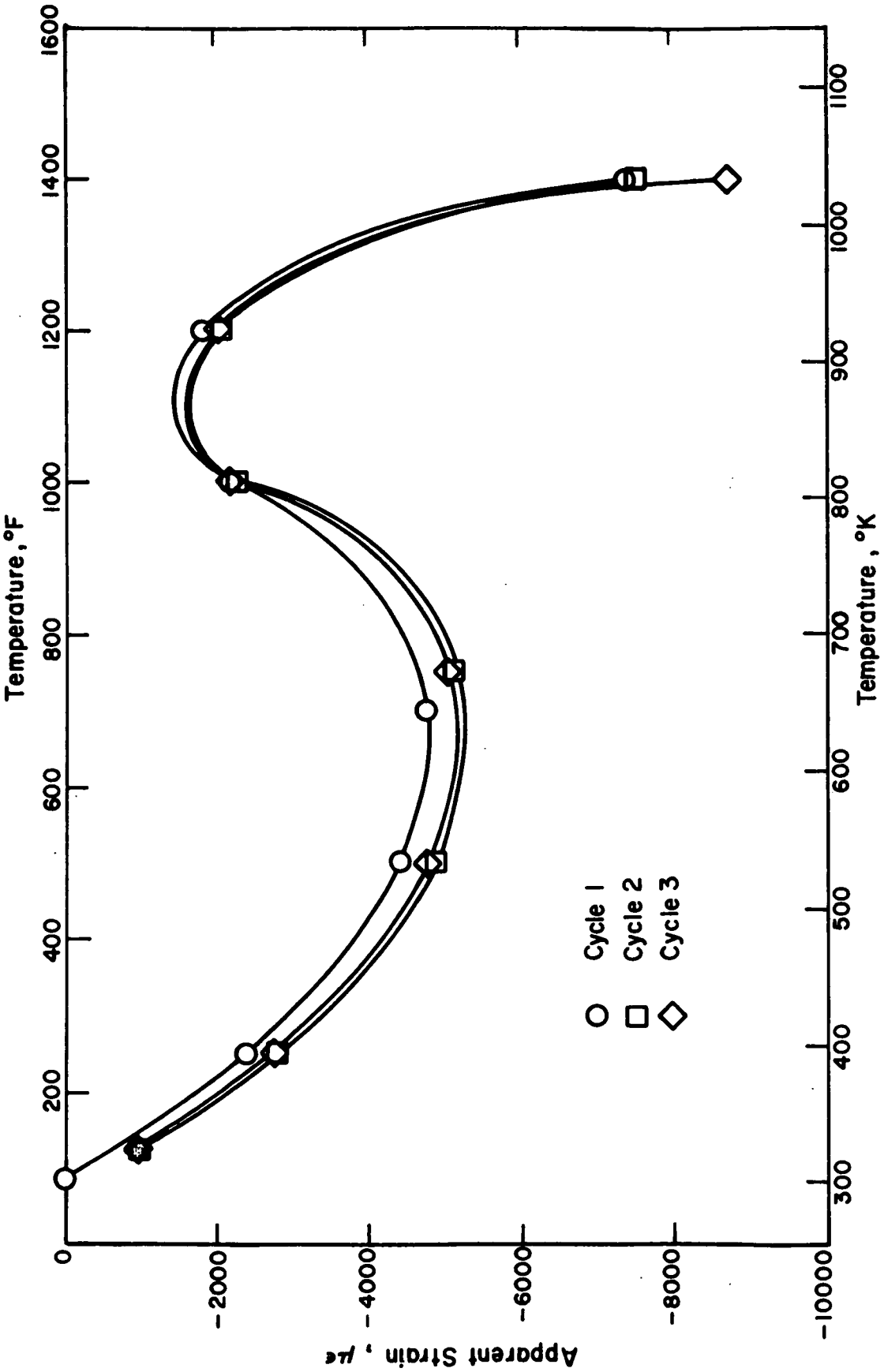

FIGURE 31. SPECIMEN H-21, APPARENT STRAIN TO 1033°K (1400°F)

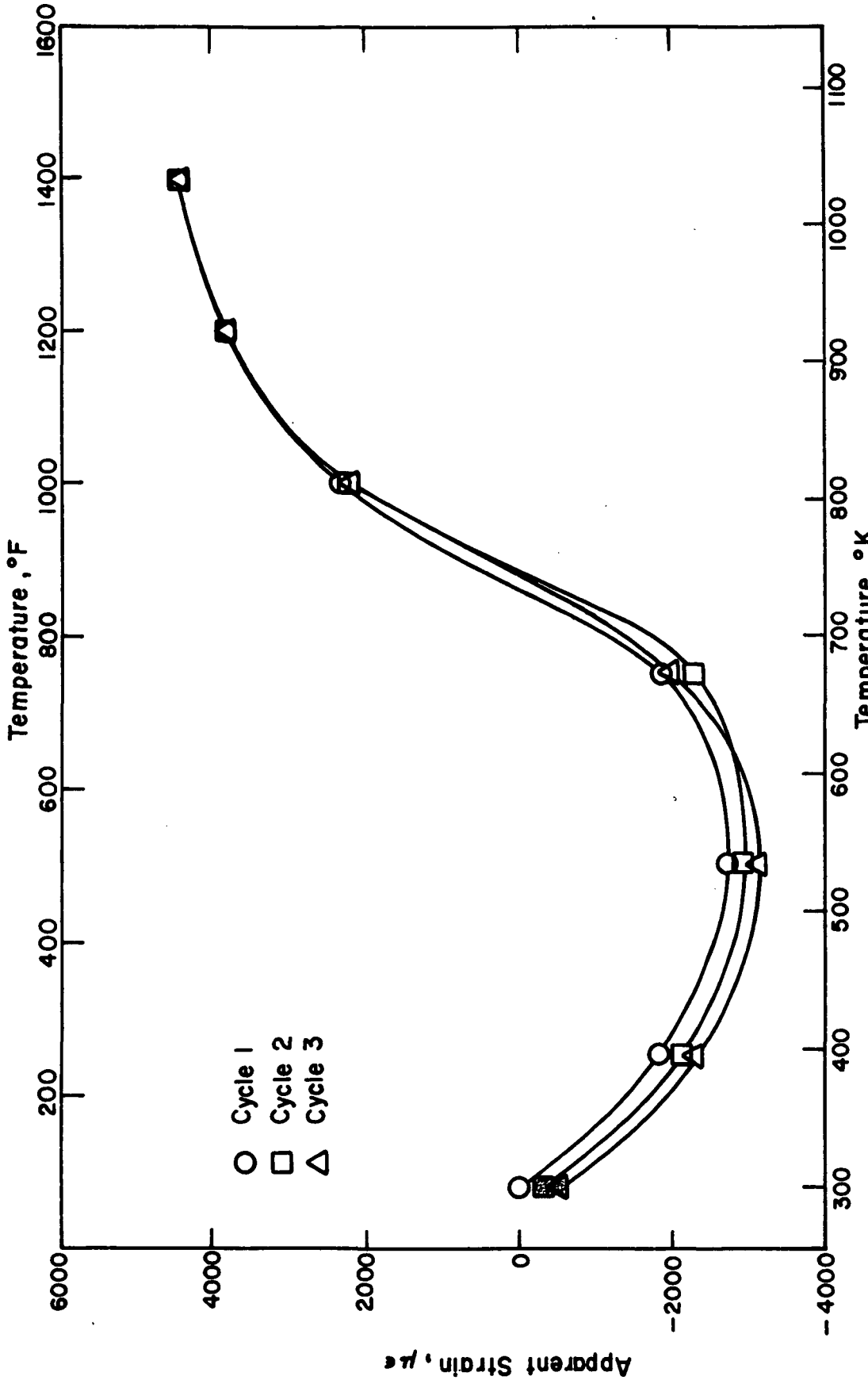

FIGURE 32. SPECIMEN H-22, APPARENT STRAIN TO 1033°K (1400°F)

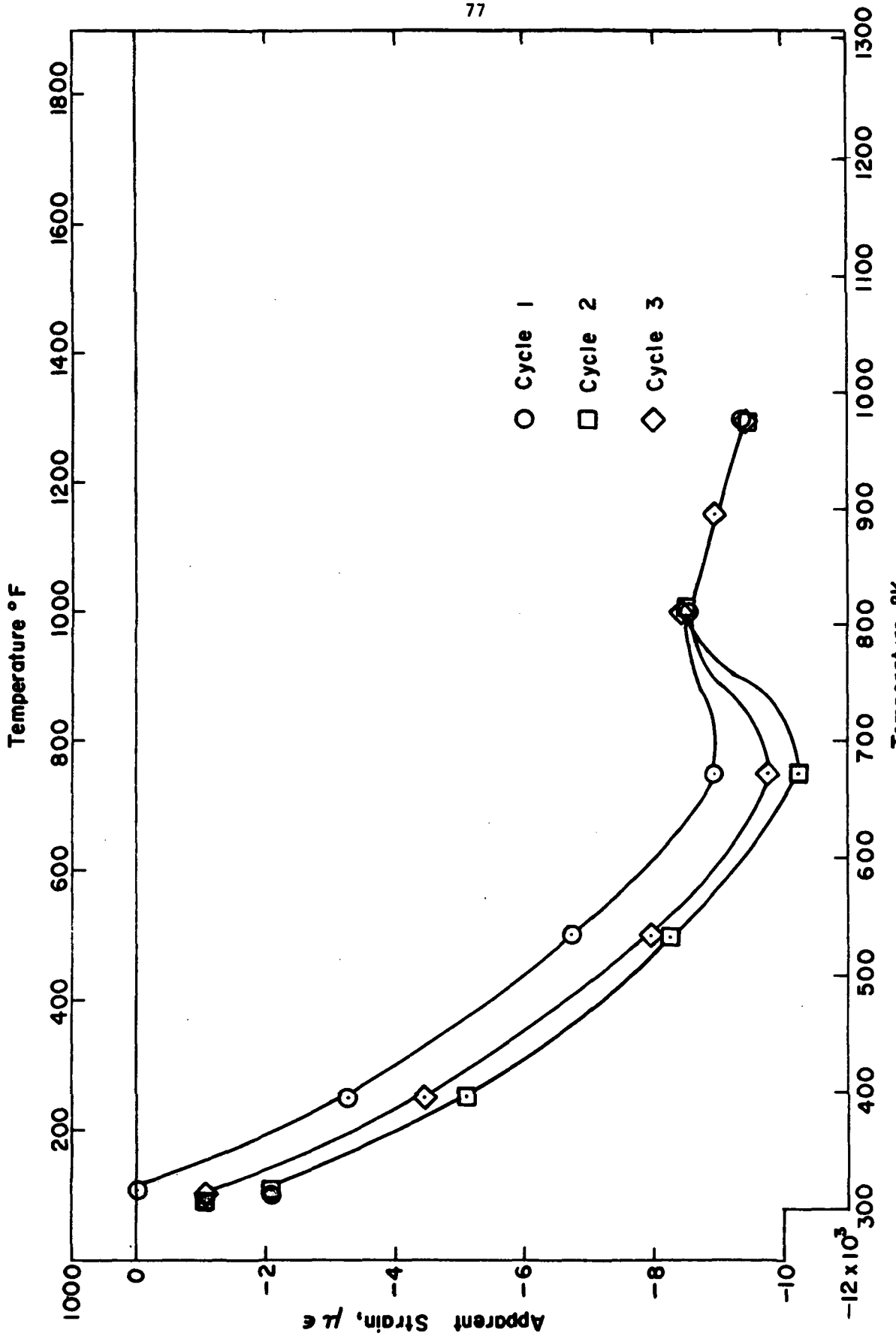

FIGURE 33. SPECIMEN H-23, APPARENT STRAIN TO 978°K (1300°F), CHROMEL A LEADS

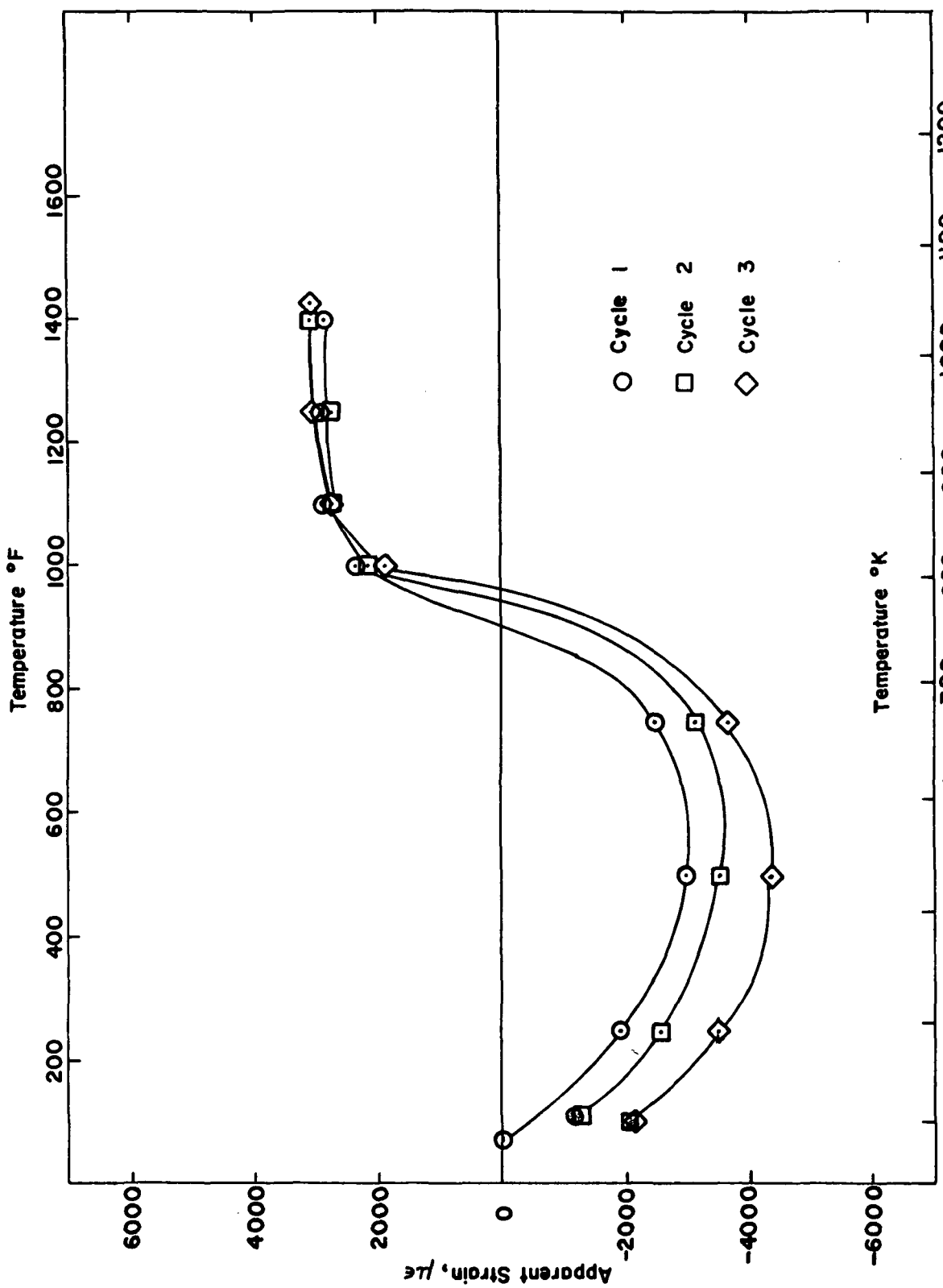

FIGURE 34. SPECIMEN H-23, APPARENT STRAIN TO 1033°K (1400°F), CHROMEL A LEADS

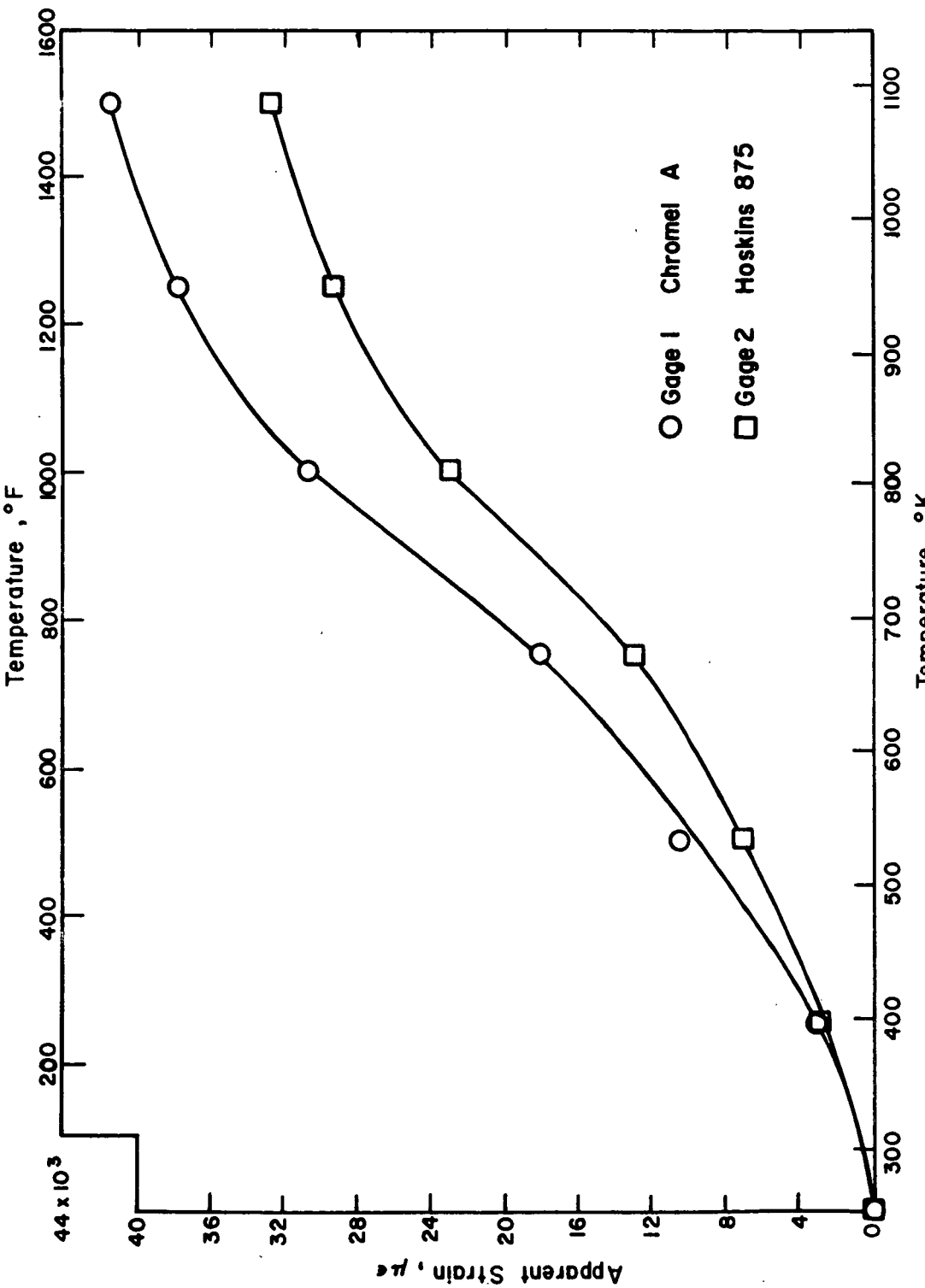

FIGURE 35. SPECIMEN H-25, APPARENT STRAINS TO 1085°K (1500°F), CHROMEL A AND HOSKINS 875 LEADS

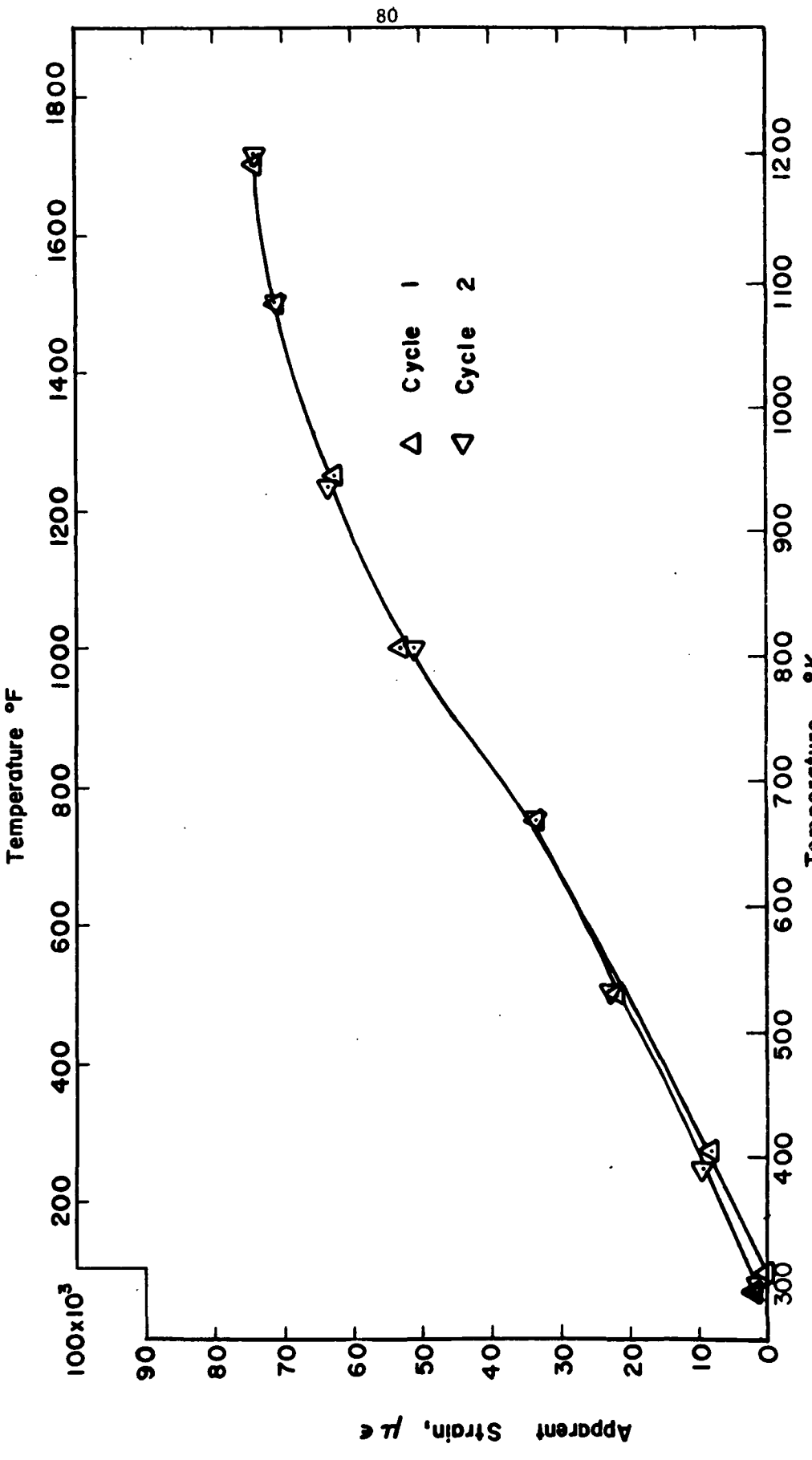

FIGURE 36. SPECIMEN H-25, APPARENT STRAIN TO 1198°K (1700°F), CHROMEL A LEADS

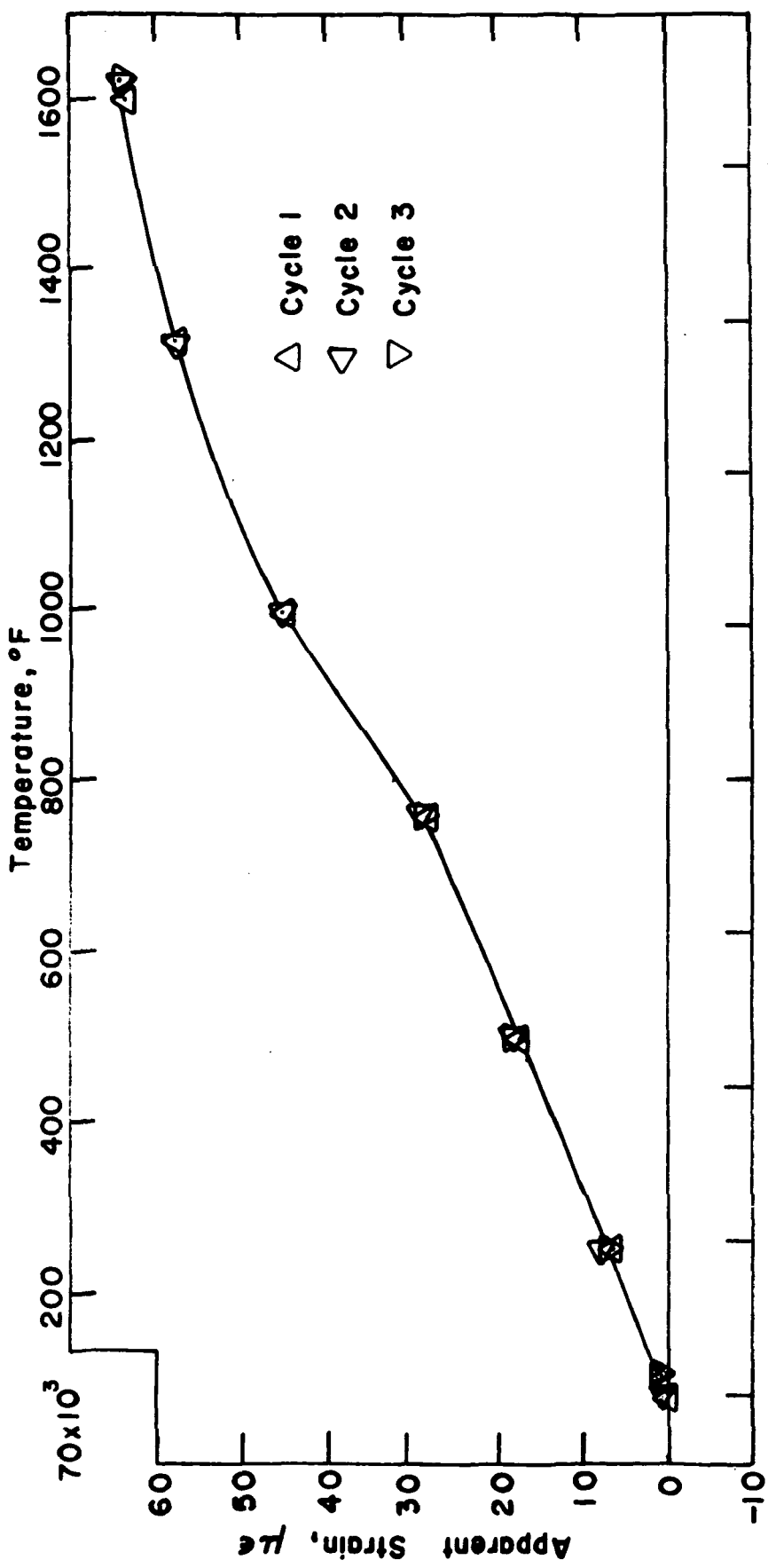

FIGURE 37. SPECIMEN H-26, APPARENT STRAIN TO 1144°K (1600°F), CHROMEL A LEADS

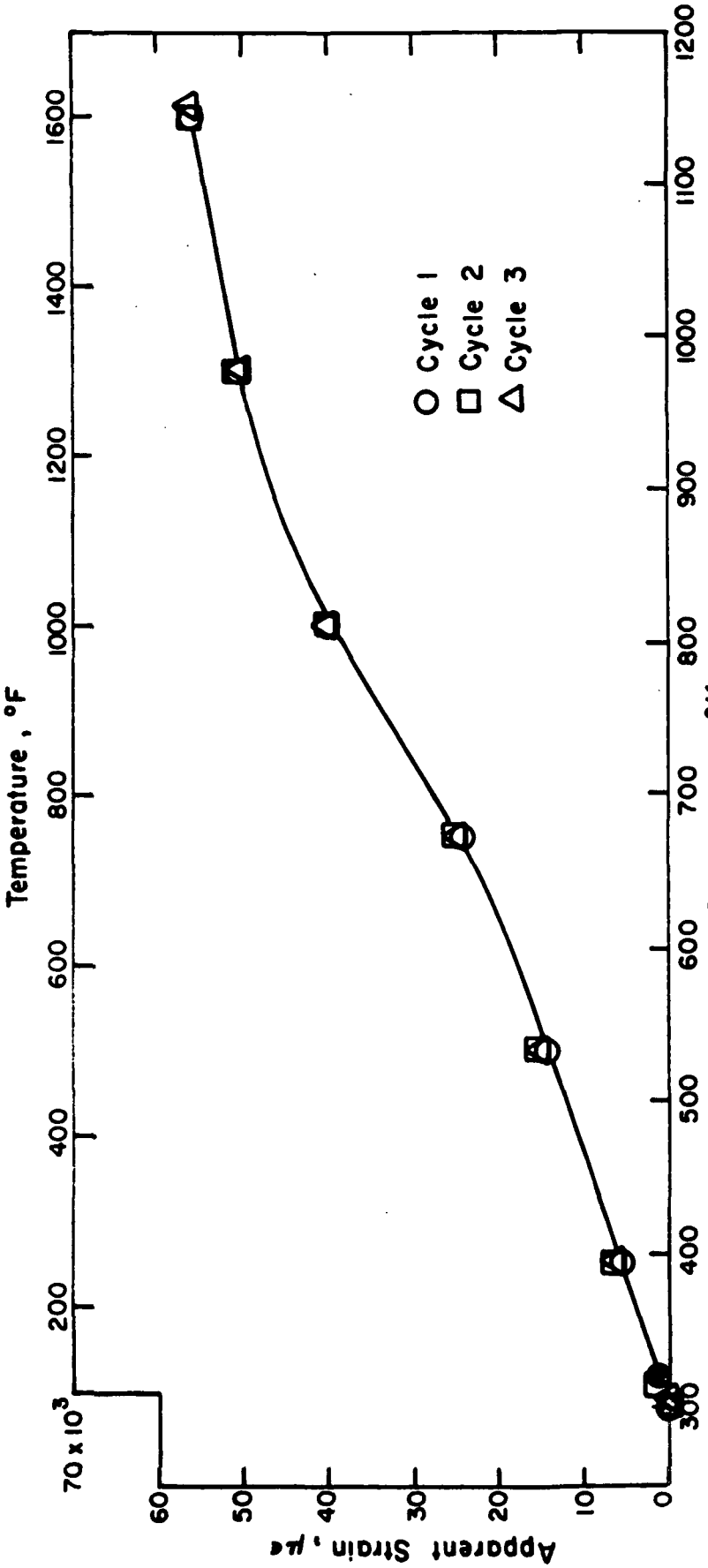

FIGURE 38. SPECIMEN H-26, APPARENT STRAIN TO 1144°K (1600°F), HOSKINS 875 LEADS

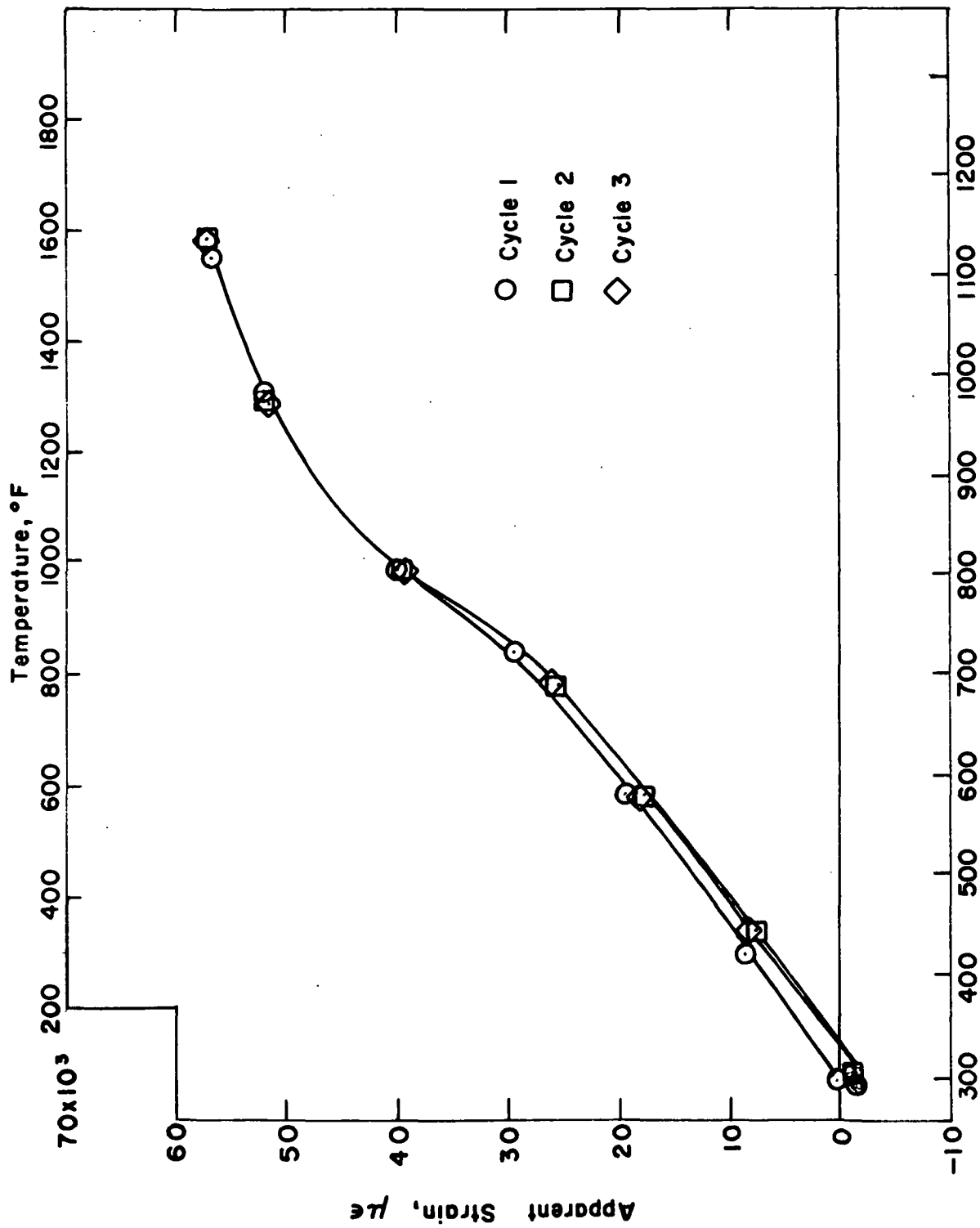

FIGURE 39. SPECIMEN H-27, APPARENT STRAIN TO 1144°K (1600°F)

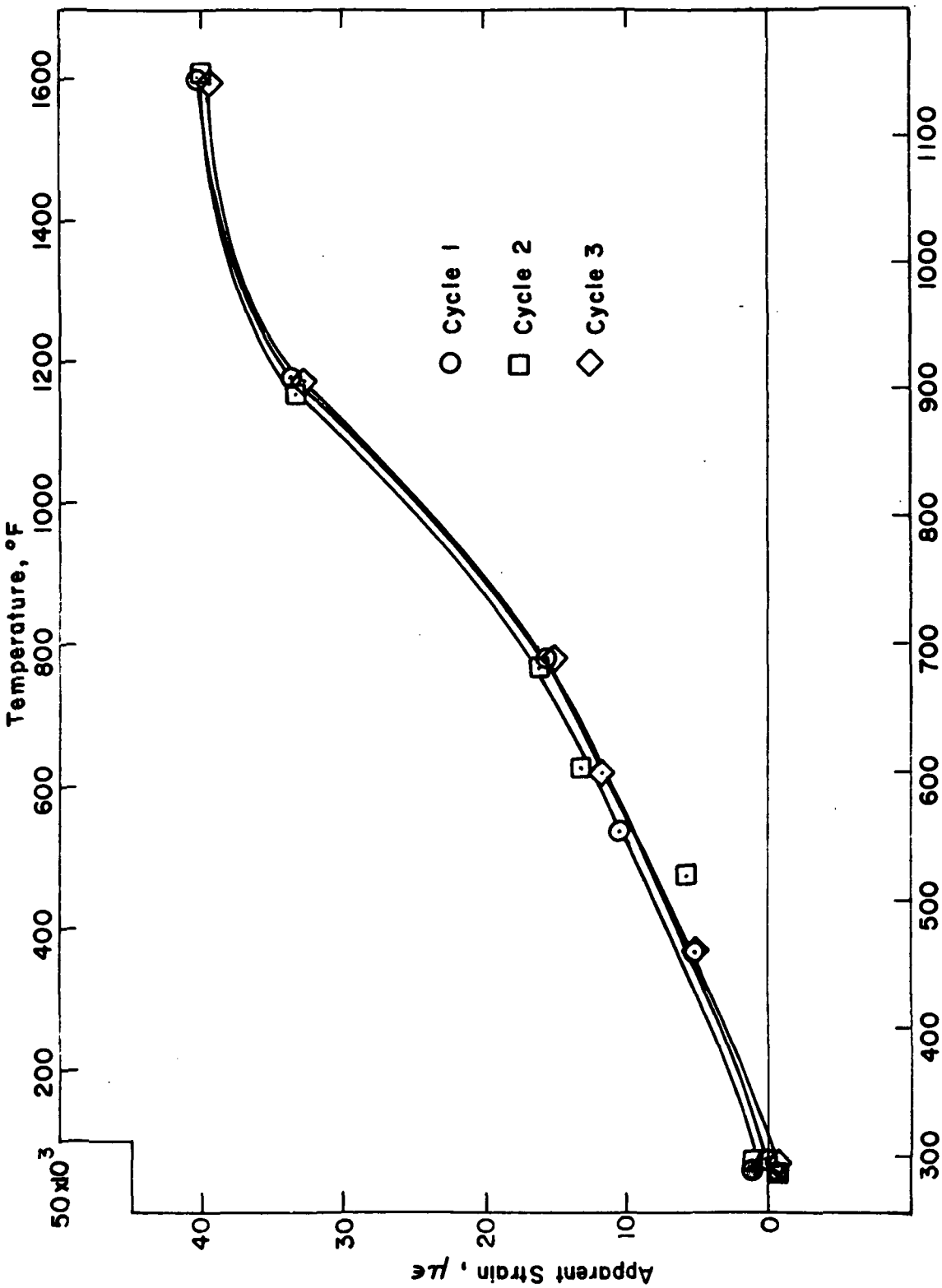

FIGURE 40. SPECIMEN H-27A, APPARENT STRAIN TO 1144°K (1600°F)

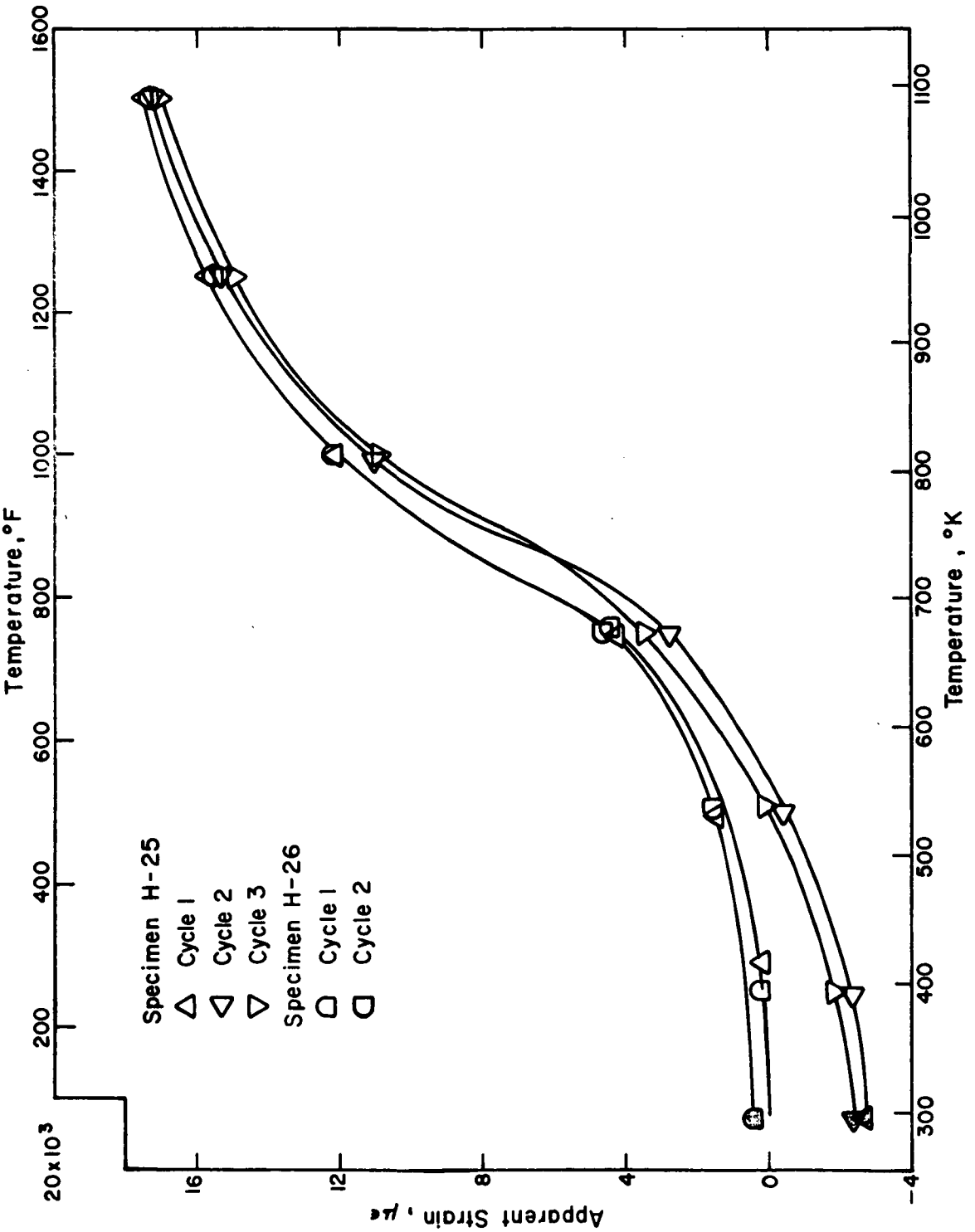

FIGURE 41. SPECIMENS H-25, H-26, APPARENT STRAINS TO 1085°K (1500°F) CHROMEL A LEADS

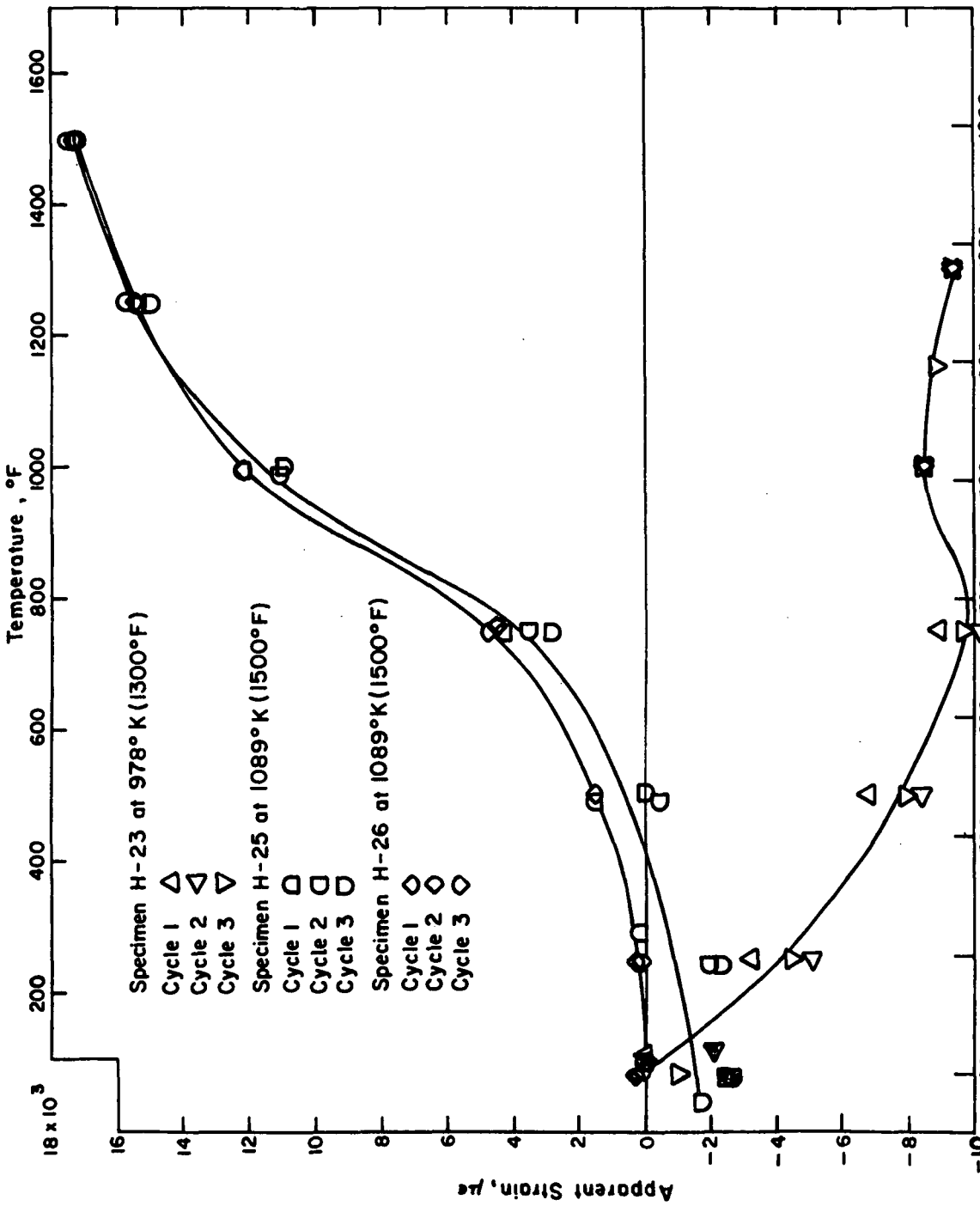

FIGURE 42. SPECIMENS H-23, H-25, H-26, APPARENT STRAINS, CHROMEL A LEADS

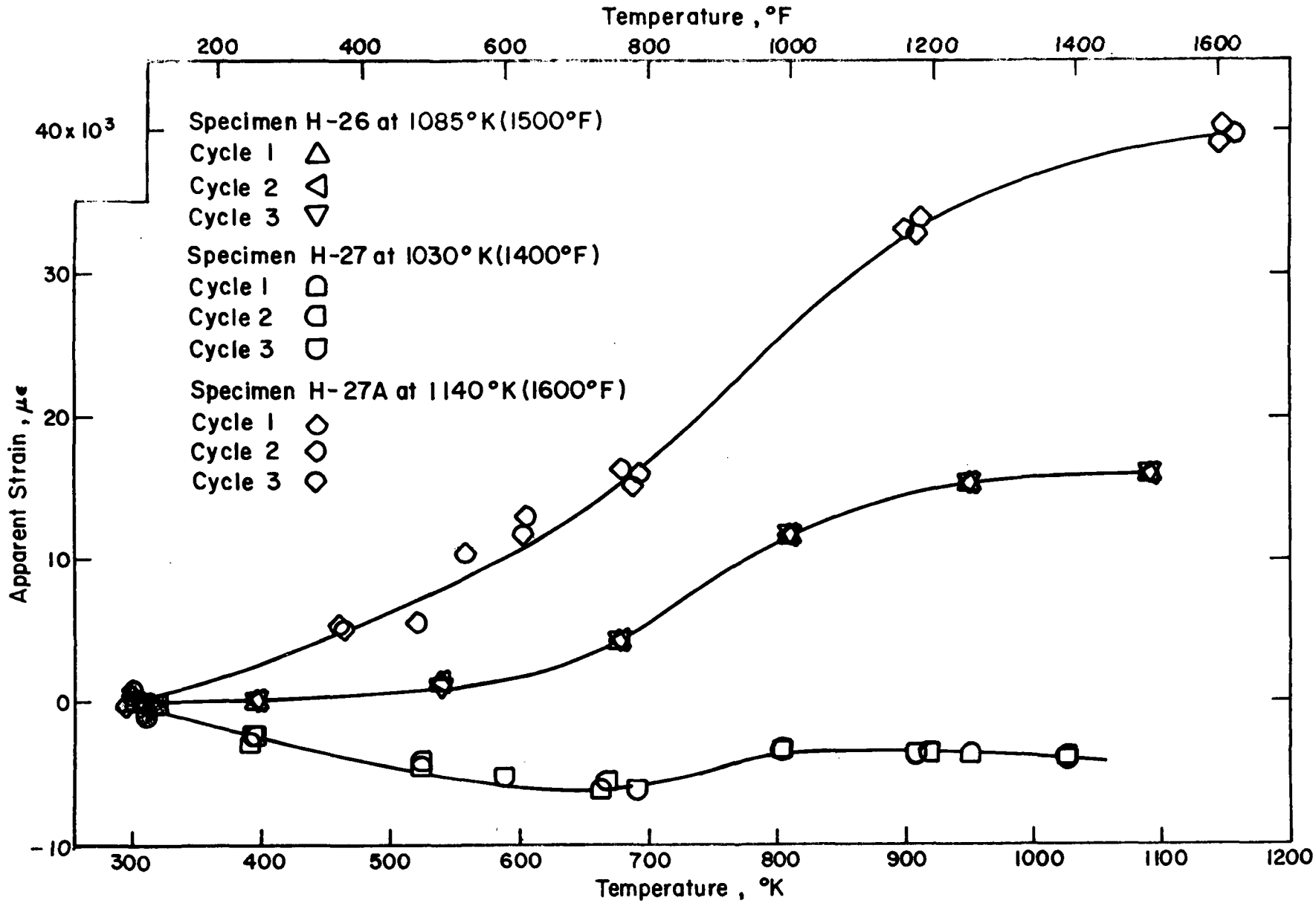

FIGURE 43. SPECIMENS H-26, H-27, H-27A, APPARENT STRAINS, HOSKINS LEADS

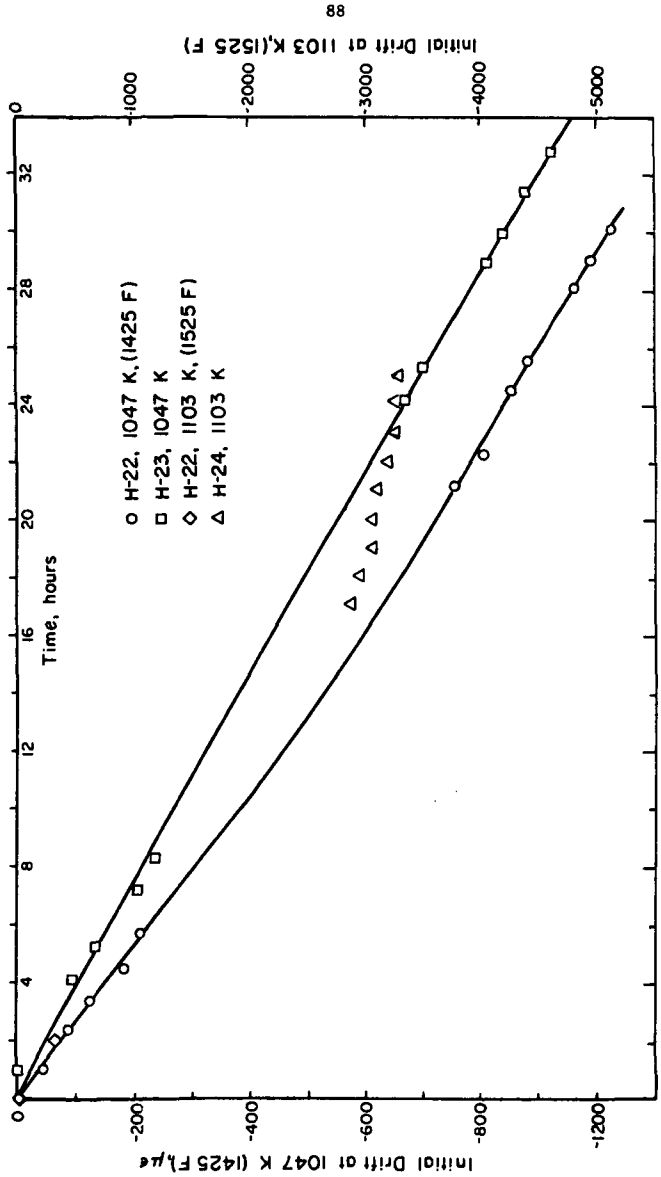

FIGURE 44. SPECIMENS H-22, H-23, H-24, INITIAL DRIFTS AT VARING TEMPERATURES, CHROMEL A LEADS

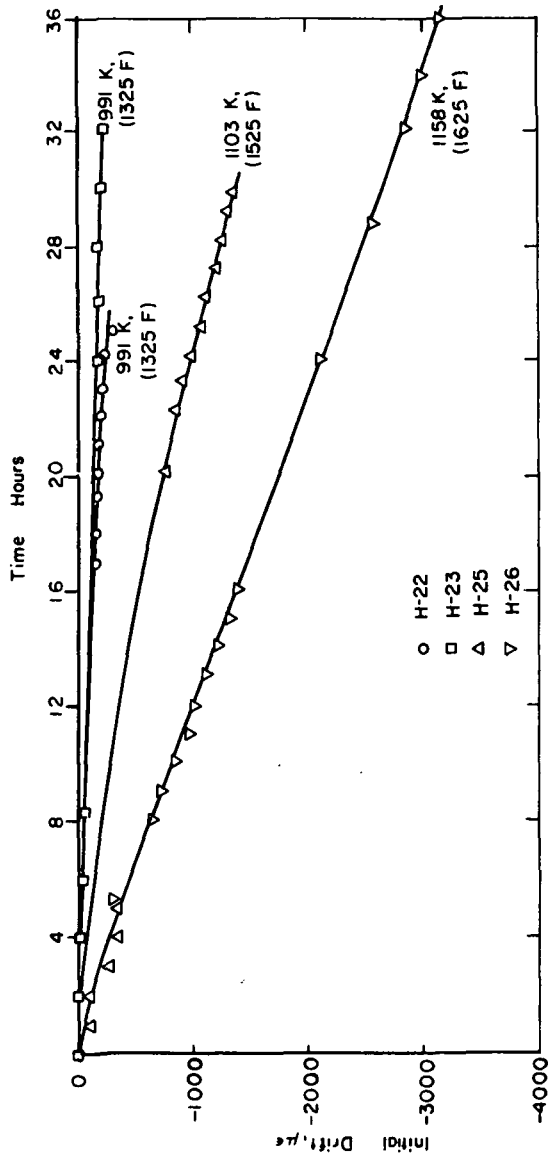

FIGURE 45. SPECIMENS H-22, H-23, H-25, H-26, INITIAL DRIFTS AT VARYING TEMPERATURES, CHROMEL A LEADS

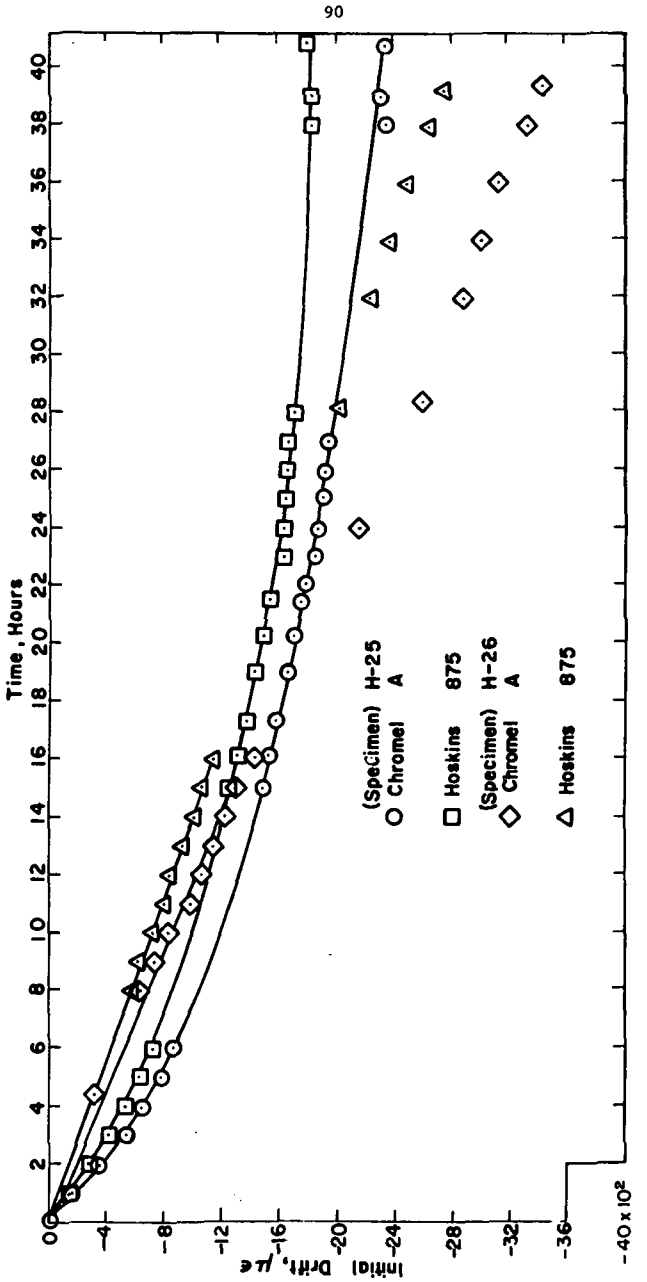

FIGURE 46. SPECIMENS H-25, H-26, INITIAL DRIFTS AT 1200°K (1700°F)

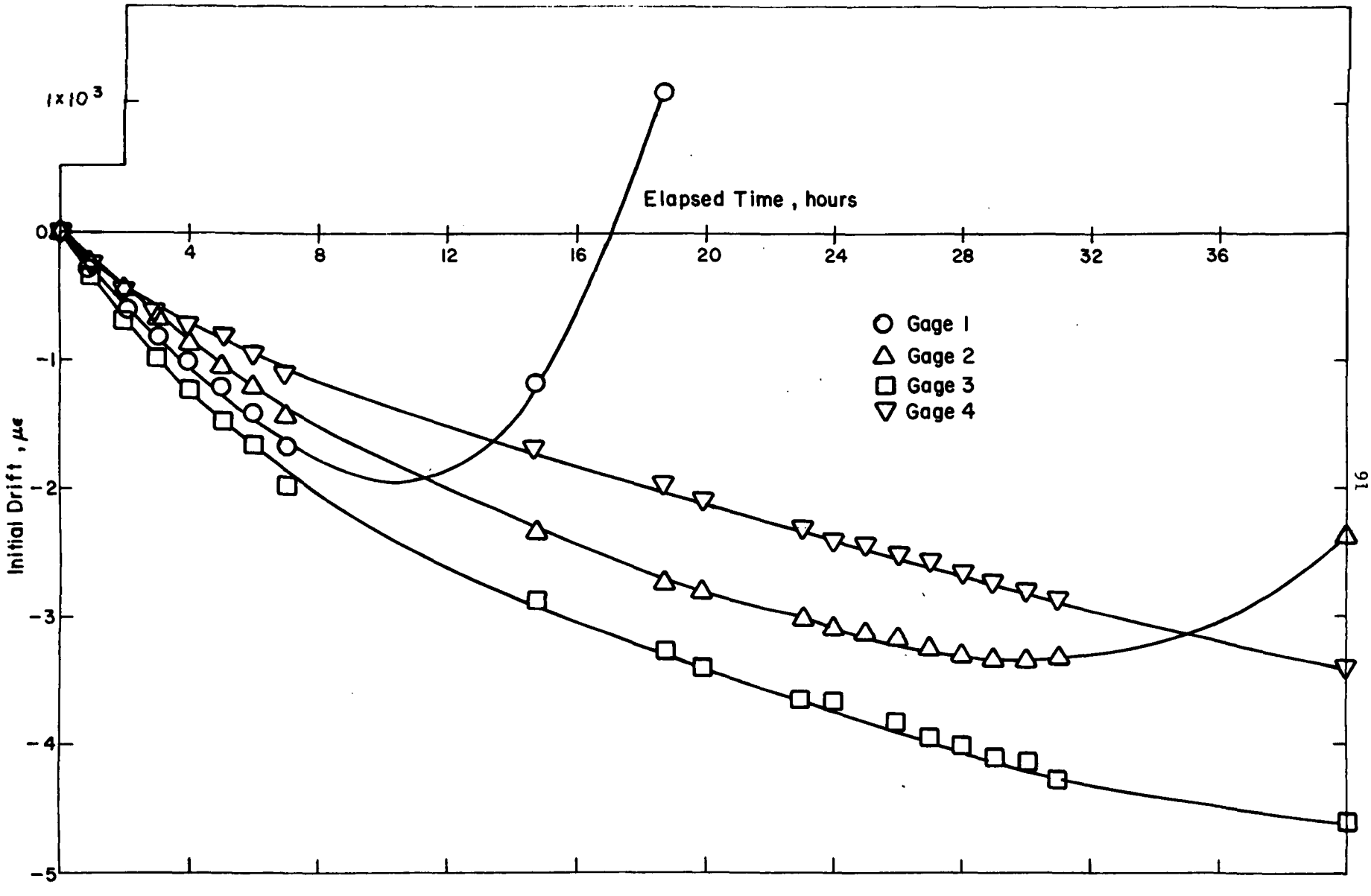

FIGURE 47. SPECIMEN H-26, INITIAL DRIFT AT 1269°K (1825°F)

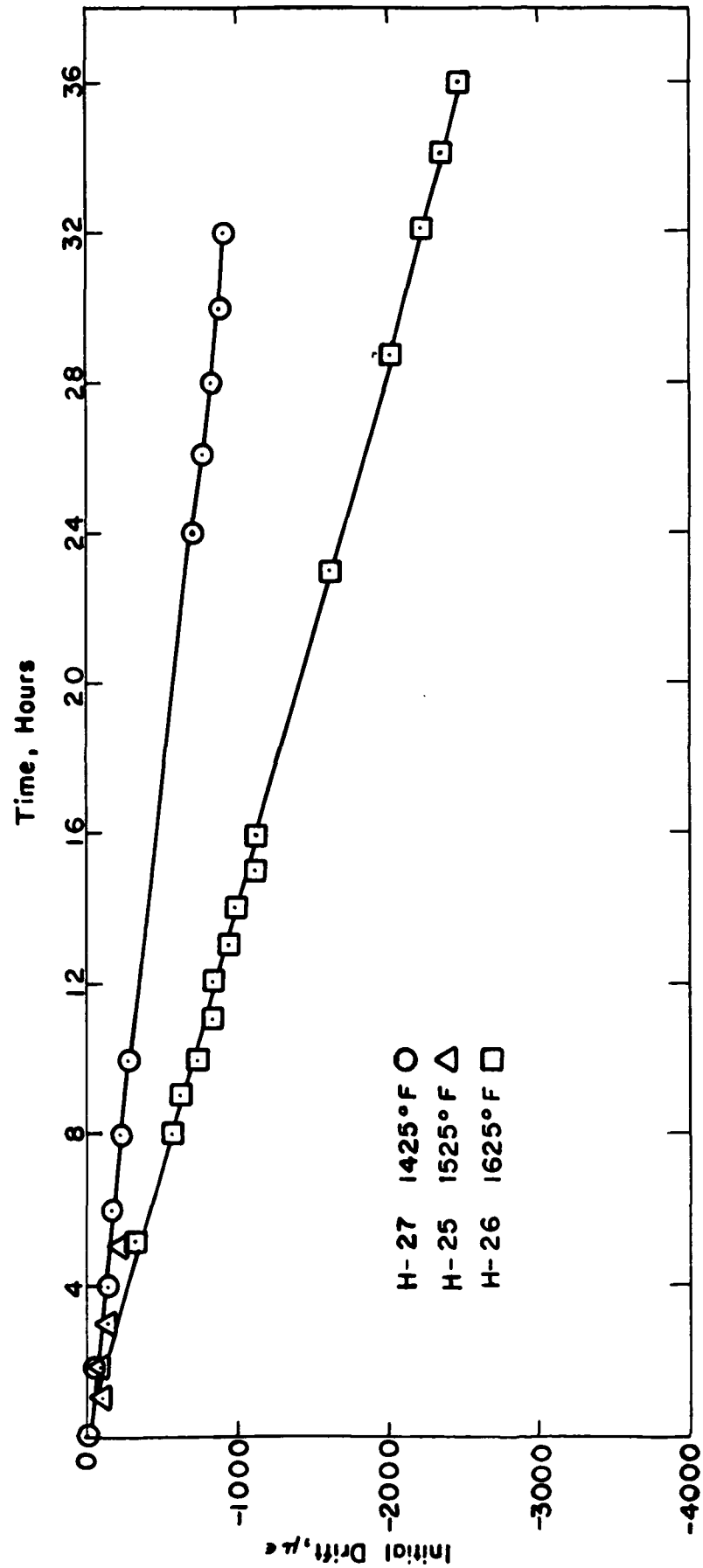

FIGURE 48. SPECIMENS H-25, H-26, H-27, INITIAL DRIFTS AT VARYING TEMPERATURES, HOSKINS 875 LEADS

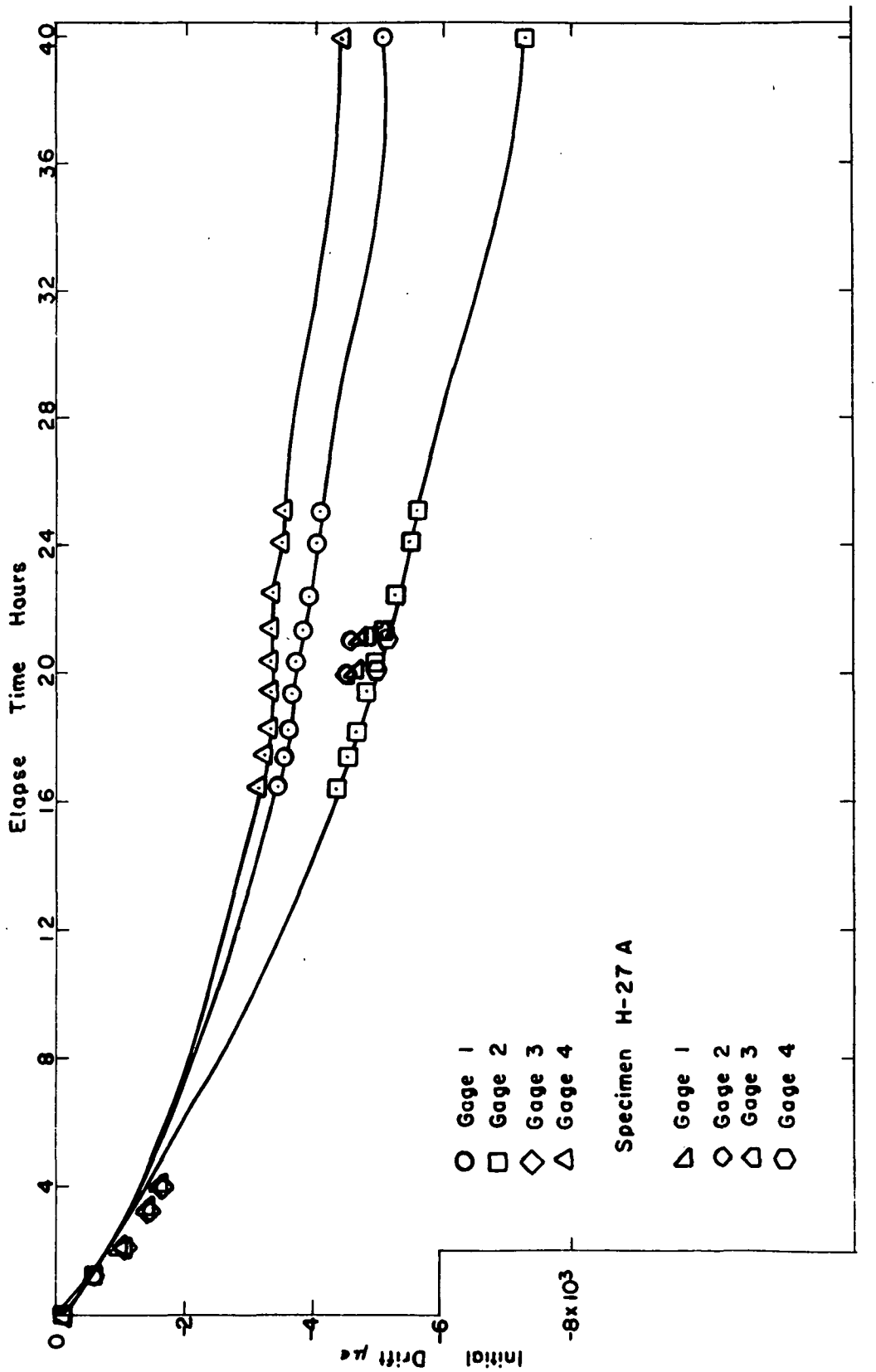

FIGURE 49. SPECIMENS H-27, H-27A INITIAL DRIFTS AT 1158°K (1625°F)

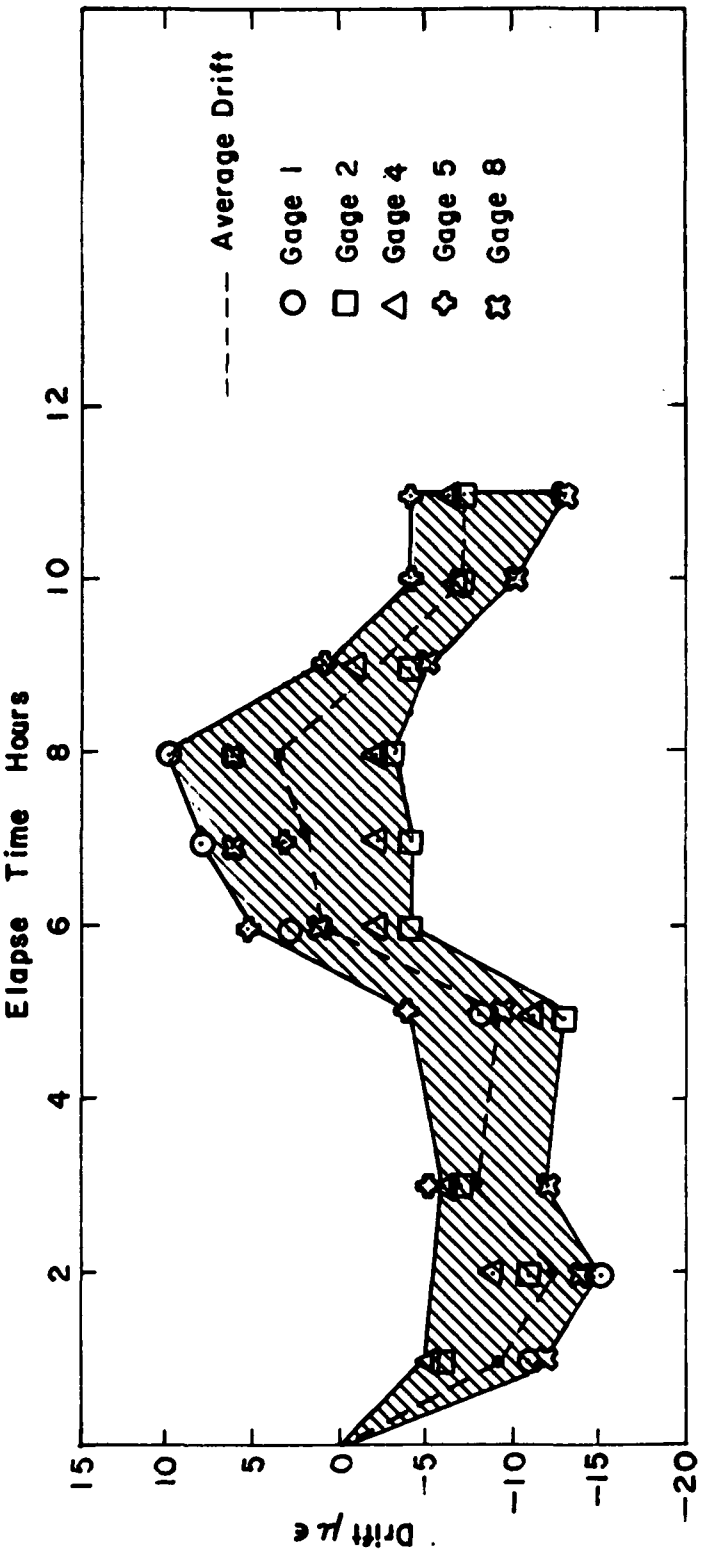

FIGURE 50. SPECIMEN H-21, DRIFT AT 922°K (1200°F)

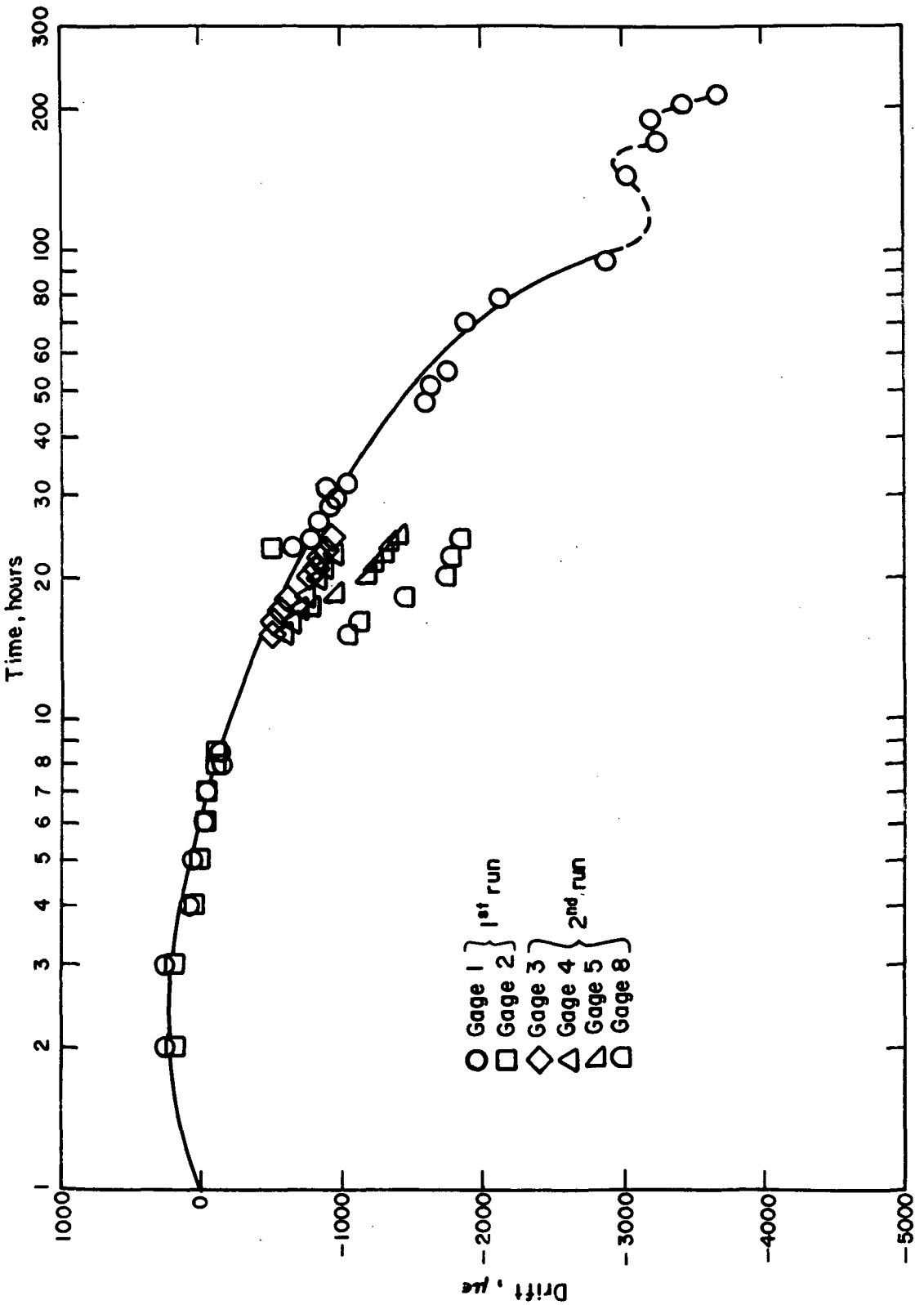

FIGURE 51. SPECIMEN H-21, DRIFT AT 1033°K (1400°F)

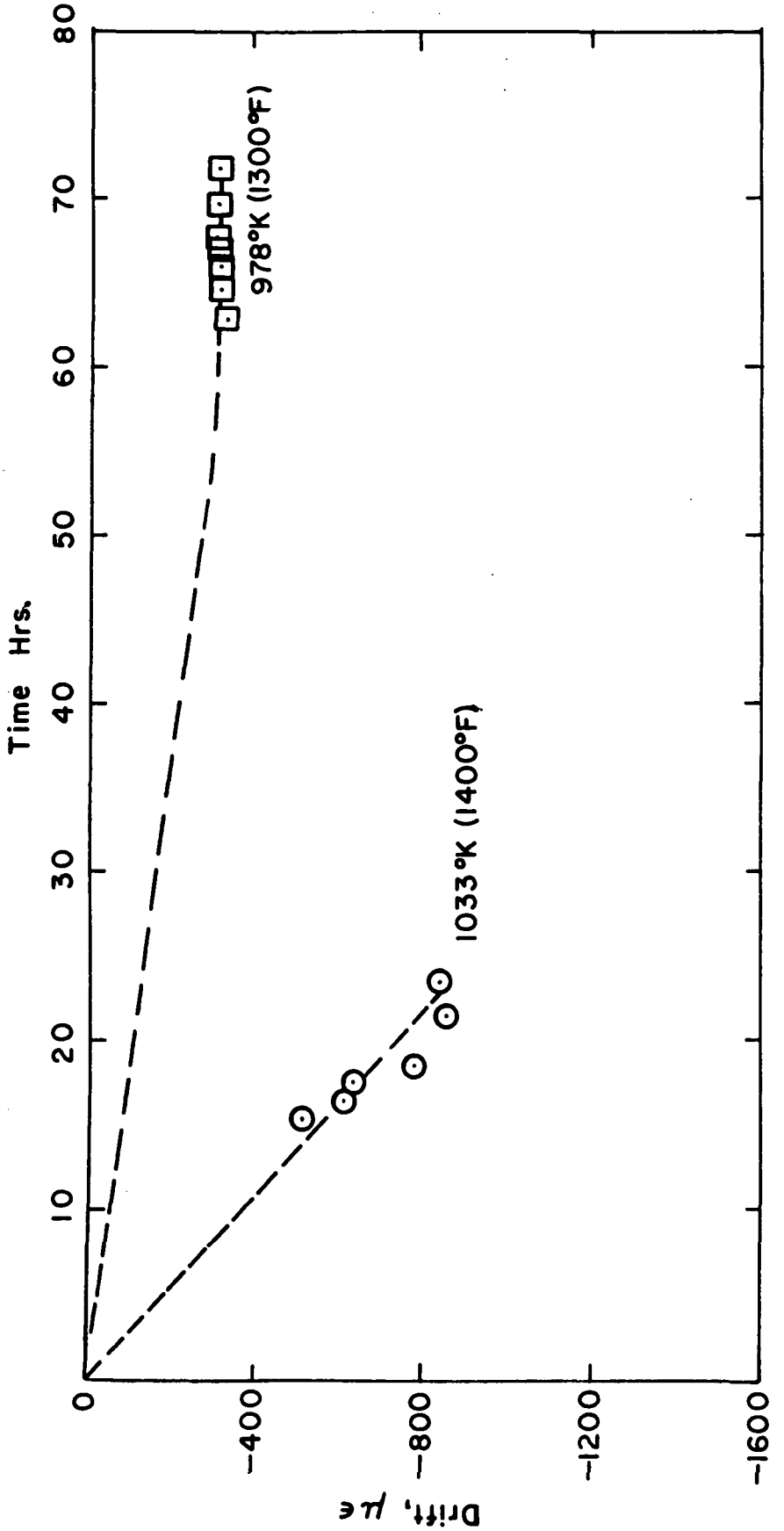

FIGURE 52. SPECIMEN H-23, DRIFT @ 978°K (1300°F) AND 1033°K (1400°F)

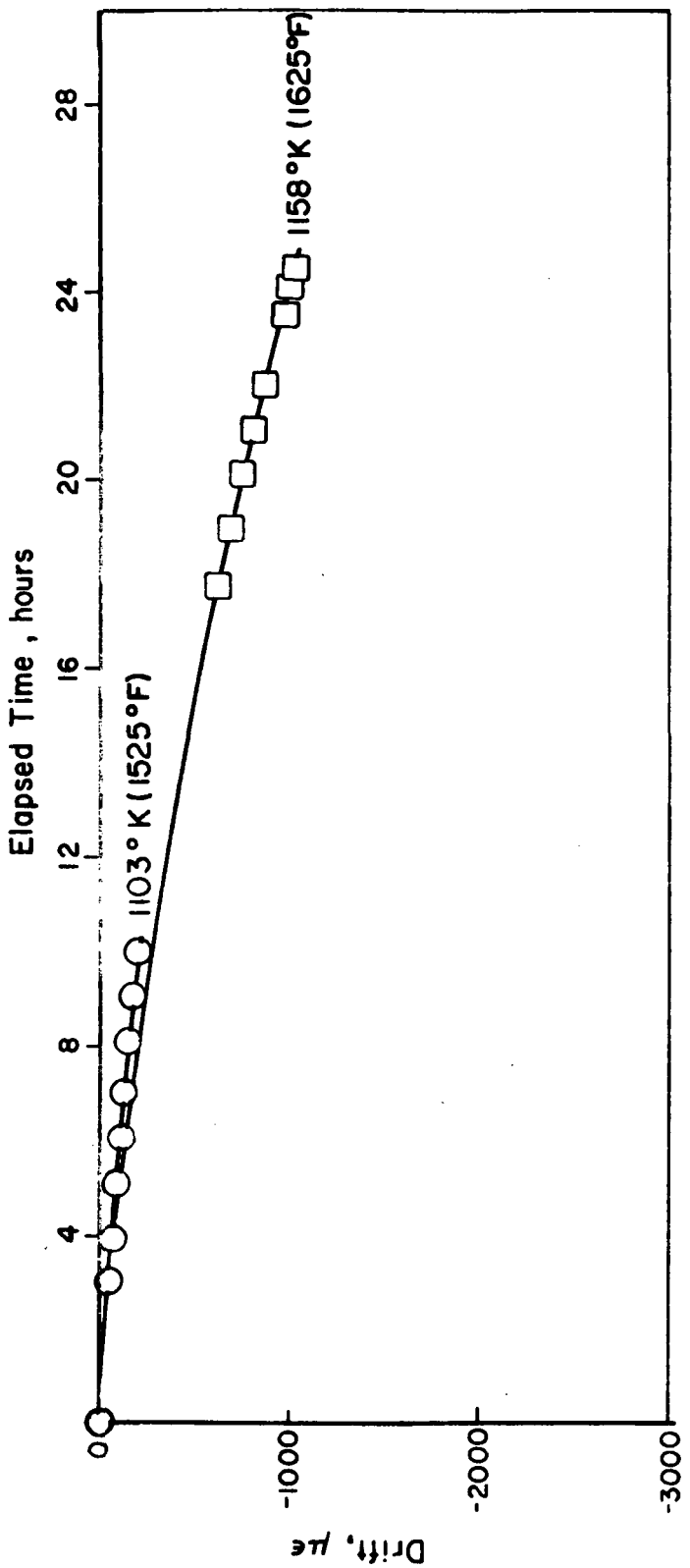

FIGURE 53. SPECIMEN H—26, DRIFT AT 1089° K (1500° F) AND 1144° K (1600° F), CHROMEL A LEADS

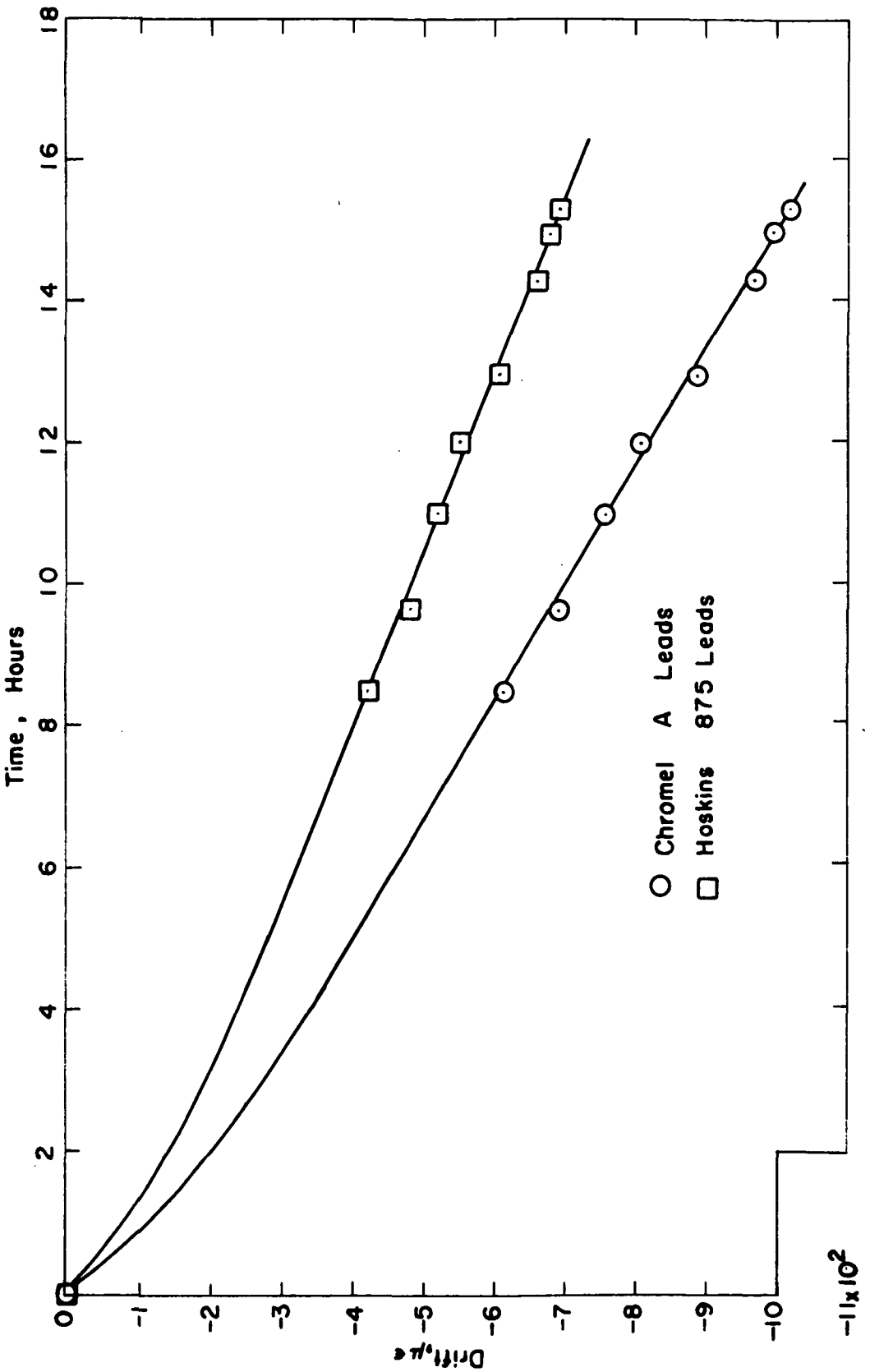

FIGURE 54. SPECIMEN H-26 DRIFTS AT 1144°K (1600°F), CHROMEL A AND HOSKINS 875 LEADS

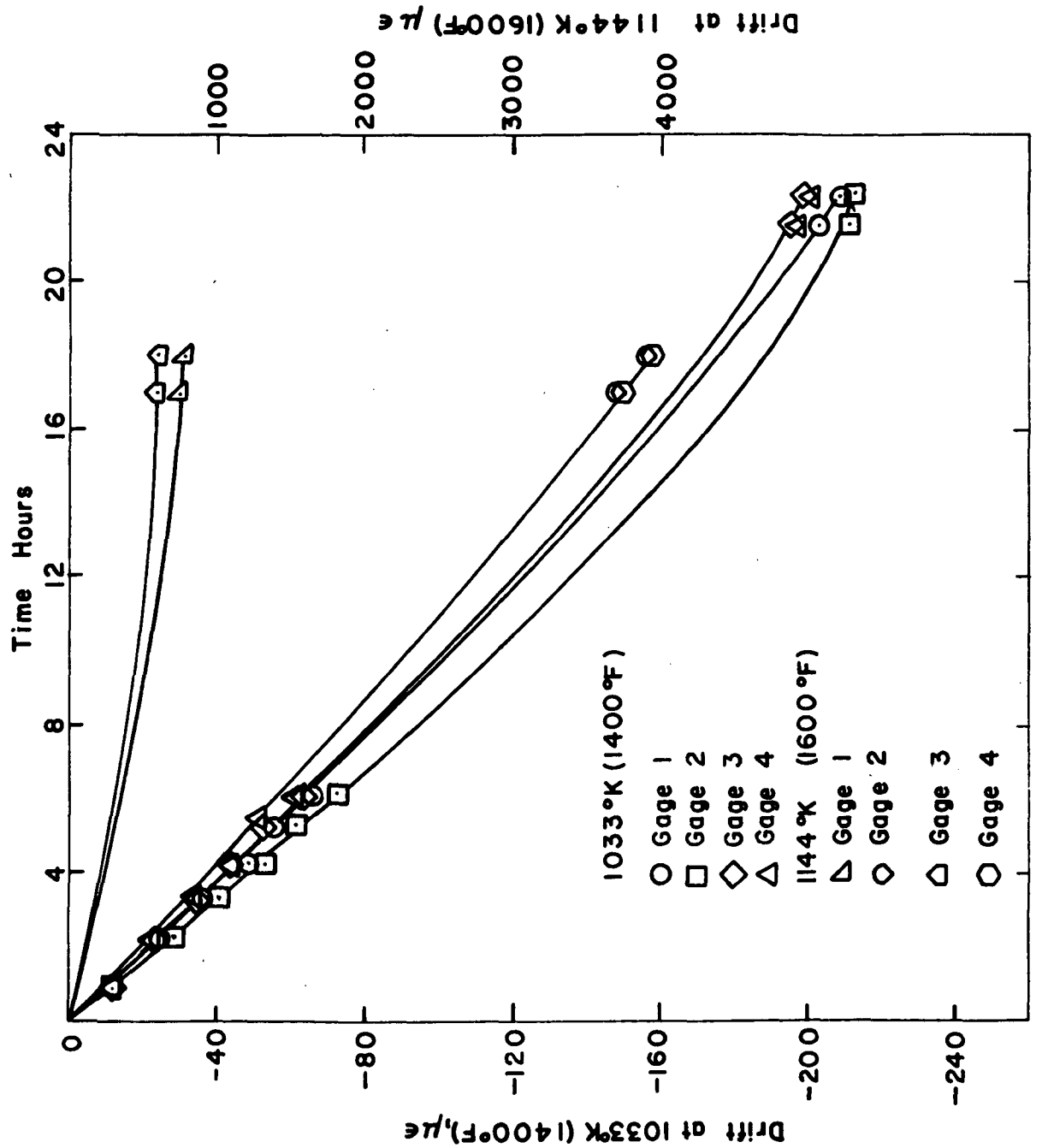

FIGURE 55. SPECIMEN H-27, DRIFT AT 1033°K (1400°F) AND 1144°K (1600°F)

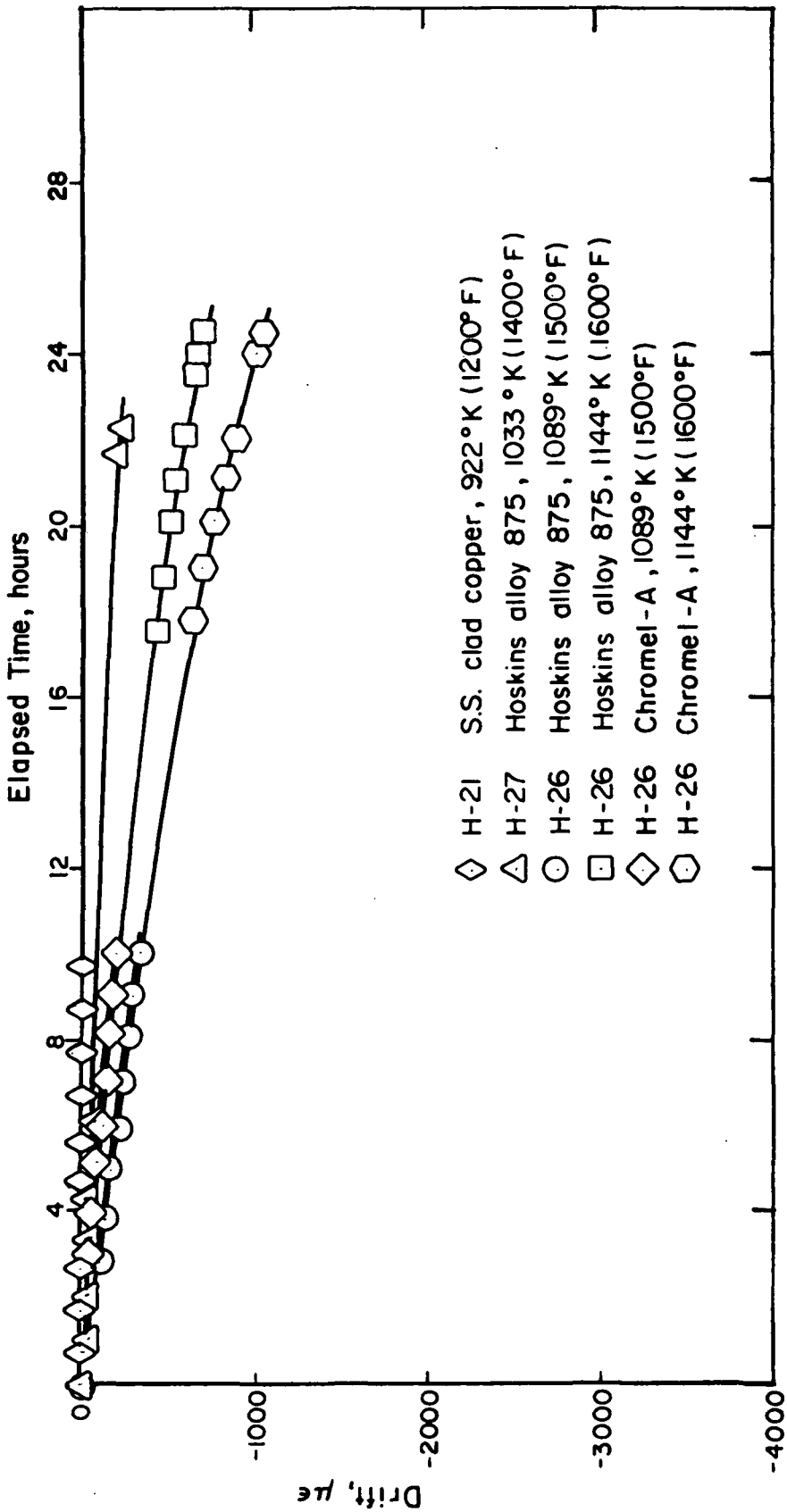

FIGURE 56. SPECIMENS H-21, H-26, H-27, DRIFT AT VARIOUS TEMPERATURES

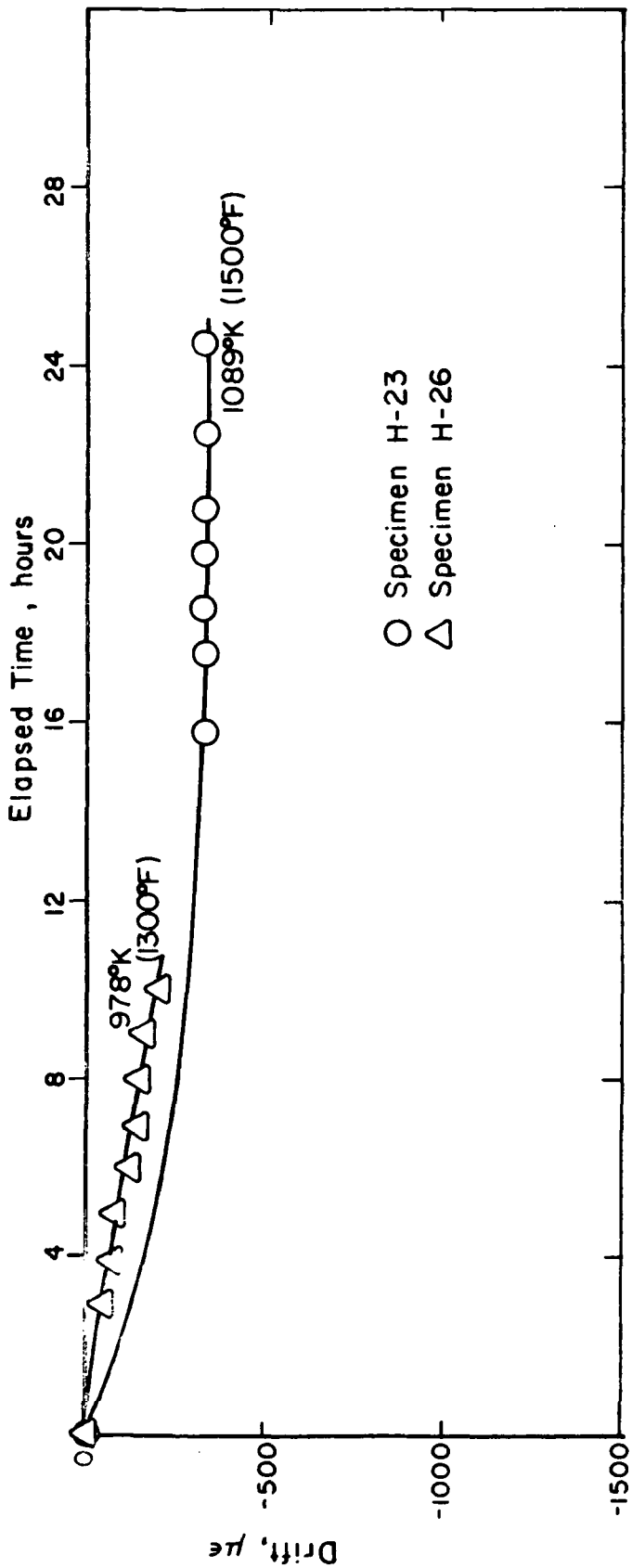

FIGURE 57. SPECIMENS H-23, H-26, DRIFTS AT 978°K (1300°F) AND 1089°K (1500°F) CHROMEL A LEADS

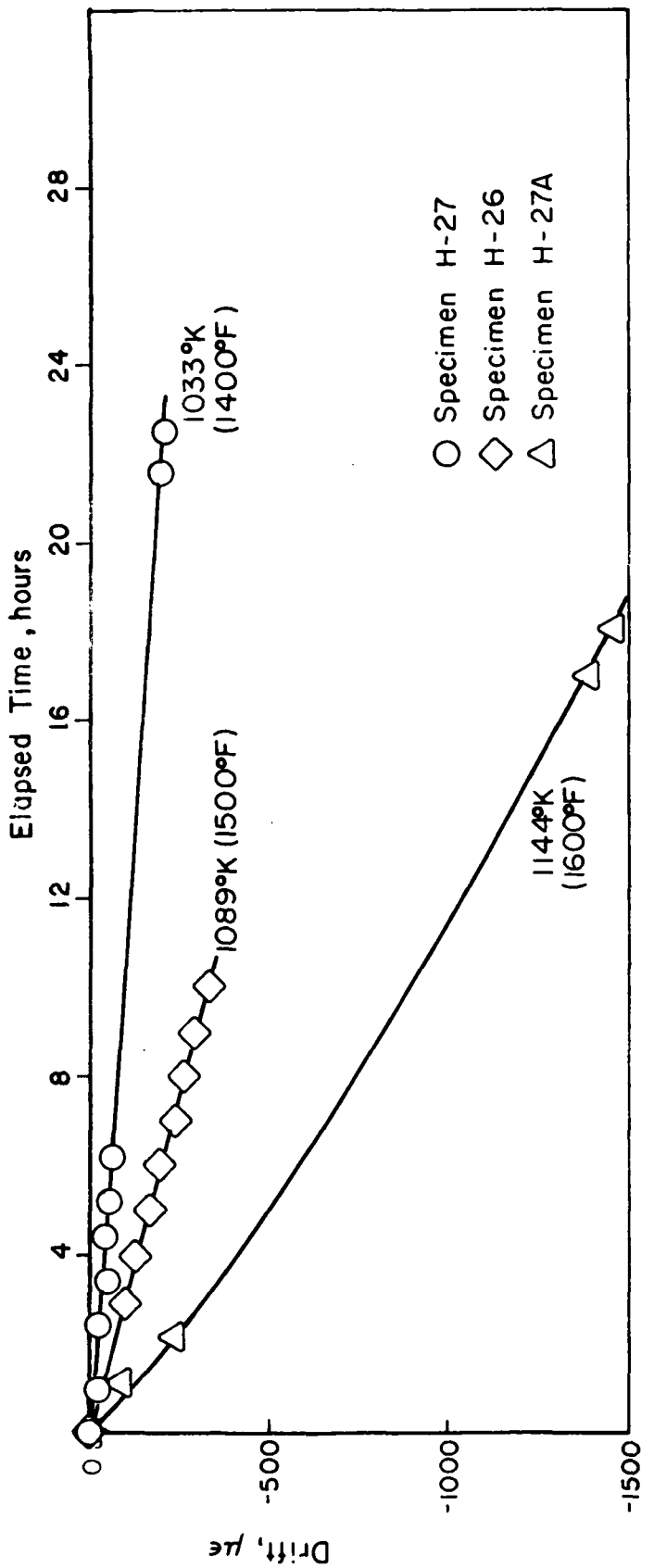

FIGURE 58. SPECIMENS H-26, H-27, H-27A, DRIFTS AT 1089°K (1500°F), 1033°K (1400°F), HOSKINS LEADS

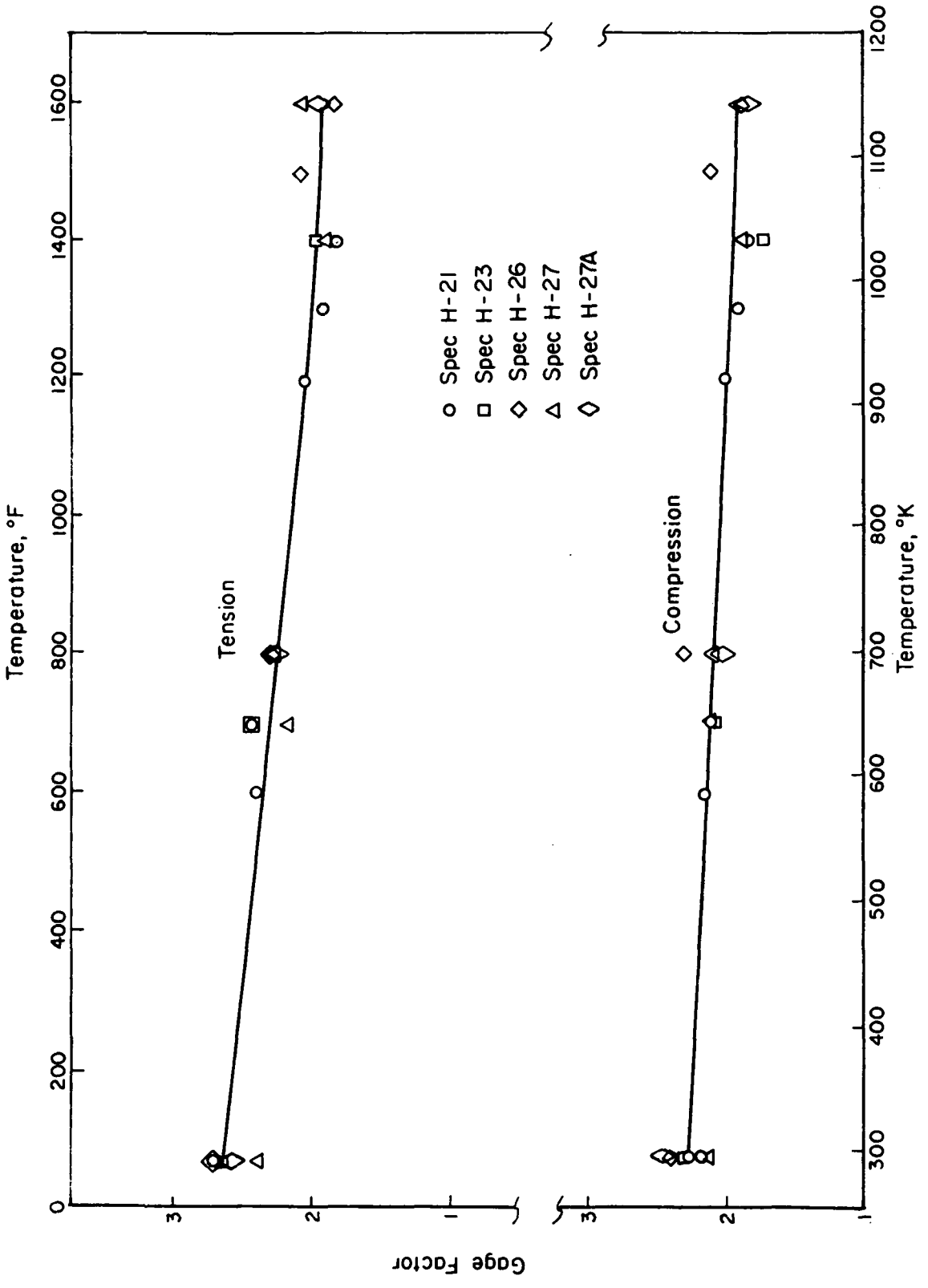

FIGURE 59. GAGE FACTOR VS TEMPERATURE

APPENDIX A

GAGE FABRICATION PROCEDURE

APPENDIX A. GAGE FABRICATION PROCEDURE

A1. General Remarks

This Appendix describes the equipment, fixtures, and procedures used to fabricate the 70 ohm gages, from two mil dia. BCL-3, air-annealed wire. These gages have a nominal gage length of 0.8 in. Figure A-1 shows the pertinent gage dimensions.

Skill and cleanliness requirements for fabrication of these gages are believed no different from those pertaining to fabrication or handling wire gages, in general. It is also imperative that the wire and completed gages be stored in an inert moisture free, and dust free atmosphere.

A2. Description of Equipment

A2.1 Winding Fixture

Figure A-2 shows the pertinent features of the winding fixture.

The gage filament is produced by winding the wire around the pins which retract into the two bakelite blocks upon actuation of the pin retracting levers. The fixed block has two wire grips, G1 and G2; three retracting pins, P1, P3, and P5, which are operated by the levers L1, L3, and L5, respectively; and two Lavite ceramic buttons, which serve as welding bases. The movable block has two retractable pins, P2 and P4, which are actuated by levers L2 and L4, and a micrometer head for establishing a precise gage length. The blocks, pins, buttons, and micrometer comprise the "head" of the fixture. To wind a gage, the head is rotated about the vertical spindle with the "bat" shaped handle.

A2.2 Welding Equipment

The gage filament to lead tab joints of the gages evaluated in this program were made of the following pieces of DC parallel gap welding equipment:

(1) Hughes constant voltage welding power supply, Model No. MCW-550.

(2) Hughes parallel gap weld head Model No. VTA-66.

(3) Hughes Type MCW electrodes Catalog No. ESQ-1525-02 (0.015 in. x 0.025 in.).

(4) Bausch and Lomb microscope, Hughes Model No. MCW-552.

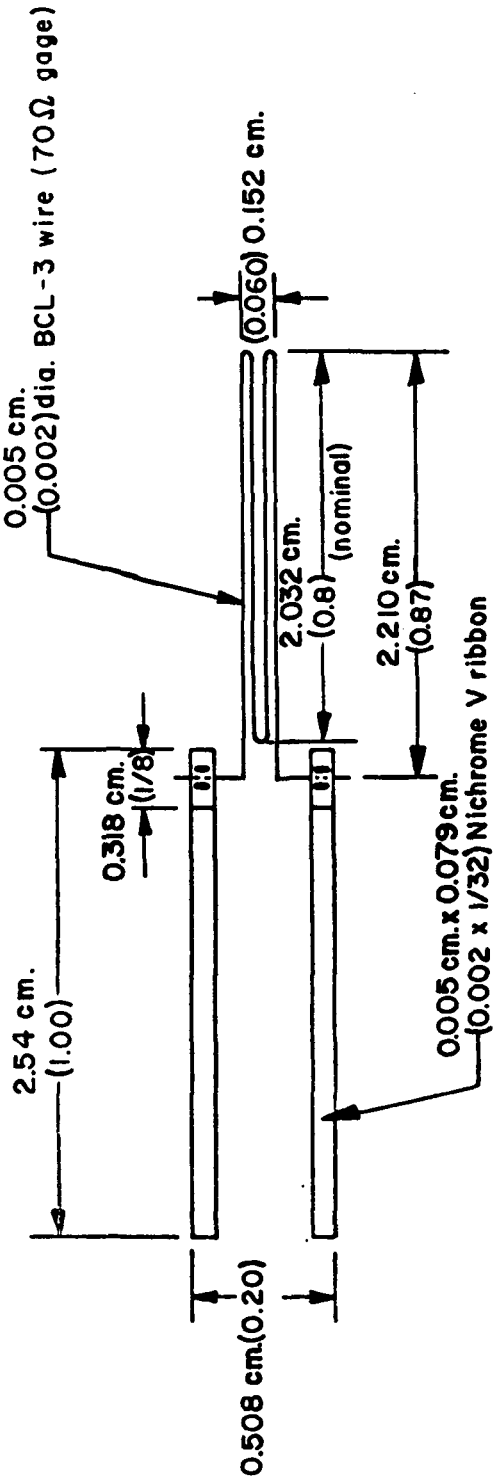

FIGURE A-1. GAGE GEOMETRY

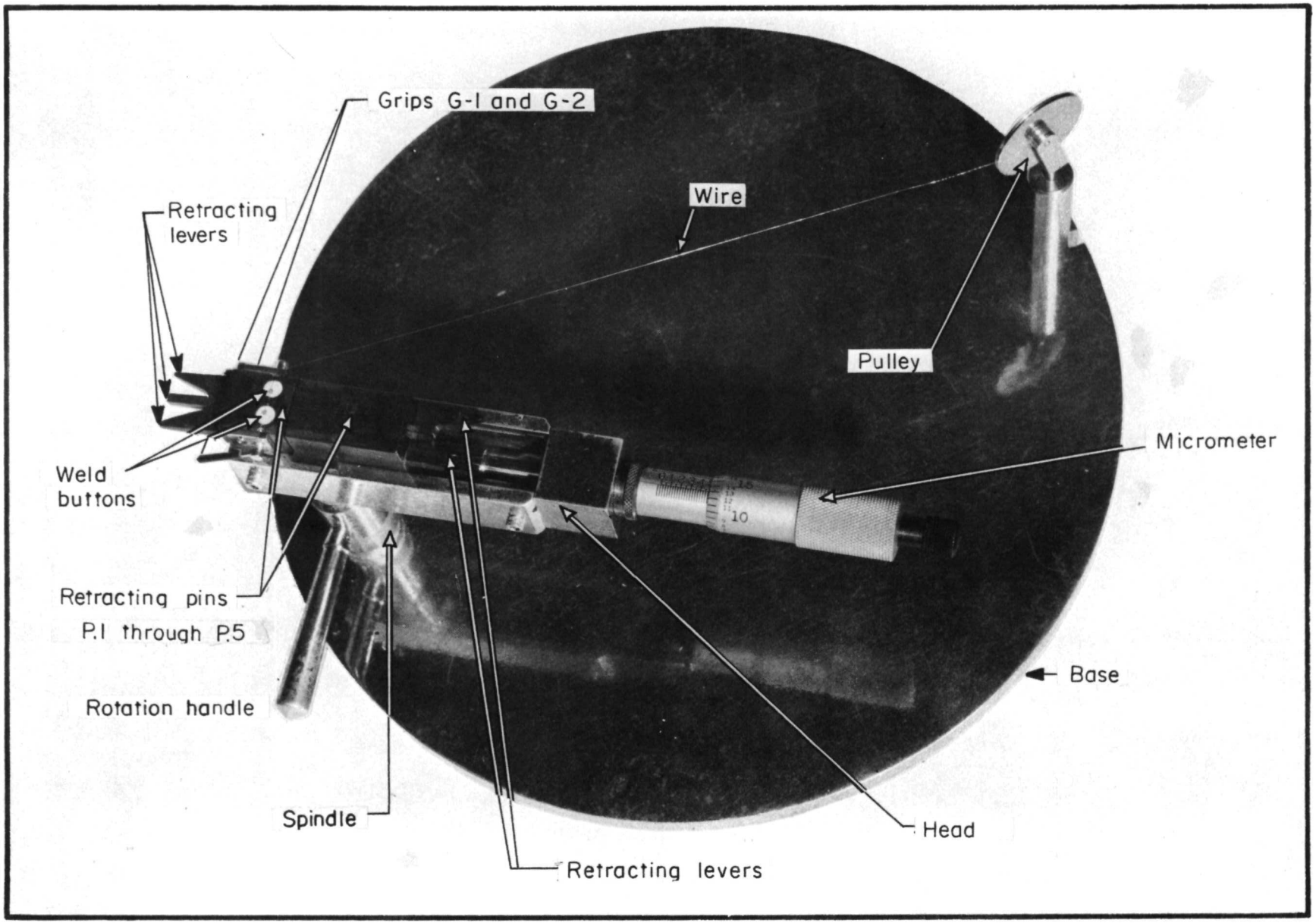

FIGURE A-2a. GAGE WINDING FIXTURE ASSEMBLY

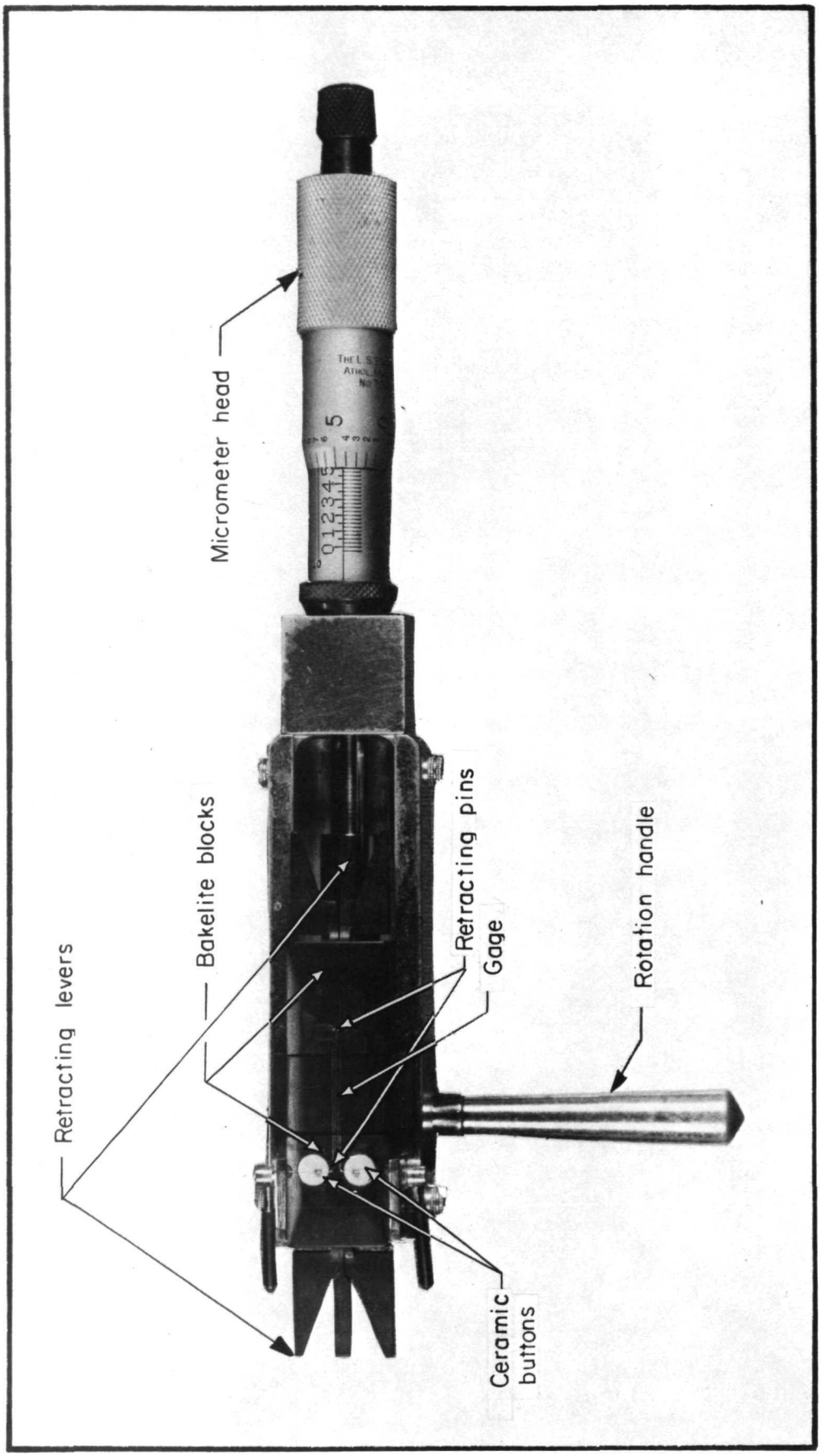

FIGURE A-2b. GAGE WINDING FIXTURE HEAD

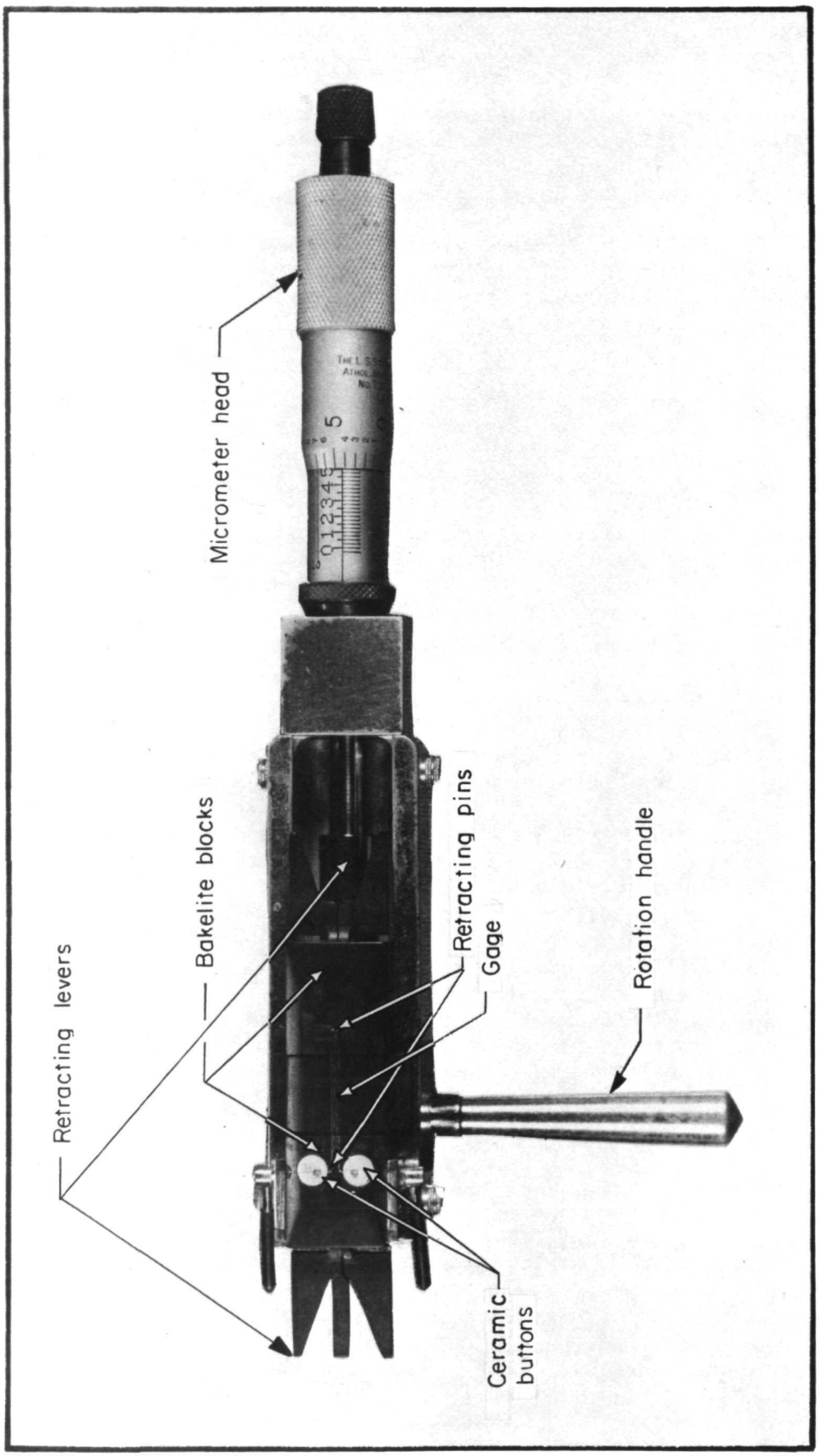

FIGURE A-2b. GAGE WINDING FIXTURE HEAD

The power supply settings which proved most successful for this application were a voltage setting of 0.70 and a 28 millisecond pulse duration with an electrode pressure of 7 lb. and a gap of 0.010 in. There were no deviations from the general operating procedures in the manufacturers' handbook.

It was found that maintenance of the proper electrode tip dimensions and electrode cleanliness were essential to making sound and uniform welds. Corroded or unevenly worn electrodes produced unreliable joints.

A3. Gage Fabrication Procedure

A3.1 General

The lead tabs, carrier type, and teflon backing should be prepared prior to winding the gage filament. The use of a binocular microscope is essential during gage fabrication. The following describes the steps involved in making the above-mentioned gage elements, and in winding the gage filaments.

A3.2 Preparation of Lead Tab Ribbons

The lead tabs are made by cutting tabs 1-1/4 in. long from 0.002 x 1/32 in. Nichrome V ribbon. To prepare a ribbon, place a piece of 0.001 to 0.003 in. shim stock 1/4 in. from the end of the ribbon. Holding the shim securely, abrade the ribbon with 320 grit silicon carbide paper, and then with 600 grit silicon carbide paper. Turn the ribbon over and abrade this surface in the same manner as the previous surface. The abrading should remove all oxide or other film from the surface of the ribbon. Next place the shim over the ribbon 1/8 in. from the abraded end. While holding the shim down, then with a scalpel or other thin edged instrument, lift the exposed end of the ribbon and fold it back over the shim. Depress the bend to form a sharp bend. Next remove the ribbon from the shim and clean with alcohol applied with a small brush. Then place ribbons in a container or otherwise store to avoid contamination from grease or dust.

A3.3 Preparation of Carrier Tape

The carrier tape used is teflon impregnated glass fiber tape 3M type X-1132. A 9-hole pattern is cut on 1-1/2 in. x 1 in. pieces of the tape, in accordance with the geometry shown in Figure A-3 using a hole cutter. It is imperative that the holes be cut clean so that no fibers extend into the hole pattern. The use of a sharp die or other cutting tool is essential. Experience has shown that best results will be achieved by taping the carrier material to a clean piece of material such as Plexiglas and cutting the holes in the carrier while it is still taped to the Plexiglas. The perforated tape may be left on the Plexiglas until it is needed.

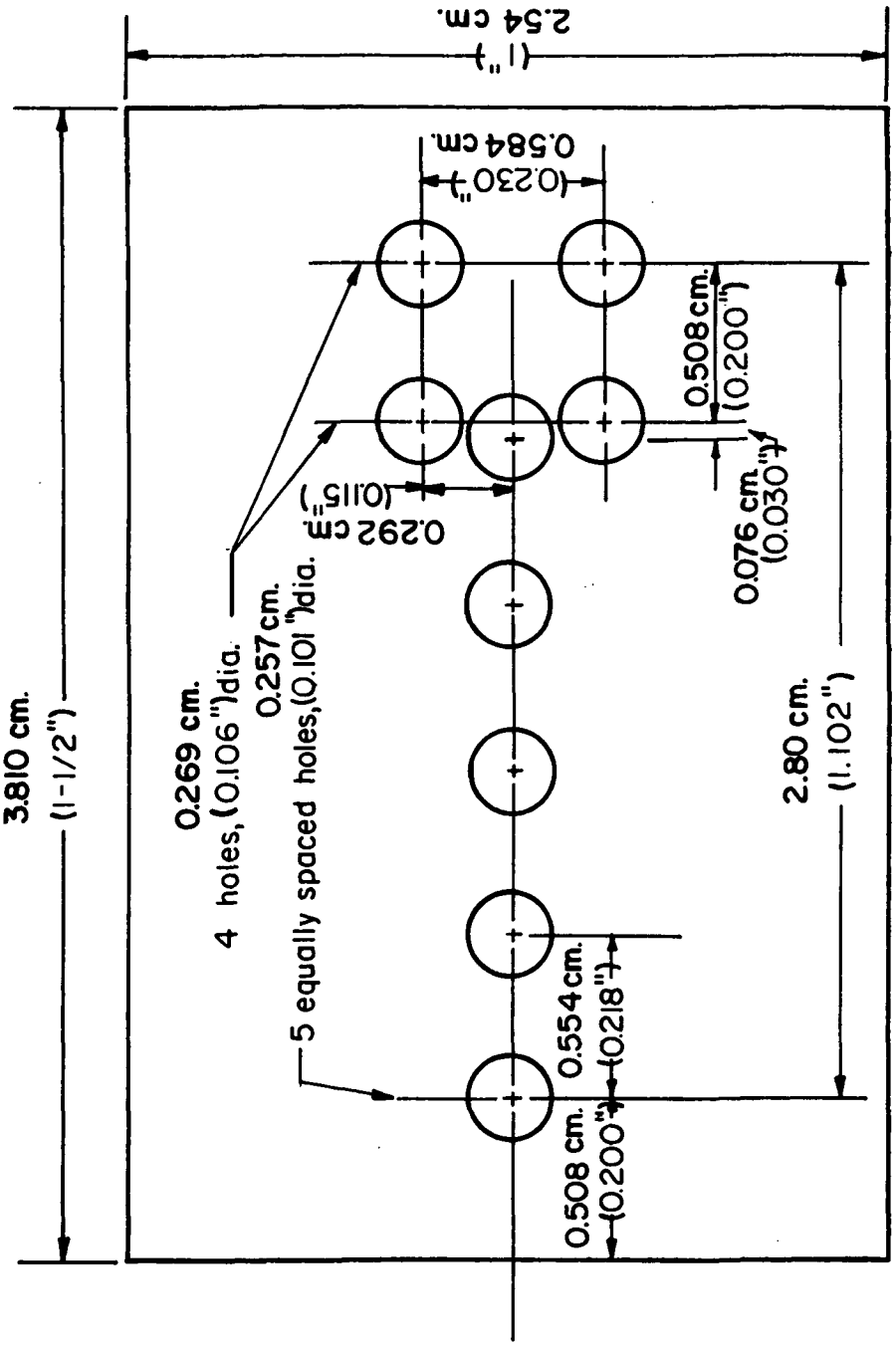

FIGURE A-3. GEOMETRY OF PERFORATED CARRIER TAPE

A3.4 Preparation of Backing

The backings are made from teflon sheet, approximately 1/32 in. thick. They should be cut in pieces 1 in. x 1-1/2 in. After cutting the pieces should be degreased with Xylene, and then stored in a clean container.

A3.5 Gage Winding and Assembly

Care must be exercised at all times to avoid handling the previously prepared and cleaned lead tabs, and backing pieces with the bare hands. Likewise, the wire used to wind the gages should not be touched with bare hands, and care must also be exercised to avoid overstressing or nicking the wire with instruments while handling or winding the gages.

To facilitate gage winding, the fixture should be placed near the edge of the workbench. The micrometer setting should be increased 0.500 in. from a lesser setting. A 12 gm weight should then be attached to a 30 in. length of 2 mil BCL-3 wire, and suspended from grip G-1 over the adjustable height pulley. Next position the lead tab ribbon on the fixture head by slipping the ribbon under the wire and positioning ribbon so that wire is sandwiched between the ribbon fold. The ribbon should then be carefully centered over the Lavite weld button closest to G-1. Next raise pin P-1 by depressing L-1 and rotate the head 90° counterclockwise with the bat shaped handle. The micrometer should never be used to rotate the head, since this may change the micrometer setting. Next raise pin P-2 and rotate 180° clockwise. Then raise pin P-3 and rotate 180° counterclockwise. Next raise pin P-4 and rotate 180° clockwise. Finally, raise pin P-5 and rotate the head 90° counterclockwise. Then insert another ribbon under the wire, as before, and position over the Lavite welding button nearest G-2. Then place a toothpick or some instrument on the wire, between the head and the pulley, and depress the wire gently and guide the end of the wire nearest the head into grip G-2 and lock grip. Depressing the wire insures uniform tension up to the final grip. Then cut the wire and secure the loose end. This completes the gage winding.

Next, remove the head from the spindle of the winding fixture and secure to an intermediate base plate, which then is placed on the platen of the DC parallel gap welder. Then, using a micrometer microscope with a reticle, space the ribbons 0.200 in. apart, with the ribbons positioned over the welding buttons. Next, increase the micrometer setting to 0.503 in. to provide the proper tension. Then weld the ribbons to the wire, using the settings specified in A2.2, and in accordance with the general instructions contained in the manufacturers' handbook for the equipment.

The carrier tape is then used to remove the gage from the winding head. The tape should be positioned over the gage, making sure that all four strands of the gage are visible and centered with respect to the holes and that the pins protrude through the appropriate holes. Then smooth down the tape over the filament and ribbon areas.

The carrier tape and gage are then removed from the head, by turning the micrometer setting back to 0.500 in., retracting all pins, releasing the grips, and carefully and slowly pulling the tape off the head at a low angle. Cut the excess wire from the outside edges of the ribbon and discard. Then place the carrier tape with gage on a prepared backing and smooth the tape down.

Store all finished gages and unused wire in a container having an inert atmosphere (argon) and desiccant.

APPENDIX B

GAGE ATTACHMENT PROCEDURE

APPENDIX B. GAGE ATTACHMENT PROCEDURE

B1. General Remarks

This Appendix describes the equipment, fixtures, and procedures used to attach the gages evaluated in this program, by means of the Rokide flame spray process. Unless otherwise noted, the general procedures recommended by BLH Electronics were followed for flame spray bonding with their equipment. Skill and cleanliness requirements for attachment of these gages are believed no different from that pertaining to the attachment of commercially available gages of this type.

B2. Description of Equipment

B2.1 Flame-Spray Equipment

The BLH portable Rokide flame-spray system with the 1/4 inch Rokide coating gun, Type R-3, and associated equipment was used. The accessories include two stage acelylene and oxygen regulators, automatic air aridifier, gas arrestor, air cleaner and dryer, and hoses. The material used was 1/4 inch Rokide BLH Type H rod, which is a high purity alumina (Al_2O_3).

B2.2 Welding Equipment

The welding equipment used to attach the lead wire to the gage lead tabs consisted of a Unitek Model 1-065-03 resistance spot welder and the Model 34066 hand-piece with a Model 13-012-04-02 electrode. It was found that a 10 to 12 watt-second setting with moderate pressure works best.

B3. Gage Attachment Procedure

The Haynes 25 specimen is first degreased with Xylene. Next an area about 3/4 in. x 2 in. is masked off for each gage with BLH Type 64 teflon impregnated tape. The area is then grit-blasted with -30 + 100 mesh brown fused alumina oxide, at a pressure of 30 psi. This was done with a slow, sweeping motion, at a distance of about 4 to 6 inches from the specimen. If properly done, the surface will be dull, unstreaked, and uniform in appearance.

After completion of the blasting, the specimen is again cleaned, using Xylene, and the specimen is again blasted with filtered air, at a pressure of about 40 psi to remove any tissue or cloth fibers. The grit-blasted area is

then remasked, using the No. 64 tape. The thickness of the specimen in the gage area is checked with a clean micrometer to obtain the final specimen thickness. The substrate is then deposited on the prepared surface by means of the Rokide process. A thickness of 4 mils was found satisfactory at the lower temperatures (< 1300°F); however, at the higher temperatures, a substrate thickness of 5 mils was found necessary. The gun is held about 8 to 10 inches from the specimen surface during flame-spraying which was done in a slow and even motion, with the gun perpendicular to the surface.

It appeared that better results were obtained by depositing the substrate in 2 or 3 separate layers, rather than one thick substrate. It was also found that a substrate with a somewhat glazed appearance produced a better substrate, electrically and mechanically, than one having a grainy appearance, which usually results from having the gun too far from the work piece.

The gage location and alignment is then established with marks from a 4H pencil, the marks being away from the area occupied by the gage filament. The teflon backing is then removed from the gage by bending the backing away from the carrier tape. The gage/carrier tape is then carefully positioned on the specimen with respect to the pencil markings. The tape is then smoothed down by pressing firmly, making certain that the tape is "down" in the hole areas. The remaining areas of the substrate, not covered by the carrier tape, are than masked off.

Next, the "tack-coat" is applied by flame-spraying through the holes in the carrier tape, moving the gun in a slow, sweeping motion parallel, if possible, to the gage filaments. The tack coat is considered complete when the grid wires are slightly visible through the coating. This corresponds to a thickness in the neighborhood of one to two mils. To secure the ribbons, a thicker tack is required. This is done by covering the upper portion of the gage with a piece of tape, and spraying an additional layer onto the ribbon until the "button" is flush with the tape surface. Any Al_2O_3 that has bridged from the button to the tape should be carefully chipped away. The chipping should be done under magnification to avoid damaging the button or gage.

The carrier tape is then removed by folding the end opposite the ribbons back over the gage at a low angle pulling the tape toward the ribbon end and keeping it as close to the specimen as possible; otherwise, the gage filament may be broken.

The gage is then remasked leaving only the elements and buttons exposed. The ribbons beyond the button should also be covered. The next coat is then flame-sprayed, using the same procedure as previously. The coat should be sufficient to just encapsulate the gage wires.

A piece of tape is again applied over the upper portion of the gage, and the final coat applied to the ribbons to securely anchor them. This will require a heavier coat than used to just encapsulate the gage filaments.

Next, all masking tape is removed and the area remasked leaving all of the substrate and one gage exposed, except the area beyond that of the

ribbon tackdown, including the ribbon. The gage coat is then applied until the wires are evenly coated and the total thickness of the coating is 10 to 15 mils thick, including the substrate thickness.

All masking is then removed, and the area remasked, leaving the area of the substrate beyond the ribbon tackdowns exposed. The ribbons are then folded over the gage and covered with tape. The exposed area is then sprayed until it is the same thickness as the rest of the substrate.

The lead wires are then attached to the lead tab ribbons with the Unitek welder, hand-piece, and electrode. It was found that a 10 to 12 watt-second setting with moderate pressure gave the best results for the lead wire systems used.

APPENDIX C

RESISTANCE TO GROUND MEASUREMENTS

TABLE C-1. RESISTANCE TO GROUND MEASUREMENTS
-SPECIMEN H-21 (3 MIL SUBSTRATE)-

Maximum Run Temperature	Step Number	Cycle Number	Gage Temperature °K	Gage Temperature °F	Gage Number	Resistance to Ground Kilohms	Resistance to Ground Megohms
922 K (1200 F)	2	---	936	1225	1	---	7.0
					2	3.5	---
					3	48.0	---
					4	---	1.7
					5	650.0	---
					6	450.0	---
					7	---	1.4
					8	190.0	---
922 K (1200 F)	4	---	922	1200	1	---	7.5
					2	3.8	---
					4	---	2.0
					5	---	1.0
					8	290.0	---
978 K (1300 F)	2	---	991	1325	1	---	3.0
					4	4.0	---
					5	---	1.4
					8	350.0	---
978 K (1300 F)	3	3	991	1325	1	---	3.8
					2	---	3.6
					4	---	3.8
					5	---	1.6
					8	---	1.0
978 K (1300 F)	4	3	978	1300	1	---	3.0
					2	4.5	---
					3	20.0	---
					4	3.8	---
					5	---	1.4
					8	---	2.5
978 K (1300 F)	5	---	978	1300	1	---	2.0
					2	4.2	---
					3	15.0	---
					4	3.6	---
					5	---	1.4
					8	---	2.8

TABLE C-1. RESISTANCE TO GROUND MEASUREMENTS
-SPECIMEN H-21 (3 MIL SUBSTRATE)-
(Continued)

Maximum Run Temperature	Step Number	Cycle Number	Gage Temperature °K	Gage Temperature °F	Gage Number	Resistance to Ground Kilohms	Resistance to Ground Megohms
1033 K (1400 F)	4	3	1033	1400	1	---	1.0
					2	5.0	---
					3	5.6	---
					4	1.6	---
					5	600.0	---
					8	200.0	---
1033 K (1400 F)	5	---	1033	1400	1	---	1.0
					2	5.0	---
					3	7.5	---
					4	1.8	---
					5	600.0	---
					8	200.0	---

TABLE C-2. RESISTANCE TO GROUND MEASUREMENTS
-SPECIMEN H-22 (4 MIL SUBSTRATE)-

Maximum Run Temperature	Step Number	Cycle Number	Gage Temperature °K	Gage Temperature °F	Gage Number	Resistance to Ground Kilohms	Resistance to Ground Megohms
978 K (1300 F)	2	---	991	1325	1	350	---
					2	---	1
					3	500	---
					4	---	1
978 K (1300 F)	3	3	978	1300	1	---	200
					2	---	100
					3	---	100
					4	---	100
978 K (1300 F)	6	3	978	1300	2	---	2
					3	---	5
					4	3	---
978 K (1300 F)	7	---	978	1300	2	---	2
					3	---	5
					4	3	---
1033 K (1400 F)	2	---	1047	1425	2	---	2
					3	---	5
					4	3	---
1033 K (1400 F)	3	3	1033	1400	2	---	4.4
					3	---	2.3
					4	13	---
1033 K (1400 F)	6	1	299	78	2	---	100
					3	---	70
					4	---	150
1033 K (1400 F)	7	---	297	75	2	---	100
					3	---	100
					4	---	150
1089 K (1500 F)	3	---	1103	1500	2	200	---
					3	300	---
					4	10	---

TABLE C-3. RESISTANCE TO GROUND MEASUREMENTS
-SPECIMEN H-23 (4.5 MIL SUBSTRATE)-

Maximum Run Temperature	Step Number	Cycle Number	Gage Temperature °K	Gage Temperature °F	Gage Number	Resistance to Ground Kilohms	Resistance to Ground Megohms
978 K (1300 F)	2	---	296	74	1	---	500
					2	---	150
					3	---	500
					4	---	400
978 K (1300 F)	2	---	1005	1350	1	---	∞
					2	---	10
					3	---	6
					4	---	1.2
978 K (1300 F)	3	3	978	1300	1	---	13
					2	---	9.5
					3	---	9.5
					4	---	6
978 K (1300 F)	3	3	301	82	1	---	90
					2	---	90
					3	---	50
					4	---	50
978 K (1300 F)	4	1	978	1300	1	---	7.5
					2	---	4.8
					3	---	5.5
					4	---	0.5
978 K (1300 F)	5	3	315	108	1	---	∞
					2	---	∞
					3	---	∞
					4	---	50
978 K (1300 F)	6	3	978	1300	1	---	11
					2	---	9
					3	---	7.5
					4	---	2
978 K (1300 F)	7	---	978	1300	1	---	30
					2	---	35
					3	---	30
					4	---	19
1033 K (1400 F)	2	---	1047	1425	1	---	8
					2	---	6
					3	---	9
					4	---	2.5

TABLE C-3. RESISTANCE TO GROUND MEASUREMENTS
-SPECIMEN H-23 (4.5 MIL SUBSTRATE)-
(Continued)

Maximum Run Temperature	Step Number	Cycle Number	Gage Temperature °K	Gage Temperature °F	Gage Number	Resistance to Ground Kilohms	Resistance to Ground Megohms
1033 K (1400 F)	3	---	1039	1410	1	---	14
					2	---	12
					3	---	11.5
					4	---	8.5
1033 K (1400 F)	6	3	313	103	1	---	400
					2	---	1000
					3	---	1000
					4	---	1000
1033 K (1400 F)	7	---	1033	1400	1	20	---
					2	100	---
					3	20	---
					4	100	---
1033 K (1400 F)	7	---	296	74	1	---	1000
					2	---	300
					3	---	500
					4	---	100
1089 K (1500 F)		---	1103	1525	1	---	700
					2	40	---
					3	---	1000
					4	45	---

TABLE C-4. RESISTANCE TO GROUND MEASUREMENTS
-SPECIMEN H-24 (5 MIL SUBSTRATE)-

Maximum Run Temperature	Step Number	Cycle Number	Gage Temperature °K	Gage Temperature °F	Gage Number	Resistance to Ground Kilohms	Resistance to Ground Megohms
1089 K (1500 F)	2	---	1103	1525	1	---	12
					2	---	10
					3	---	11
					4	---	9
1089 K (1500 F)	2	---	1103	1525	1	---	1
					2	---	8
					3	---	1.2
					4	---	5.6
1089 K (1500 F)	3	3	1089	1500	1	---	1
					2	---	2
					4	---	2.2
1089 K (1500 F)	4	2	299	78	1	---	∞
					2	---	1000
					4	---	500

TABLE C-5. RESISTANCE TO GROUND MEASUREMENTS
-SPECIMEN H-25 (5 MIL SUBSTRATE)-

Maximum Run Temperature	Step Number	Cycle Number	Gage Temperature °K	Gage Temperature °F	Gage Number	Resistance to Ground Kilohms	Resistance to Ground Megohms
1200 K (1700 F)	6	2	1200	1700	1	100	100
					2	---	2.4
1089 K (1500 F)	6	4	1089	1500	1	40	---
					2	100	---
1144 K (1600 F)	2	---	1158	1625	1	---	30
					2	---	17
					3	---	30
					4	---	30
1144 K (1600 F)	2	---	1158	1625	1	---	10
					2	---	15
					3	---	16
					4	---	12
1089 K (1500 F)	3	3	1089	1500	1	---	70
					2	---	30
					3	---	60
					4	---	70
1089 K (1500 F)	4	1	1089	1500	1	---	60
					2	---	29
					3	---	50
					4	---	45
1089 K (1500 F)	6	3	1089	1500	1	---	36
					2	---	17
					3	---	42
					4	---	45
1144 K (1600 F)	3	3	1144	1600	1	---	45
					2	---	17
					3	---	45
					4	---	24

TABLE C-6. RESISTANCE TO GROUND MEASUREMENTS
- SPECIMEN H-26 (5 MIL SUBSTRATE)-

Maximum Run Temperature	Step Number	Cycle Number	Gage Temperature °K	Gage Temperature °F	Gage Number	Resistance to Ground Kilohms	Resistance to Ground Megohms
1144 K (1600 F)	6	2	1141	1595	1	---	24
					2	---	12
					3	---	26
					4	---	20
1255 K (1800 F)	2	---	1269	1825	1	---	4
					2	---	8.5
					3	---	8
					4	---	10
1255 K (1800 F)	3	2	1255	1800	1	---	3.8
					2	---	2.9
					3	---	5.2
					4	---	5.8
1255 K (1800 F)	4	2	1255	1800	1	---	2.8
					2	---	2.2
					3	---	4.2
					4	---	5

TABLE C-7. RESISTANCE TO GROUND MEASUREMENTS -SPECIMEN H-27 and H-27A (5 MIL SUBSTRATE)

Maximum Run Temperature	Step Number	Cycle Number	Gage Temperature °K	Gage Temperature °F	Gage Number	Resistance to Ground Kilohms	Resistance to Ground Megohms
1144 K (1600 F)	2	---	308	95	1	---	∞
					2	---	∞
					3	---	∞
					4	---	∞